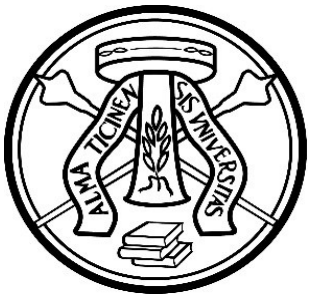

UNIVERSITY OF PAVIA
Department of Brain and Behavioral Sciences
Doctoral Program in Psychology, Neuroscience and Data Science
Doctorate cycle: XXXIII
Coordinator: Prof. Gabriella Bottini

EFFECTS OF MAGNETIC RESONANCE ON TEMPERATURE AND ADHESION EFFICACY OF ORTHODONTIC DEVICES

Supervisor: Prof. Luisa Bernardinelli

Doctoral Thesis of:
Andrea Scribante
Matr. N. 462090

Academic Year 2019/2020

To Stefania, Elena and Luca

To my parents

To Cairoli College Brothers

Acknowledgements.

The present Study has been conducted in five different Laboratories:

Section of Statistics - Department of Brain and Behavioral Sciences, University of Pavia

Unit of Orthodontics and Paediatric Dentistry, Section of Dentistry, Department of Clinical, Surgical, Diagnostic and Paediatric Sciences, University of Pavia

Department of Diagnostic and Interventional Radiology—Fondazione IRCCS Policlinico San Matteo, Pavia

CNAO Foundation Diagnostic Imaging Unit, National Center of Oncological Hadrontherapy (CNAO) Pavia

Section of Radiology - Department of Clinical, Surgical, Diagnostic and Paediatric Sciences, University of Pavia

I would like to thank:

Prof. Luisa Bernardinelli for her continuous training and precious support before and during PhD

Prof. Paola Gandini for great teaching precision and outstanding research organization

Prof. Maria Francesca Sfondrini for her constant help in improving my scientific activity and knowledge

Prof. Fabrizio Calliada for wise supervision of the 1.5T tests

Prof. Lorenzo Preda for bright oversight of the 3T tests

Dr. Luca Lungarotti, my brother and "son" in Cairoli College, for excellent radiologic assistance

Maria Luisa Valsecchi (3M Unitek), and Renzo Erinni (Leone) for providing the materials tested in the present investigation

Prof. Giuseppe Sfondrini, life master

Stefania, Elena and Luca for love, energy and support.

Table of contents.

1. Abstract and Keywords.

2. Introduction.
2.1. History of magnetic resonance.
2.2. Physics of magnetic resonance.
2.3. The hardware of an MRI imaging system.
2.4. Advantages and disadvantages of MRI.
2.5. Applications of MRI in medicine and dentistry.
2.6. Safety and compatibility of dental alloys.
2.7. Orthodontic appliances.
2.8. Interactions between fixed orthodontic appliances and magnetic fields.
2.9. Magnetic behavior of orthodontic alloys.
2.10. Interaction between metal orthodontic devices and MRI.
2.11. Artifact production.
2.12. Overheating.
2.13. Detachment and displacement.
2.14. Bracket adhesion to enamel
2.15. Shear bond strength test in orthodontics.
2.16. Rationale of the study.

3. Materials and Methods.
3.1 Specimen preparation.
3.2. Temperature test and MRI.
3.3. Shear bond strength test.
3.4. Adhesive remnant index test.

4. Statistical analysis.
4.1. The Software R.
4.2. The R environment.

4.3. Descriptive Statistics.
4.4. Mean.
4.5. Standard deviation.
4.6. Median.
4.7. Minimum and Maximum.
4.8. Linear regression.
4.9. Kolmogorov and Smirnov test.
4.10. ANOVA (Analysis of variance).
4.11. Pairwise comparison: Tukey test.
4.12. Fisher exact test.
4.13. P values.
4.14. Statistical Analysis on the R software.

5. Results.
5.1. Linear regressions.
5.2. Temperature test.
5.3. Shear bond strength test.
5.4. ARI scores analysis.

6. Discussion.
6.1. Overall.
6.2. The first null hypothesis. Temperature variations.
6.3. The second null hypothesis. The shear bond strength.
6.4. Third null hypothesis. The ARI Scores.
6.5. Limitations and general considerations.

7. Conclusions.

8. Statements and publication.

9. References.

1. Abstract and keywords.

Abstract.

Magnetic resonance (MRI) is a widely used diagnostic technique. Often, patients wearing orthodontic appliances are requested to remove appliance even when the MRI exam involves anatomic areas far from mouth, in order to avoid metal heating and appliance detachment. The purpose of the present investigation was to measure and compare temperature changes and adhesion to enamel of orthodontic appliances after different MRIs. 220 orthodontic bracket were bonded on bovine incisors and wires with different materials (stainless steel and nickel titanium) and sizes (0.014'' and 0.019''x0.025'') were engaged. Appliances were submitted to MRI at two different powers (1.5T and 3T). Temperatures of brackets and wires were measured before and after MRI. Subsequently, shear bond strength (SBS) and adhesive remnant index (ARI) scores were recorded. Statistical analysis was performed. After MRI a significant increase of temperatures was found both for brackets and wires in some groups, even if the mean temperature increase was clinically not significant, as it ranged between 0.05°C and 2.4°C for brackets and between 0.42°C and 1.74°C for wires. MRI did not conditioned bracket adhesion in any group. No differences were reported when comparing 1.5T with 3T groups. ARI Scores were significantly lower after MRI. The results of the present report show that under MRI orthodontic appliances present low temperature rise and no debonding risk. Therefore, the removal of orthodontic appliance would not be recommended routinely, but could be suggested only in case of void risk or interference in image quality.

Keywords.

Dentistry; Orthodontics; Nuclear; Magnetic; Resonance; Shear; Bond; Strength; Temperature; Adhesion; Bracket; Wire.

2. Introduction.

2. Introduction.

2.1. History of magnetic resonance.

Nuclear magnetic resonance was first described and measured in molecular beams by Isidor Rabi in 1938 [Rabi et al., 1938]. Magnetic nuclei, like hydrogen and potassium, could absorb radio frequency energy when placed in a magnetic field. When this absorption occurs, the nucleus is described as being in resonance. Different atomic nuclei within a molecule resonate at different (radio) frequencies for the same magnetic field strength [Haacke et al., 2014]. The observation of such magnetic resonance frequencies of the nuclei present in a molecule allows any trained user to discover essential chemical and structural information about the molecule.

The development of nuclear magnetic resonance as a technique in analytical chemistry and biochemistry parallels the development of electromagnetic technology and advanced electronics and their introduction into civilian use [Mitchell, 1999].

The inventor of the first magnetic resonance apparatus for medical science was Raymond Vahan Damadian. His early work on NMR concerned investigating potassium ions inside cells [Cope and Damadian 1970]. Seven years after, the first nuclear magnetic resonance for a body exam imaging was realized. In 1980, Edelstein and his collaborators experimented whole body imaging. A single image could be acquired in about five minutes. Over the years, the progress made has allowed a thorough knowledge of the various organs of the human body. MRI imaging is a relatively young technique, but in rapid and continuous evolution [Haacke et al., 2014].

2.2. Physics of magnetic resonance.

MRI systems produce images using the magnetic properties of the hydrogen core, which is the most abundant element in the body [Parker, 2018]. The magnetic resonance phenomenon is based on the intrinsic ability to rotate around its axis, possessed by the nuclei of some elements with an odd number of protons and / or neutrons (eg H +): this phenomenon is called spin or magnetic moment. Since every moving electric charge produces a magnetic field, these nuclei, electrically charged and spinning, are also associated with a microscopic magnetic field called nuclear magnetic moment or

magnetic dipole [Karunakaran, 2018]. Nuclei with magnetic moment can be visualized as "magnetic needles" capable of orienting themselves in the presence of a magnetic field (Figure 1); they can take two directions, one parallel (lower energy level) and the other antiparallel (higher energy level) to the field itself [Strikman et al., 2014].

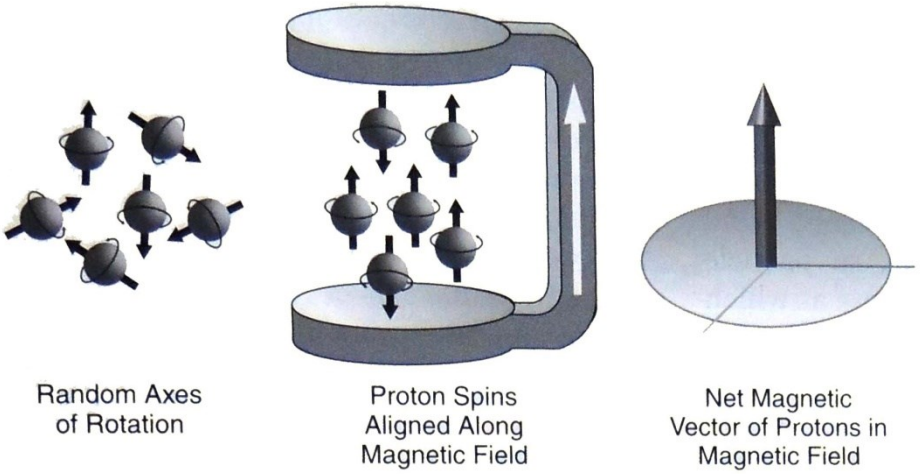

Figure 1. Alignment of protons to the magnetic field and net magnetization vector [White and Pharoah, 2009].

The preferred energy state is the one with the lowest energy level. This causes a net excess of protons aligned parallel to the external magnetic field, which produces a resulting longitudinal magnetization M.

The magnetic axis of the proton tends to arrange itself in an oscillating manner according to the direction of the magnetic field. This oscillation is combined with the spin motion of the particle (spin), resulting in a complex rotation movement on a conical surface having the direction of the magnetic field. This movement, called precession (Figure 2), occurs with a frequency, called the Larmor frequency, specific to each element and variable according to the intensity of the magnetic field in which it is inserted [Morris., 2014].

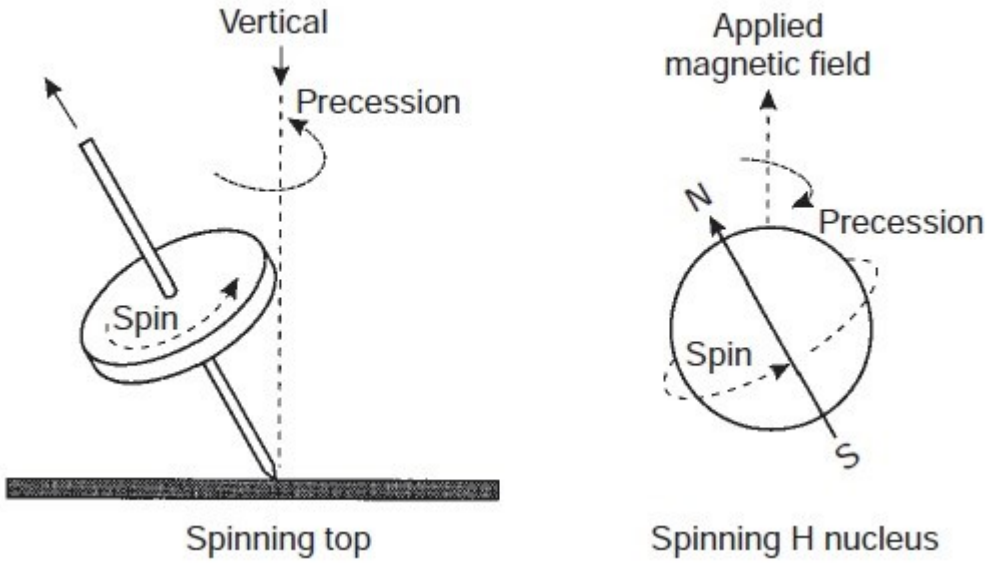

Figure 2. Precession phenomenon [White and Pharoah, 2009].

The resulting magnetization M cannot be quantified as long as it lies parallel to the external magnetic field. For this reason, it is necessary to perturb the system in order to generate a new magnetization with transversal orientation with respect to the previous one [Parker, 2018]. This occurs by subjecting the spins to a magnetic field B1 oscillating on a plane perpendicular to B0. The resonance is induced by sending a radiofrequency (RF) pulse, by applying the B1 field, for a defined time, to the Larmor precession frequency. Only the pulses with a frequency equal to that of the protons can give them the energy necessary to generate an RM signal detectable by a receiving antenna.

Once the application of the RF impulse has ceased, the magnetization vector gradually returns to its original state (relaxation). The new transverse magnetization begins to disappear (transverse relaxation process that takes place in time T2) and the longitudinal magnetization returns to its original state (longitudinal relaxation that occurs in a T1 time).

The T1 or longitudinal relaxation time is the time required for the protons to return to the initial equilibrium conditions, with the transfer of energy to the surrounding microenvironment. This process is described by an exponential type function (Figure 3) and indicates the time required to recover 63% of the longitudinal magnetization. The speed of T1 depends on numerous factors, including the intensity of the B0 field and the

size of the molecule itself (for example, DNA has a long T1, short lipids). On average, the structures of the human body in a magnetic field of intensity 0.1-0.5 T have a T1 between 300 and 700 milliseconds [Morris., 2014].

The T2 or transversal relaxation time is the time required for the protons (spin) to desynchronize in relation to the reciprocal exchange of energy. T2 is also a process described by an exponential type function (Figure 3) and indicates the time required for the transverse magnetization to decay at 37% of the initial value. The efficiency of T2 depends on various factors such as the size of the molecules (specifically, large molecules have shorter T2: water therefore has a long T2). In biological tissues, T2 is between 50 and 150 milliseconds. Unlike T1, T2 is little affected by the change in B0 [Morris., 2014].

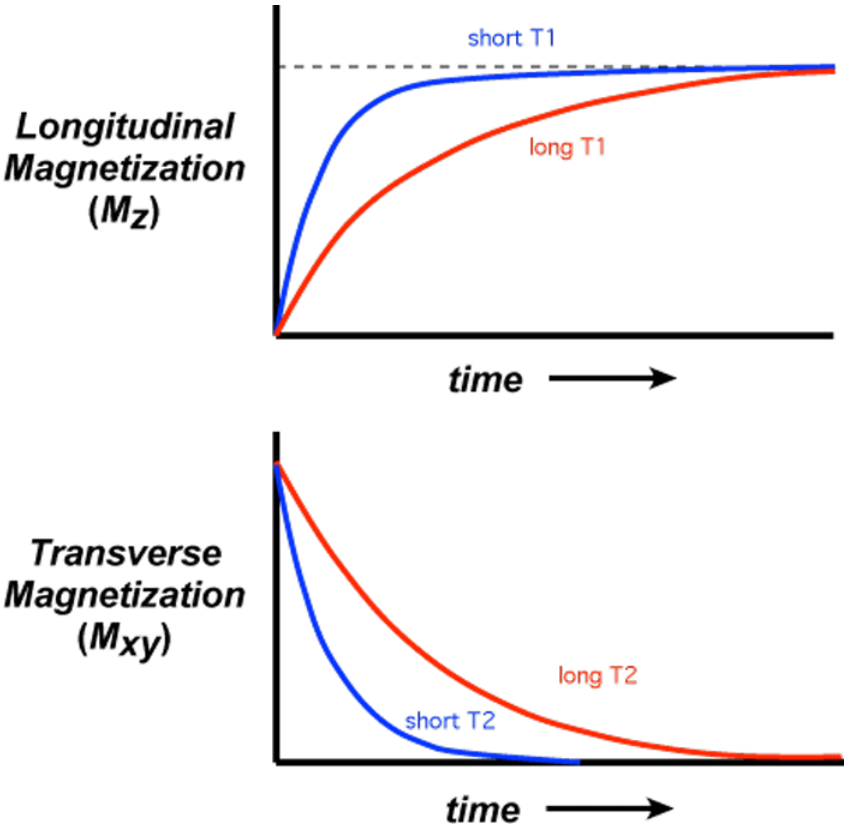

Figure 3 T1 and T2 relaxation curves. [Elster et al., 1988]

The magnetic resonance signal is the result of the sum of a multiplicity of signals from the individual spins, each of which is characterized by a frequency value and by the relaxation times T1 and T2. It varies in relation to the type of sequence used. Magnetic

resonance imaging provides multiparametric imaging, which gives the possibility to evaluate different characteristics of the tissue, linked to the intrinsic magnetic properties of the different tissue components, represented by relaxation time T1, proton density and relaxation time T2 [Elster, 1988].

In conditions of equilibrium, in the presence of a uniform magnetic field, all protons have the same frequency, but not the same precession phase. For each proton, two vector components are considered: longitudinal and transversal.

Longitudinal are oriented along the z-axis (longitudinal magnetization). It is the sum of the single moments.

Transversal are perpendicular to B0, which rotates in the x, y plane. There is no transverse magnetization in the x, y plane because the transverse components of the individual nuclei are scattered and cancel each other [Parker, 2018].

The equilibrium state just described can be altered by applying radio frequencies (electromagnetic waves) equal to the radiofrequency of protons precession (Larmor frequency). Only in these conditions does the phenomenon of nuclear magnetic resonance occur, i.e. the passage of energy from RF to protons. For RF with frequency different from that of Larmor no exchange of occurs energy [Strikman et al., 2014].

2.3. The hardware of an MRI imaging system.

The main components of an MRI imaging system are [Inam et al., 2020]:

- a cylindrical magnet capable of producing the static magnetic field B0;
- three generators of magnetic fields of variable intensity in space and time (gradients) that deform the B0 field in a controlled way;
- a radio frequency coil, capable of generating and receiving radio frequencies;
- a computerized system capable of controlling all components, calculating and displaying MRI images and data, managing archiving, printing and transfer of studies.

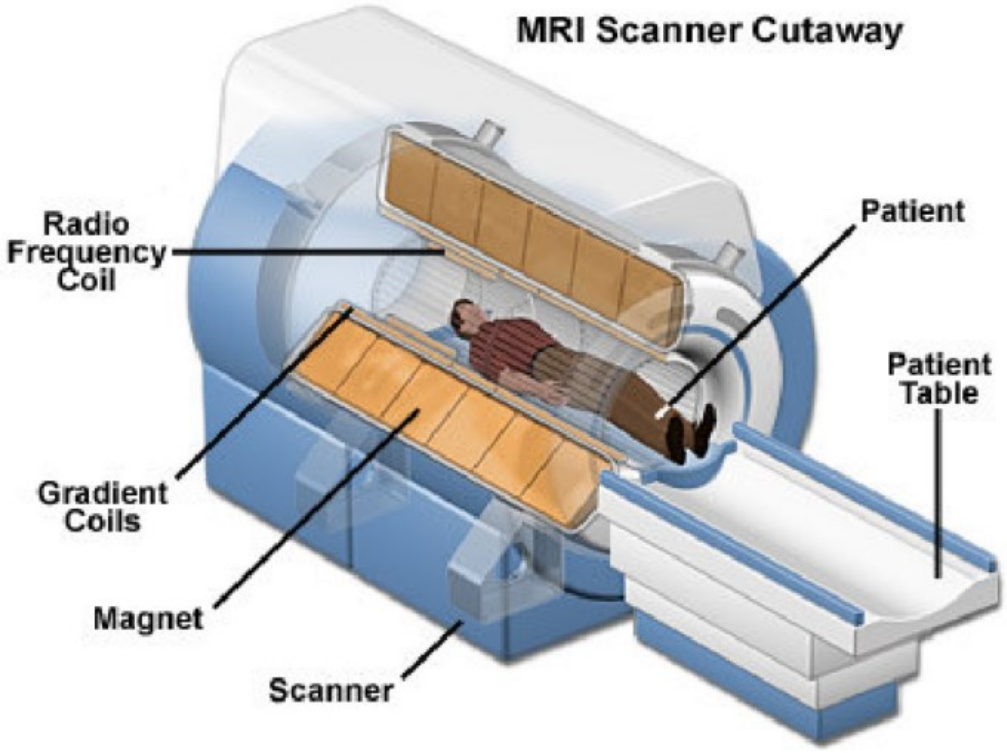

Figure 4. Hardware components of the imaging system [Schweber, 2019].

The magnet produces the static magnetic field B0. Inside the magnet, there are the coils to produce the field gradients B0 in the X, Y and Z directions. In the innermost position, the radiofrequency coil is located. It produces the magnetic field B1 necessary to rotate the spins by 90 ° , 180 ° or any other angle specified by the pulse sequence; it also receives the signal from the spins inside the body.

The patient is positioned inside the magnet (Figure 4) by means of a computer-controlled couch with millimeter accuracy. A radio frequency screen surrounds the room where the scan takes place. A magnetic shield is always present, unless the magnet is self-shielding. (5) The control of the magnetic resonance equipment and all its components is carried out with a computer. The imaging sequences are selected and customized by the operator through a control station (console). The images produced can be either displayed on a video belonging to the console or printed on film [Arun et al., 2020].

2.4. Advantages and disadvantages of MRI.

There are numerous advantages of MRI. Firstly, it is a non-invasive test that does not emit ionizing radiation. For this reason, it is increasingly used mainly in pediatric field [Yassi et al., 2007; Görgülü et al., 2014]. Additionally, the good spatial resolution improves the quality of the images, in particular of the smaller structures such as the inner ear, the brachial plexus, the biliary tract and the vascular system. No artifacts due to bone structures are present and excellent contrast resolution for soft tissues is reported. Therefore, it is used for head, spine, spinal cord, musculoskeletal system and internal organs in the detection of malformations, morbid processes of a vascular, tumor and traumatic nature [Parker, 2018].

MRI also allows to obtain direct multiplanar scans (adjustable according to different planes), without need of patient repositioning. This feature allows a panoramic view of large districts (e.g. spine) and offers the possibility of obtaining different images (different sequences), each with additional information, for each anatomical structure [Patel et al., 2006].

The main disadvantages of MRI essentially consist of very long acquisition times (25-60 minutes), and rather high costs of purchasing machinery and operating costs. Furthermore, it is not suitable for the evaluation of tissues poor of hydrogen protons such as the pulmonary parenchyma and the compact bone. The presence of metallic objects can create artifacts with loss of information. It is not recommended as a precaution to women in the first trimester of pregnancy. Additionally, also claustrophobic patients may show impatience, due to the enclosed space and long scan times. Patients with metal implants, pacemakers, implanted cardiac defibrillators, in situ ferromagnetic surgical clips / metal aneurysmal clips, neurostimulators, etc. they cannot perform this type of examination, even if RM-compatible materials have been used more and more since the 1990s [White and Pharoah, 2009].

2.5. Applications of MRI in medicine and dentistry.

MRI has become a fundamental tool for the diagnosis of various pathological conditions of the cephalic district, including migraine and cluster headache, epilepsy and other seizure disorders, multiple sclerosis, Alzheimer's disease, autism, head, neck and cable cancers oral, sinus atresia and sinusitis, cerebrovascular stroke, aneurysms, cerebral

palsy, and many other intra and extracranial lesions [Shalish et al., 2015; Elison et al., 2008]

MRI also finds application in dentistry; new approaches have recently been proposed for the application in various branches [Cox et al., 2012; Tymofiyeva et al., 2013], such as:

-endodontics, as a potential method to evaluate longitudinally teeth in which the pulp and root structures have been regenerated;

-conservative dentistry, for the diagnosis of dental caries and demineralization;

-prosthodontics, for the design of customized prosthetic products;

-implantology, for accurate positioning of the fixtures;

-orthodontics, for taking impressions indirectly, for the 3D evaluation of dental elements included and the degree of resorption of the roots

In clinical routine, however, MRI finds its main use in gnathology in the imaging of the anatomy and pathophysiology of temporo mandibular articulation [Wylezinska et al., 2015].

It is precisely when patients have to undergo MRI especially for temporo mandibular problems that the radiologist and orthodontist are faced with the question of whether or not to remove orthodontic appliances [Beau et al., 2015].

2.6. Safety and compatibility of dental alloys.

Before performing a MRI, the clinician has to considerate the safety of the patient undergoing the exam and the compatibility of the dental alloys used [Blankenstein et al., 2015].

Each of the three types of magnetic field (static, gradient and radiofrequency), to which the patient is exposed during the examination, carries a potential risk to his safety. As regards the static magnetic field (B0), the main safety problem consists in the attraction of ferromagnetic material towards the magnet. Ferromagnetic materials external to the patient (such as keys or coins) can become bullets inside the scanning room; the patient, the staff and the machinery run the risk of being hit. Static magnetic fields can also exert mechanical forces on ferromagnetic components within implanted medical devices, such as pacemakers, aneurysmal clips and cardiac defibrillators. The devices

can rotate or detach, resulting in serious injury to the patient, sometimes resulting in death [Haacke et al., 2014].

High static magnetic fields exert greater forces on ferromagnetic materials [Blankenstein et al., 2015]. Access control to the magnet room is essential to minimize the associated risks.

As far as gradient fields are concerned, the main concerns are excessive noise and potential hearing damage. The rapid alterations of the currents inside the gradient coils, in the presence of a strong magnetic field, generate a significant force that acts on the coils and manifests itself with loud noises. For this reason, it is advisable for patients to wear ear protection devices [Morris, 2014].

The radiofrequency impulses can lead to heating of the local tissue through the dissipation of energy. Normally this effect is negligible in clinical imaging, as the temperature rise is <1 °C, but it is potentially serious in patients with implanted devices. A pacemaker cable, for example, can act as an antenna and concentrate radiofrequency energy, resulting in significant local heating, tissue damage and cardiac dysfunction. Currently, more and more compatible medical devices and magnetic resonance equipment are available on the market nowadays [Haacke et al., 2014].

The decisive parameter for all the compatibility modes of a material is magnetic susceptibility (χ) or a measure of the variation of the magnetic field within the material with respect to the external field [Blankenstein et al., 2015].

Unit χ is dimensionless and can vary from -1 to ∞. Based on its value, the materials are divided into three categories. Susceptibilities between -1 and 0 indicate that the material is diamagnetic, such as Cu, Au, Zi, C, Bi, Pb. Instead, small positive values indicate a paramagnetic property. This category includes materials such as Cr, Mn, Al, Ti ($\chi \approx 0.000182$) and Ti-V-Al alloys ($\chi \approx 0.000189$). These materials do not create any problems if exposed to magnetic resonance. At values $\chi > 0.01$, ferromagnetic properties emerge, as for Fe, Ni, Co. This physical threshold value, however, does not strictly correspond to what is experienced in practice, as non-magnetic alloys with values $\chi \leq 0$ can also be found [Currie et al., 2013].

The American Society for Testing and Materials (ASTM) define ferromagnetism as the property of a material which, when exposed to a strong magnetic field, is influenced by a force greater than the gravitational force acting on it [Shellock and Crues, 1988].

In addition to the safety problem related to the possible movement of the metal objects that are inside the Field of View (FOV) if subjected to considerable forces, there is also the problem of artifacts.

The image artifact is defined as distortion, modification of signal intensity or signal emptiness, which does not originate from the anatomical elements present in the scanned section; it is made up of pixels that do not faithfully represent the components of the studied fabric. The metal artifact is caused by the inhomogeneity of the B0 field due to the presence of metal components with magnetic susceptibility. The formation of artifacts depends on the properties of the material (shape, sample size, crystal structure) and on the characteristics of the RM system used (strength of the magnetic field, type of sequence, etc.). [Blankenstein et al., 2017]. The image in the graphics window shows a region with a homogeneous magnetic field in which an object with a high magnetic susceptibility has been placed [Parker, 2018].

The result is that the magnetic field lines curve within the object. As a result, the field will be more intense or weaker as the position around the object changes. This distortion affects the static magnetic field B0, the radiofrequency magnetic field B1 and the field gradients [Mitchell et al., 1999].

Given the increasing use of magnetic resonance imaging for diagnostics, with the consequent need to have clear images, free of artifacts, efforts have been made to classify materials based on their magnetic resonance compatibility.

In 1996, Schenck identified two compatibility categories for medical devices. The first-order magnetic resonance compatibility is typical of devices that do not cause significant effects on the surrounding tissue when exposed to magnetic forces. These objects do not produce mechanical or torque forces, but they can generate significant distortions and degradation of the image if placed close to the imaging region. The second-order magnetic resonance compatibility is typical of materials that do not generate forces and do not produce clinically relevant imaging artifacts. The first definition focuses on patient safety and was later associated with the expression “MRI safe”. The second definition, on the other hand, focuses on diagnostic quality, and it is assimilated to the expression “MRI compatible” [Schenck et al., 1996].

In 2005, the American Society for Testing and Materials (ASTM) modified these definitions. Since then, the term "RMI compatibility" has been formally abandoned. The new system defines three risk classes.

"MRI safe" means that a device does not present any risks whatsoever for patients, medical personnel, or other individuals present within the controlled area, while an MRI is being prepared or execution.

On the contrary, a device considered "MRI unsafe" can generate these risks.

A third class called "MRI conditional" indicates devices that require specific conditions to be safe (labeling that explicitly states these conditions is mandatory).

This new classification (Figure 5) stresses greater importance to patient safety, totally ignoring the diagnostic quality [Blankestein et al., 2015].

Figure 5 ASTM symbols on RM safety: the first square (green) corresponds to "MRI safe"; the triangle (yellow) corresponds to "MRI conditional"; the circle (red) corresponds to "MR unsafe".

2.7. Orthodontic appliances.

The orthodontic appliance is a prosthesis or medical device. The orthodontist use it to align the teeth, in order to obtain correct chewing, cleaner oral hygiene and a better smile aesthetic [Cerroni et al., 2018]. Orthodontic movement can be managed with mobile or fixed appliances.

Figure 6. Mobile orthodontic appliances. They can be removed during MRI [Staley and Reske, 2013].

Mobile appliances (Figure 6) are used for the correction of serious malocclusions and for dento-facial dysmorphias. They allow limited movements of the teeth, generated by screws, springs and arches, but allow a harmonious rebalancing of the lower third of the face from a functional and aesthetic point of view. They obtain not only an orthodontic effect but also an orthopedic remodeling, as they correct and guide the growth of the bone bases [Caplin et al., 2020].

Mobile devices are mainly used in interceptive orthodontics to modify incorrect habits and incorrect behaviors (for example the sucking of the finger) during the developmental age [Mostafiz, 2019].

Functional and orthopedic mobile appliances positively affect the growth and development of the arches and jaws, acting on both the bone and the muscle component, something that the fixed appliance cannot do. They have a generally lower cost than fixed appliances, are prepared directly in the laboratory, and, unlike fixed ones, do not require special equipment to be regulated, requiring instead a deeper knowledge of the stomatognathic apparatus. A great advantage is that they do not create difficulties in oral hygiene, since they must be removed when eating [Ritcher et al., 2011].

For some years, now other transparent mobile devices have been used called aligners or more generically bites. They are manufactured for any type of dental arch and being

transparent, they do not significantly alter the aesthetics of the smile during treatment. These are light, temporary bites, changed on average every 2-4 weeks during the treatment. They are studied on the computer through a software program, which, based on a scan of the casts of the patient's arches, produces 8-16 different progressive bites, to be applied over 1-2 years. This system progressively allow the teeth to find the right position. With these types of appliances, functional cases can also be treated through root movements. However, their precision in the teeth positioning is still not equal to the precision of fixed appliances [Sfondrini et al., 2018].

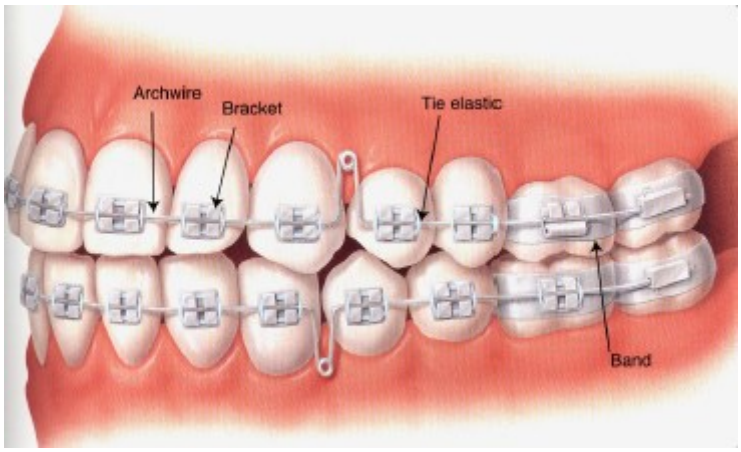

Figure 7. Fixed orthodontic appliances. They cannot be removed during MRI [Staley and Reske, 2013].

Fixed orthodontic appliances (Figure 7) are used to treat misalignments, as they are able to move the teeth in the direction desired by orthodontics. They are often used in the last phase or finishing [Fleming et al., 2015]. However, they complicate oral hygiene because they are made of various metallic wires, elastic bands, brackets, tubes or bands on the molars, which increase the difficulty in correctly removing the bacterial plaque from the teeth and make the use of the wire problematic flossing. It is often recommended to use other tools such as the water jet, thanks to which, by spraying thin jets of water between the teeth, it is possible to remove most of the food residues. It is also sometimes recommended to use the mouthwash after the brush, because, in addition to improving the breath, protection from caries is increased [Reichardt et al., 2019].

The fixed appliance is made up of plates (also called plates, tiles, attachments or brackets) that hold the orthodontic wire (or arch), metal, the main means in straightening the teeth [Pasha et al., 2015]. Depending on the technique, which usually takes the name of the author, the brackets have different angles that characterize the slot (seat where the orthodontic arch is located). Different techniques correspond to small corner differences in dental alignments [Banks et al., 2010]. Today, for aesthetic reasons, there are ceramic or composite brackets that come close to the natural color of the teeth. Additionally there are brackets that are applied on the internal surface of the teeth, resulting almost invisible from the outside. On molars, normally the brackets are not applied directly on the tooth enamel, but on metal rings called bands that embrace the dental crown. In some cases, the orthodontic effect cannot be obtained only with the use of the orthodontic arch, but the application of elastic bands is necessary to obtain the displacement of the dental elements. Another component of the appliance are the hooks, located near the plates of the canines, premolars and molars, on which the elastics are hooked. The wire is held in place in the brackets by metal or elastic ligatures, which allow it to more or less slide according to the orthodontic technique used. Finally, there is a type of bracket, called self-ligating or with low friction, in which no ligatures are used since it is designed to fit the arch and keep it in place with a flap [Papageorgiou et al., 2016].

Concerning MRI exposure, obviously mobile appliance can be removed before the exam. On the other hand, fixed appliances has to be left in the mouth, thus leading their interaction with magnetic field [Görgülü et al., 2014].

2.8. Interactions between fixed orthodontic appliances and magnetic fields.

When orthodontic patients have to undergo MRI, the orthodontist and radiologist are faced with a doubt: remove or not remove the equipment. In fact, it in addition to potentially damaging the enamel, debonding procedures take a long time, interrupt orthodontic treatment, elongate the treatment time, are annoying for the patient, and expensive [Wylezinska et al., 2015].

Among the scholars who have been interested in the problem, Shellock and Crues first detected the presence of a ferromagnetism measurable only in the orthodontic wire (chromium alloy), so in their opinion it was enough to anchor the wire in several points

to elements that were not ferromagnetic to avoid displacement or detachment [Shellock and Crues, 1988].

Other Authors evaluated MRI scans of patients with TMJ dysfunction under fixed orthodontic treatment [Sadowsky et al., 1988]. They found that the devices produce significant artifacts, particularly in the areas closest to them. Artifacts were not considered serious enough to alter the diagnostic quality brain and ATM scans, because they were concentrated in the region of the mouth and face. Therefore, they recommend disengaging arches, removable palatal bars, lingual arches and mobile devices. On the other hand, they suggest maintaining bands and brackets, checking their adhesion and ensuring them through passive ligatures.

More recently, other authors [Okano et al., 2003 Klocke et al., 2005; Klocke et al., 2006; Hatch et al., 2014] confirmed these considerations. Some guidelines were proposed [Patel et al., 2006]:

• Always leave the bracket in place if the area of investigation is not the oral cavity

• Remove steel arches, palatal bars and removable lingual arches.

• Verify that all bonded bands and brackets are secure

• For greater safety, strengthen the binding of the brackets with an elastic chain or non-ferromagnetic metal ligatures.

A recent article has drawn up exhaustive, but not absolute, rules of clinical behavior when dealing with various materials (Figure 8) used in orthodontics [Poorsattar-Bejeh Mir et al., 2016].

Suggested guideline for various materials frequently used in orthodontics.

Product	Comment
SS bracket [a,b]	Should be removed in head and neck MRI
Ceramic bracket[b]	MRI-safe
Ceramic bracket with SS slot	Should be removed in oral cavity MRI
Titanium bracket[b]	Better to be removed in oral cavity MRI
Plastic bracket	MRI-safe
SS wire	Should be removed in head and neck MRI
Ni-Ti wire[c]	Relatively MRI- compatible
Composite wire	Probably MRI-safe[d]
Palatal/lingual arch	Should be removed in head and neck MRI
Fixed bonded retainer	Should be removed in oral cavity MRI
Ligature wire	Better to be removed in oral cavity MRI
Miniscrew and Miniplates	Should be removed in oral cavity MRI[d,e]

[a] SS: stainless steel.
[b] Self-ligating brackets maybe made of either stainless steel, nickel titanium, nickel-free SS or ceramic, hence decision should be made based on bracket composition and anatomic location of interest and clip and slot material.
[c] Ni-Ti: nickel-titanium.
[d] Needs further investigation.
[e] Miniplates and miniscrews near to TMJ, maxillary sinus and palatal implants may be decided individually.

Figure 8. Recommended guidelines for different orthodontic materials [Poorsattar-Bejeh Mir et al., 2016].

These Authors, recommend removing brackets and steel wires when scanning the head and neck region. They stress the importance of being more scrupulous in the use of self-ligating brackets, which are equated, as magnetic behavior, to ceramic brackets. Brackets can be manufactured in Stainless Steel, Nickel Titanium, Nickel-free Stainless Steel or ceramic. Even a single bracket can have different types of SS for the mesh, the base and the fins, assembled with silver-based brazing alloys. Therefore, the decision to

remove has to be made basing on the composition of the bracket, the anatomical site of interest and the material of the clip and slot. Authors agree with other studies in considering the “MRI safe” ceramic and plastic brackets. They recommends instead the removal of ceramic brackets with Stainless Steel metal slot, when the site of investigation is the oral cavity. They consider “relatively MR-compatible” the Nickel Titanium wires, aesthetic wires. They it recommend the removal of fixed splinting and binding threads. For miniscrews and miniplates near the TMJ, maxillary sinus, and palatal implants, it is necessary to decide on a case-by-case basis [Poorsattar-Bejeh Mir et al., 2016].

2.9. Magnetic behavior of orthodontic alloys.

Even today, the knowledge of the magnetic properties of the metal alloys used for orthodontic devices is rather lacking. So far, the behavior of more than 1000 metal biomedical devices has been tested and information has been collected on the “MRIsafety.com” web page, recently created and periodically updated [Thompson et al., 2020].

Unfortunately, manufacturers of orthodontic devices are not obliged to declare the magnetic properties of their products or any other useful parameter for this purpose. Neither is the detailed composition of brackets, bands and orthodontic wires known, nor the weights of the various components of the alloy, but even if the composition was known, it would not be possible to deduce the magnetic properties of an alloy starting from behavior of the individual elements [Blankestein et al., 2015]. For example, steel alloys or highly ferromagnetic substances such as Fe, Co, Ni, are almost non-magnetic in alloy. Stainless steels are a group of alloys based on iron (Fe) that contain 10-30% chromium (Cr) and from 0.03% to about 1.2% carbon (C): other elements, such as Ni, Md, Ti and Al, are commonly added to obtain the desired characteristics [Schenck et al., 1996].

Different types of steel can be used for the various elements, both for the brackets and for other components of the appliances, in order to obtain optimal mechanical properties. Great rigidity is required for the brackets, while a certain malleability is expected for the bands, in order to be able to adapt them to the dental surface [Wang et al., 2015].

Three basic crystalline structures of stainless steel can be distinguished: ferrite, austenite and martensite [Tian et al., 2017].

Ferrites do not contain nickel or contain it in minimal quantities. These types of steel can be magnetized. In fact they can be magnetized, even those with a low ferrite content (for example, duplex stainless steel),

Austenites contain at least 8% nickel to optimize structural stability. They cannot be magnetized. Thanks to their flexibility, they are suitable for orthodontic purposes. In the 1990s, nickel-free austenitic steels such as Menzanium were used for the production of orthodontic wires. This material contains more nitrogen and manganese than nickel, but it is ultimately more prone to corrosion.

Martensites are formed by specific cooling processes or by cold hardening of the austenites, which makes martensitic materials particularly suitable for devices such as cutting tools. Martensitic structures have magnetic properties.

The main magnetic susceptibility characteristics of the three main alloys most commonly used in orthodontics has been summarized as follows: Titanium alloys with nickel, Cobalt-chromium-nickel-iron-molybdenum alloys, various types of stainless steel [Blankenstein et al., 2015]. Titanium alloys with nickel (for example, Nitinol, Titanol, Rematitan) or molybdenum (for example, TMA, Rematitan Special) usually have a susceptibility of less than 0.0002. Since they cannot be magnetized, they are not subject to acceleration even at 3 Tesla and generate only minimal artifacts. They can be left in situ, without creating risks.

Cobalt-chromium-nickel-iron-molybdenum alloys (for example, Remaloy, Elgiloy / Phynox, Forestalloy) are used only in wires and have a very low magnetic susceptibility. Their artifacts are about two times larger than those seen with titanium alloys. For spin-echo sequences, which have a low tendency to form artifacts, they can be left in situ.

The various types of stainless steel include a wide range of available alloys and products, which differ significantly in their magnetic behavior. Therefore, it is not possible to make clear recommendations as the other abovementioned materials. The magnetic susceptibility of a steel product depends on its crystalline structure and the formation process [Phukaoluan et al., 2016].

2.10. Interaction between metal orthodontic devices and MRI.

The interaction between MRI and orthodontic metal devices can cause different phenomena. The most relevant effects are three: generation of artifacts, which can make it difficult to read the images, overheating, that could lead to tissue heat lesions, and detachment or movement of the device from its location [Patel et al., 2006].

2.11. Artifact production.

The artifact, as previously explained, is caused by the inhomogeneity of the B0 field, which occurs in the presence of metal components: in fact, by presenting a different magnetic susceptibility to the surrounding tissues, they cause a variation of the Larmor frequency in the same [Shalish et al., 2015]. This determines the loss of phase coherence of the transverse magnetization with consequent reduction or vacuum of the signal, and the distortion of the image itself due to alteration of the position-based decoding mechanisms based on frequency. The production of artifacts alters the images, affecting their quality, making it more difficult to formulate a correct diagnosis [Zhylich et al., 2017; Chockattu et al., 2018].

Authors [Zachriat et al., 2015] found that there is a significant distortion of MRI images in patients wearing steel brackets; however, the decision whether to remove or maintain the brackets should be made on a case-by-case basis, considering the anatomical region of investigation and the type of bracket. [Wang et al., 2018].

Ceramic brackets produce less image noise [Harris et al., 2006], but are more prone to wing fracture, enamel fracture when debonding, greater friction during dental movements [Okano et al., 2003.]

A study proposed a general rule of common sense: the greater the distance between the brackets and the place of interest, the less the signal gap, the image artifacts and the distortion [Elison et al., 2008].

Other Authors established a decision criterion for device removal. They proposed to consider the distance between the device and the survey region in centimeters as discriminating. They suggest a maximum artifact radius of 7.4 cm for the steel brackets [Zachriat et al., 2015].

Authors concluded that orthodontic appliances, including metallic materials, sometimes produce significant measurement error in speech evaluation using MRI movies, which

often become invisible or distorted by metallic orthodontic appliances. When the distorted image is measured, caution should be exercised, as the measurement may be affected [Blankenstein et al., 2017]. Therefore, orthodontists should not necessarily remove all metallic appliances before MRI examination because the influence varies among the appliances [Ozawa et al., 2018; Miao et al., 2020].

2.12. Overheating.

During MRI, an increase in temperature can occur in orthodontic metal devices and in the surrounding tissues [Sawyer-Glover and Shellock, 2000]. The intensity of the effect depends on the type of metal, on the shape and orientation of the object, on the magnetic field and on the pulse sequence [Hasegawa et al., 2013]. The studies in the literature express different results, however most authors concluded that orthodontic devices are thermally safe [Görgülü et al., 2014]. Some Authors detected a temperature rise of less than 1 ° C, in the range of temperature variations induced by food [Yassi et al., 2007]. Another study demonstrated an increase in temperature of 3.20 °C, thus affirming the safety of orthodontic appliances and the non-dangerousness for vital tissues [Görgülü et al., 2014]. Other Authors postulated that such overheating could induce harmful effects in the adjacent tissues of the oral cavity [Mortazavi et al., 2016].
Other research pointed out that the tendency to overheat is more intense for objects with an elongated shape and larger dimensions than orthodontic appliances. A maximum temperature increase of 0.2 °C was reported during 3 T MRI, therefore negligible and not risky [Regier et al., 2009]. Other scientists, on the other hand, pointed out that the measured overheating, equal to 2.61 °C, is higher than the CENELECprEN45502-1 standard, which establishes a limit of 2.0 °C to avoid tissue damage in the patient; therefore they suggests placing a separator between the appliance and the mucosa or removing the wire from the brackets [Hasegawa et al., 2013].

2.13. Detachment and displacement.

Recently, some research has been carried out several studies to quantify the magnetic attraction forces that act on orthodontic devices in the MRI environment. The results are different.

Authors showed that brackets can be left in place at 3 T field strength, while it would be good to remove the arches in both NiTi and stainless steel for the greater attraction forces experienced [Görgülü et al., 2014]. On the other hand, Kemper et al. noticed, at the same field strength, a high magnetic attraction in the presence of stainless steel brackets, and no attraction for NiTi brackets [Kemper et al., 2007]. Another study detected significant attractive forces for steel bows, minor for CoCr bindings, none for NiTi and TMA bows [Klocke et al., 2005]. However, the authors agree that if there is an adequate adhesion between the bracket and the dental surface, usually the attractive and rotational forces of the field do not exert a significant influence.

2.14. Bracket adhesion to enamel

Bonding of orthodontic brackets to teeth is important to enable effective and efficient treatment with fixed appliances. The problem is bracket failure during treatment, which increases operator chairside time and lengthens treatment time. A prolonged treatment is likely to increase the oral health risks of orthodontic treatment with fixed appliances one of which is irreversible enamel decalcification. [Corradi-Dias et al., 2019].

It is useful for a clinician to know the best adhesive for fixing orthodontic brackets, so they do not fail during treatment. Bracket failure increases the time spent in surgery for repairs and the overall treatment time [Bakhadher et al., 2015]. At present orthodontics can choose between four groups of adhesives which may be set with a chemical reaction or curing light. Some adhesives may prevent early decay around brackets because they contain fluoride [Altmann et al., 2016].

Ideally the adhesive should be: strong enough to keep the brackets bonded to the teeth for the length of the treatment; not so strong that the tooth surface is damaged when the appliance is removed; easy to use clinically; protective against dental caries (decay); available at a reasonable cost. Adhesives currently available for bonding brackets to teeth are those with a resin/matrix composition, similar to conventional filling materials (composites) and those supplied as a powder with liquid, or powder with water (glass ionomer cements) [Mandall et al., 2018]. Bonding procedure is relatively easy and fast after a relatively short clinical learning curve [Vicente et al., 2006].

Light-curing adhesives used in orthodontic bonding are dimethacrylate based adhesive resins that contain monomers such as bis-GMA (bisphenol-A diglycidyl ether

dimethacrylate) and TEGDMA (triethylene glycol dimethacrylate). Tooth enamel is etched with orthophosphoric acid gel. After 30 seconds, the gel is rinsed. Tooth is washed and a liquid adhesive is applied on the enamel. The liquid adhesive contains methacrylate monomers and a solvent (ethanol). The liquid adhesive fills the porosities on the enamel surface created by the acid etching, and excess solvent is evaporated by air-drying. However, a thin airflow is gently applied in order to secure the evaporation process [Foersch et al., 2016]. Subsequently, a resin paste is applied on the base of the bracket, and the appliance is placed on the enamel surface. The structure and length of the resin tag formation varies, but generally it reaches depths of 5-50 μm, [Fjeld and Øgaard 2006]. However, the bond strength does not increase in proportion to the tag length [Shinchi et. al. 2000]. Finally, the adhesive and the resin are cured by a free radical polymerization reaction. This process is initiated by photons delivered from a light source that emits blue light. The dental curing lights use LEDs that produce a narrow spectrum of blue light in the 400–500 nm range (with a peak wavelength of about 460 nm), which is the useful energy range for activating the camphorquinone molecule most commonly used to initiate the photo-polymerization of dental monomers [Assaf et al., 2020].

The movement of teeth depends on the wires and springs attached to the brackets. Therefore, it is of utmost importance that these brackets remain attached to the teeth during the course of orthodontic treatment. However, brackets detachment from the teeth is one of the major concerns during orthodontic treatment with fixed appliances [Almosa and Zafar, 2018]. The bracket bonding procedure plays a major role in achieving an optimal outcome during orthodontic corrective procedures, as the required tooth movement relies upon it [Romano et al., 2012]. Bracket detachment during corrective procedures may also lead to increased treatment duration, damage to tooth enamel, and increased chairside-time due to re-bonding procedure [Roelofs et al., 2017]. Consequently, it could also raise the costs of the overall orthodontic treatment [Bishara et al., 2002].

Bracket detachment is a major concern during orthodontic treatment with fixed appliances, as it can be irritating and in some instances critical in the overall success of the treatment [Banks et al., 2010]. Presently, there is a tendency towards bonding brackets on all the teeth for providing full arch orthodontic treatment, thus making

bracket detachment more critical [Wenger et al., 2007]. Previous Authors have reported varying incidence of bracket failure following orthodontic brackets bonding [Attishia et al., 2015]. A high incidence of brackets detachment during orthodontic treatment (up to 29.3%) has been reported [Bovali et al., 2014].

2.15. Shear bond strength test in orthodontics.

Modern adhesive interfaces influence greatly clinical success of modern dentistry. Durability of the interface can be determined by using several in vitro testing methods. Shear bond strength tests are widely used in dentistry and they are well suitable for testing orthodontic materials bonded to teeth. The first study that analyzed shear bond strength of orthodontic appliances appeared in international literature in the late 1970s [Carlyle, 1978]. Nowadays, more than one thousand reports have been conducted in order to analyze various factors influencing shear bond strength of orthodontic brackets. Precise interpretation of the results of shear bond strength test should take into account other types of stress, which are occurring at the interface during testing.

Previous studies that evaluated bond strength analyzed different variables related to adhesive system (composite or resin-modified glass ionomer) [Shinya et al., 2008], bonding surface (enamel, ceramic, or metal) [Ozcan et al., 2004], antibacterial agents (added to adhesive system) [Garcia-Contreras et al., 2015], bracket material (steel, ceramic, or plastic) [Da Rocha et al., 2014], bracket type (conventional, self-ligating, or lingual) [Cetik et al., 2019], attachment base (with various mesh sizes and shapes), brace mesh [Scribante et al., 2013 A] or surface pretreatment (such as sandblasting) [Yassaei et al., 2015], bracket placement force [Montasser, 2011], enamel conditioning (with etchants or lasers) [Contreras-Bulnes et al., 2013], enamel pretreatment (with protecting agents) [Montasser and Taha, 2014] or bleaching [Scougall-Vilchis et al.,. 2011], and enamel contaminants (such as blood or saliva) [Sfondrini et al., 2013]. The effect of any of these factors may differ when rebonding orthodontic brackets [Koide et al., 2020]. Moreover, bonding studies have been applied to test not only orthodontic brackets but also other materials bonded to tooth structure during active or passive orthodontic treatment (such as customized CAD CAM bases, disinclusion buttons, and fiber reinforced composites bars and nets) [Scribante et al., 2006; Sha et al., 2018].

During over 35 years of orthodontic bonding research, a standardized technique has been reached [Fox, 1994] but many differences in methods among different studies remain [Van Meerbeek et al., 2010]. Due to increased ethical requirements, human teeth used are usually wisdom teeth or first premolars (extracted for orthodontic reasons). Bovine teeth are collected in slaughterhouses in deciduous or permanent dentition. Tooth selection include intact buccal enamel and no cracks due to extraction procedure. After extraction, teeth are stored in thymol, water or artificial saliva, whereas formalin and alcohol are no more used in order to avoid adverse effects on bond strength measurement [Rüttermann et al., 2013].

Brackets or jigs are bonded to teeth with an adhesive system and subsequently, or after artificial ageing specimens are placed in a testing machine with the adhesion surface parallel to shearing force [Klocke and Kahl-Nieke, 2006].

Predominantly a shear force is applied with a steel tip with standardized crosshead speed until adhesive failure (Figure 9).

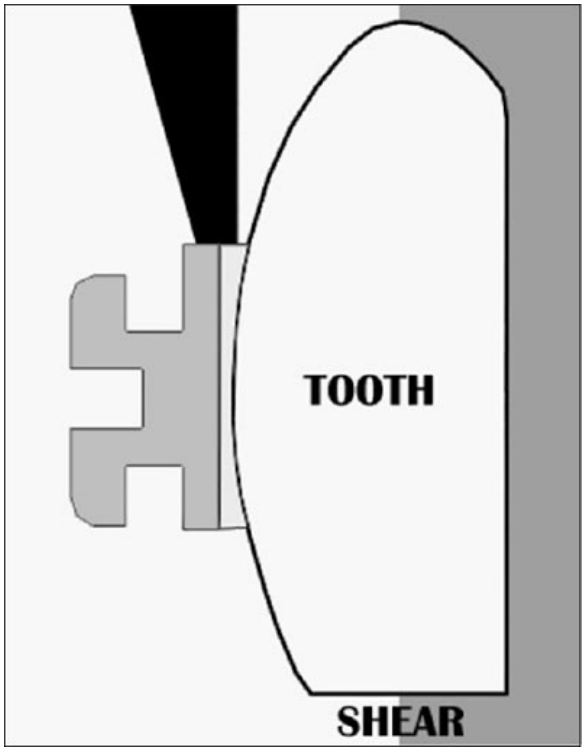

Figure 9. Diagram showing the shear debonding force applied by the Instron blades from gingival to occlusal direction at debonding [Linjawi et al., 2016].

Debonding force is recorded in newtons and then often converted into megapascals, which is the unit of stress at the interface [Oztürk et al., 2008]. Special attention needs to be paid to ensure the geometry of the bonding site of the bracket allows calculation of stress. In the case of complex form of the bonding site, it is correct to report the bonding properties as debonding load [Gaur et al., 2016]. Moreover enamel and appliance surfaces are analyzed under optic magnification and an Adhesive Remnant Index (ARI) is assigned to give information of the location of the adhesive failure [Hioki et al., 2007]. ARI score is calculated evaluating the amount of adhesive left on tooth and appliance surfaces after debonding. ARI scale usually ranges from 0 to 3 (0: no resin remaining on tooth; 1: less than 50% resin remaining on tooth; 2: more than 50% resin remaining on tooth; 3: 100% resin remaining on tooth) [Artun and Bergland, 1984].

As it is a standard procedure in biomedical research, statistical analysis are performed with high enough number of test specimens (i.e. teeth). Descriptive statistics (mean, standard deviation, minimum, median, and maximum values) are calculated for the groups which are compared. The normality of the data can be calculated (for example, using the Kolmogorov-Smirnov test). Parametric (for example, ANOVA) or not parametric (for example, Kruskal Wallis) tests are then applied and parametric (for example, Tukey) or not parametric (for example, Mann Whitney) post hoc tests are used to show differences among various groups. On the other hand, for ARI scores a Chi Squared test is often applied. Significance for all statistical tests is usually predetermined at $P < 0.05$.

In the literature there are not clear guidelines about shear force limits, but in fact a good orthodontic biomaterial should allow good adhesion in order to sustain masticatory forces (with a minimum bond strength of 5-10 MPa) [Reynolds, 1975]. On the other hand, adhesion forces should not be too strong in order to avoid enamel loss after debonding (40-50 MPa) [Gittner et al., 2012]. Therefore, the ideal orthodontic biomaterial should have bonding forces included in the interval of 5-50 MPa, even if these limits are mostly theoretical.

When considering ARI index, even if methods of measurement could influence score assignment results [Montasser and Drummond, 2009], ARI score is nowadays widely used in bonding studies to assess and discuss adhesive left on tooth surface after debonding. Generally, a score of “0” is often related to lower shear bond strength

values, and is often related to contaminants over enamel that can reduce bond strength. On the other hand, an ARI score of "3" means less risk of enamel fracture after bracket debonding but polishing procedures are longer as more adhesive is remaining on tooth surface [Ekizer et al., 2012]. Therefore, an orthodontic biomaterial should aspire to a mixed adhesion modality (ARI "1" and "2").

In conclusion, bonding studies represent one of the first steps of materials testing, and should be followed by in vivo clinical studies in order to confirm the in vitro results. Therefore, although some criticisms that have been stated against bonding studies in orthodontics, bonding tests are still a valid instrument to test new brackets, adhesives, jigs, pad and other biomaterials bonded to tooth surface.

2.16. Rationale of the study.

Magnetic resonance imaging (MRI) is a non-invasive radiologic diagnostic technique that is widely used to assess lesions, particularly those involving soft tissues [Oshagh et al., 2010]. As this procedure does not involve the use of ionizing radiations, its applicability is wide and common, both for young and aged patient [Poorsattar-Bejeh Mir et al., 2016].

Under MRI, items are magnetized according to their magnetic susceptibility and metallic devices results in a signal void that is visible in the radiographic image as a black spot [Shafiei et al., 2003]. Additionally magnetic field lures metal objects that patients could accidentally wear during examination, resulting in patient injury and damage of radiographic device [Shellock, 2002]. For this reason, the first request of the radiologist to a patient before MRI is to remove metal objects even if they are far from the anatomical region that has to be examined [Hasanin et al., 2015].

The need for a MRI of patients wearing orthodontic appliances is not uncommon. During conventional orthodontic treatment, usually stainless steel brackets are bonded to the teeth and metallic wires are engaged [Wang et al., 2015]. In these cases, the removal of orthodontic appliance is recommended in order to avoid image artifacts, unwanted bracket detachment and temperature rise of brackets and wires [Costa et al., 2009; Blankenstein et al., 2017]. However, to date no clear guidelines are available. In fact, the removal of orthodontic appliance, even if for few days or hours, is time consuming, costly and uncomfortable for both the patient and the clinician [Degrazia et

al., 2018]. Moreover, this procedure could damage enamel structure or lengthen treatment time [Yassaei et al., 2014].

Low metal or metal free orthodontic therapies represent a viable alternative [Maekawa et al., 2015; Scribante et al., 2018]. In fact, ceramic, fiber, composite and other metal free brackets are currently available on the market [Matias et al., 2018]. However, these materials are more breakable than metallic ones [Sanchez et al., 2008]. Moreover, these devices work with metallic wires and tubes, so the main problem remains partially unsolved. On the other hand, transparent removable devices (aligners) shows excellent clinical results [Ke et al., 2019], but the lack of an active appliance permanently bonded to the teeth could lead, in some cases, to lower precision in certain movements [Sfondrini et al., 2018]. For these reasons, nowadays the stainless steel orthodontic appliance still represents the golden standard in the majority of orthodontic treatments [Yassir et al., 2019].

Therefore, the purpose of the present investigation was to evaluate the effect of MRI at two different powers (1.5T and 3T) on temperature of brackets and wires and on bond strength and adhesive remnant index scores of orthodontic appliances.

The first null hypothesis of the study was that there is no significant difference in temperature of brackets and wires among various conditions tested.

The second null hypothesis of the investigation was that there is no significant difference in the values of shear bond strength among different groups.

The third null hypothesis was that there is no significant change in frequency distribution of adhesive remnant index scores.

3. Materials and Methods.

3. Materials and Methods.

3.1. Specimen preparation.

The Unit Internal Committee Board approved the study. Permanent bovine mandibular incisors were used to carry out the experimentation (Figure 10) [Sfondrini et al., 2012], collected at the Inalca slaughterhouse in Ospedaletto Lodigiano (Italy).

Teeth were cleaned from soft tissues. Elements were stored in a 0.1% thymol solution (weight / volume) for the entire duration of the experimentation, with the aim of maintaining disinfection and hydration [Santana et al., 2008].

Intact teeth in the vestibular enamel were chosen, free of carious lesions and fractures resulting from extraction maneuvers such as to affect the quality of the vestibular coronal surface used for bonding [Aydin et al., 2015].

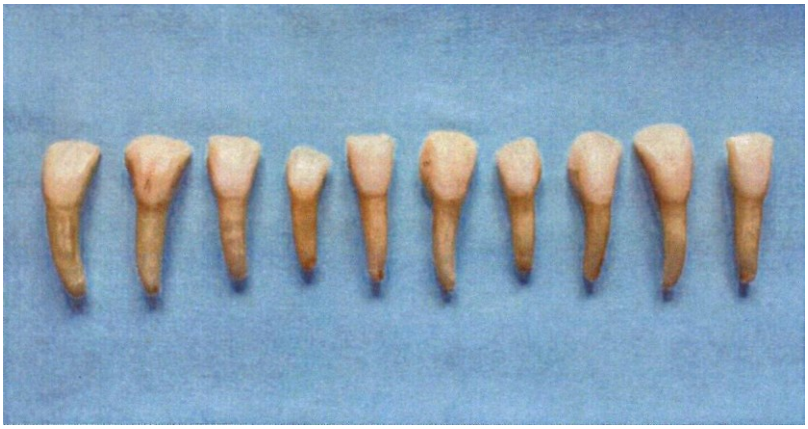

Figure 10. Bovine teeth (lower incisors).

With a scalpel, the residual root soft tissues were manually removed, instead the enamel was cleaned from the bacterial biofilm and prepared using Sof-LexTM Pop-on 2382C abrasive discs (3M ESPE, St. Paul MN, USA) mounted on a low-powered handpiece without water spray [Oduncuoğlu et al., 2020].

Subsequently 220 teeth were selected, randomly divided into 11 groups of 20 elements each.

Groups were labeled as follows:

-Group 1 - No MRI - No Wire

-Group 2 - 1.5T MRI - No wire

-Group 3 - 1.5T MRI - 0.014 inch stainless steel wire

-Group 4 - 1.5T MRI - 0.019x0.025 inch stainless steel wire

-Group 5 - 1.5T MRI - 0.014 inch nickel titanium wire

-Group 6 - 1.5T MRI - 0.019x0.025 inch nickel titanium wire

-Group 7 - 3T MRI - No wire

-Group 8 - 3T MRI - 0.014 inch stainless steel wire

-Group 9 - 3T MRI - 0.019x0.025 inch stainless steel wire

-Group 10 - 3T MRI - 0.014 inch nickel titanium wire

-Group 11 - 3T MRI - 0.019x0.025 inch nickel titanium wire

Materials (orthodontic wires, orthodontic brackets and adhesive system) tested in the present investigations are listed in Table 1.

Material	**Commercial name**	**Manufacturer**	**Composition**
0.014" Orthodontic Stainless Steel Wire	Stainless steel wire - 0.014"	Ormco, Glendora, CA, USA	17-20% chromium, 8-12% nickel, 0.08-0.15% carbon, and iron forming the balance
0.019x0.025" Orthodontic Stainless Steel Wire	Stainless steel wire - 0.019"x0.025"	Ormco, Glendora, CA, USA	17-20% chromium, 8-12% nickel, 0.08-0.15% carbon, and iron forming the balance
0.014" Orthodontic Nickel Titanium Wire	Nickel Titanium wire - 0.014"	Ormco, Glendora, CA, USA	55% Nickel and 45% Titanium
0.019x0.025" Orthodontic Nickel Titanium Wire	Nickel Titanium wire - 0.019"x0.025"	Ormco, Glendora, CA, USA	55% Nickel and 45% Titanium
Orthodontic bracket	Victory MBT	3M Unitek Monrovia, CA, USA	18–20 per cent chromium, 8–12% nickel, 0.08-0.15% carbon, and iron forming the balance
Orthodontic adhesive	Transbond XT primer	3M Unitek Monrovia, CA, USA	TEGDMA, Bis-GMA, and camphorquinone
Orthodontic paste	Transbond XT resin	3M Unitek Monrovia, CA, USA	Bis-GMA, silane, n-dimethylbenzocaine, phosphorus hexafluoride, 77% by weight of inorganic filler (silica)

Table 1. Materials tested in the present report.

For each group two blocks containing 10 teeth each were prepared [Görgülü et al., 2014]. Incisors were reduced on mesial and distal sides in order to allow an inter bracket distance of 5 mm. Vestibular enamel surface was kept parallel to the vestibular face of the resin blocks, in order to allow correct bracket placement [Scribante et al., 2013 B].
Due to the larger size of the bovine teeth compared to the human ones, in order to maintain a constant inter-bracket distance of 6 mm, the crowns of the elements were sectioned with of model trimmer machine, to coincide indicatively with the mesial-distal length with the enamel-cement junction (Figure 11).

Figure 11. Reduction of the mesial-distal dimension of the crowns.

Subsequently, 10 brackets were stabilized by elastic binding and positioned with the aid of a gauge at a distance of 6 mm from each other. Brackets were inserted on each orthodontic wire, keeping as reference the upper corner of the base (Figure 12).

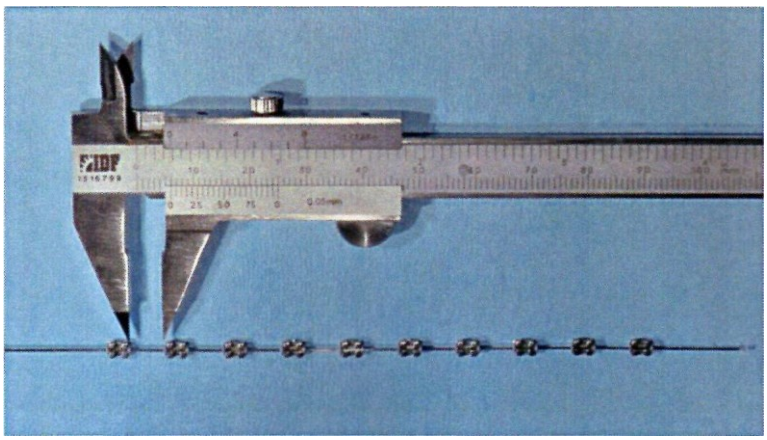

Figure 12. Inter bracket distance measurement (6mm)

Bonding procedure (Figures 13-18) involved the conditioning of enamel surface with orthophosphoric acid gel (Gerhò Etchant Gel, Gerhò Spa, Settequerce, Italy) for 30 seconds followed by washing and drying with an oil free air steam. Then, adhesive (Transbond XT primer, 3M Unitek Monrovia, CA, USA) was applied on enamel and gently dried for 3 seconds. Resin (Transbond XT resin, 3M Unitek Monrovia, CA, USA) was applied on bracket base and then bracket was squeezed on enamel [Sfondrini et al., 2006]. Excess resin was removed with a probe and adhesive was cured with a curing light (Starlight Pro, Mectron Medical Technology, Loreto, Italy) for 20 seconds (10 seconds for occlusal side and 10 seconds for gingival side) [Mollabashi et al., 2019].

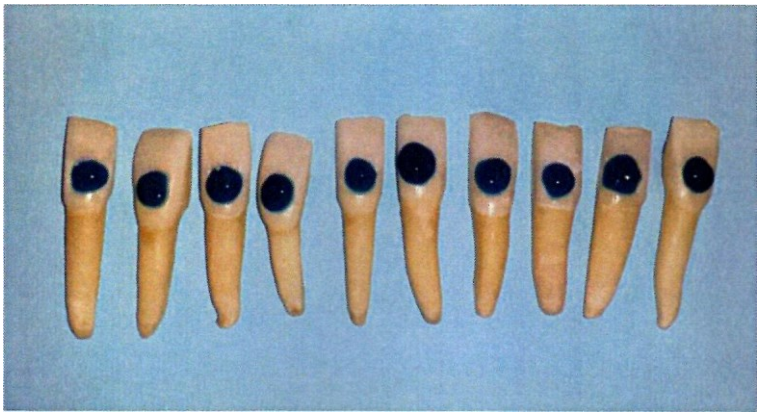

Figure 13. Orthophosphoric acid application.

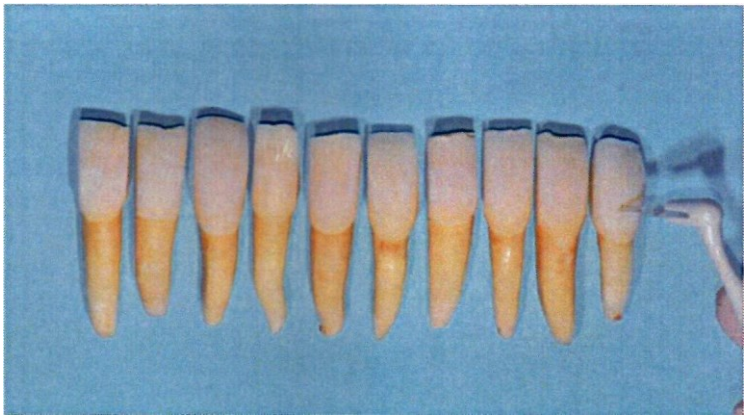

Figure 14. Primer application.

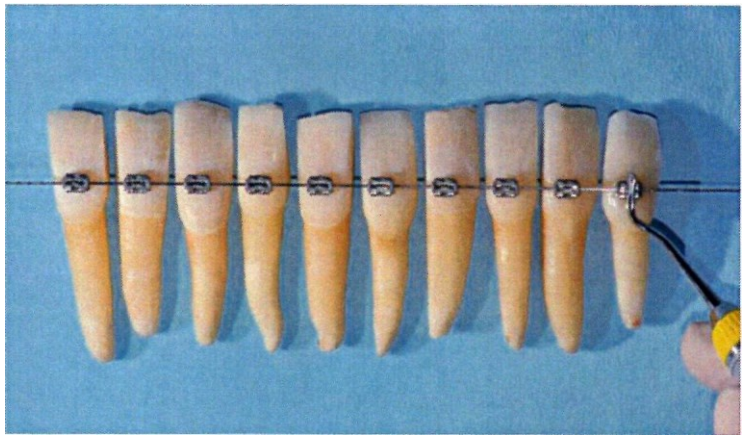

Figure 15. Bracket adhesion to enamel.

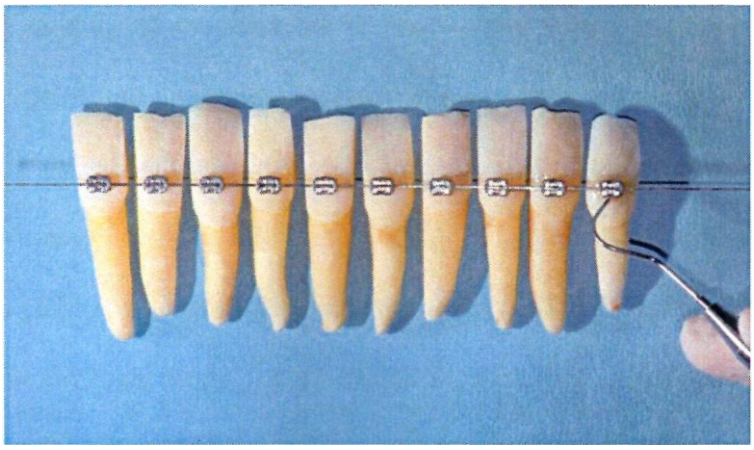

Figure 16. Composite resin excess removal.

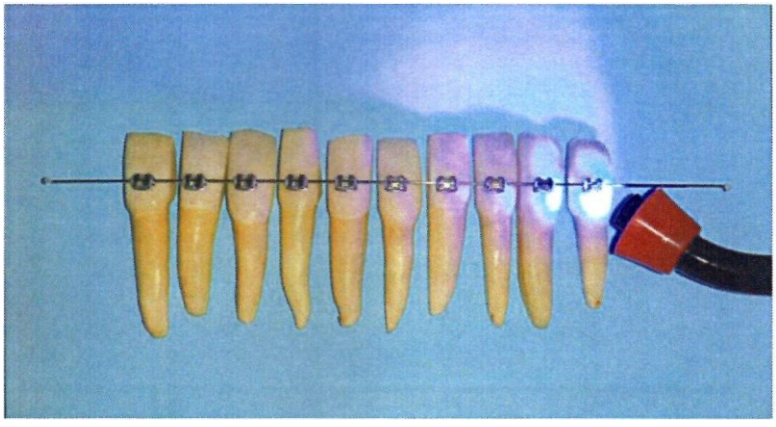

Figure 17. Cervical photopolymerization procedure.

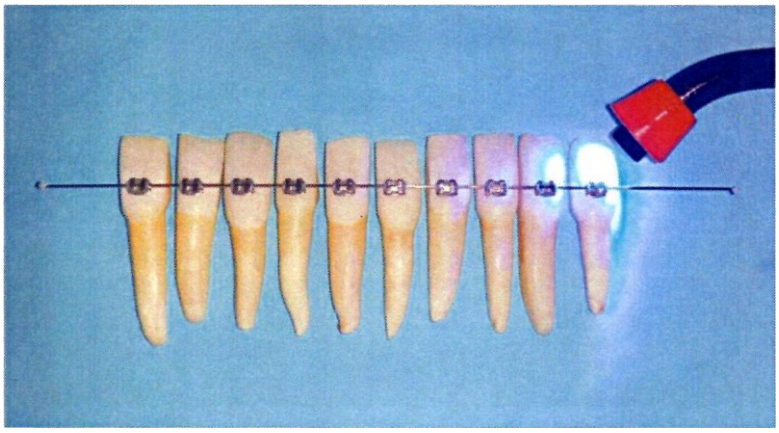

Figure 18. Incisal photopolymerization procedure.

Subsequently, where necessary, the tooth roots were reduced in length with model trimmer, to regularize the height of the elements before proceeding to incorporate the teeth in resin (Figure 19). After checking the correct inter-bracket distance (Figure), the elements were ferulised with 0-Bite (DMG, Chemisch-Pharmazeutische Fabrik GmbH, Hamburg, Germany) and Imprint II Garant Light Body (3M ESPE, St. Paul, MN, USA) applied in the lower root part (Figure 20).

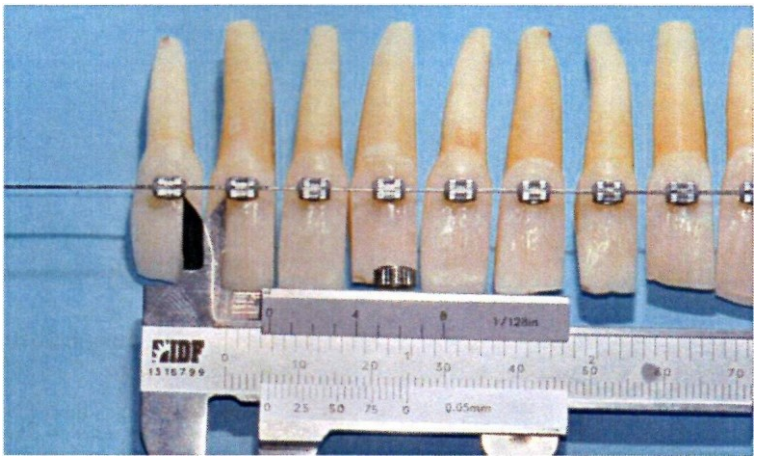

Figure 19. Inter bracket distance check.

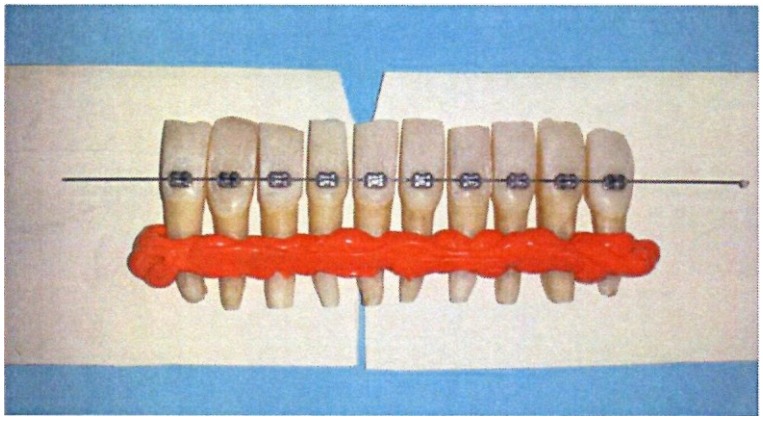

Figure 20. Roots ferulization.

Teeth were then placed in cardboard boxes of 17x2.5x3 cm, previously insulated with Vaseline. Specimens were held in position by horizontal stops made with blue edging wax (Profiled quadrangular wax, Leone Spa, Florence, Italy) so that the surface of the base of the bracket were parallel to the shear force subsequently applied (Figure 21).

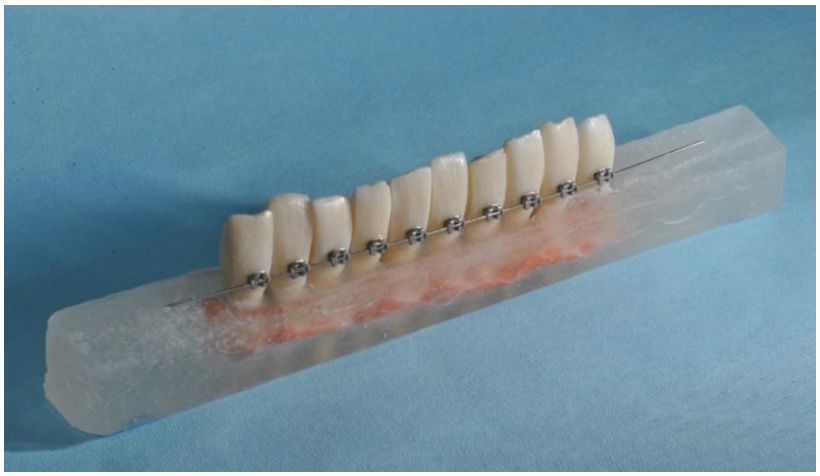

Figure 21. Block of 10 teeth ready for MRI. The inter bracket distance was set at 6 mm. Appliance was bonded on vestibular enamel and bracket base was parallel to the vestibular face of the resin block.

The whole procedure was performed keeping the dental crowns moistened with the thymol solution. Once the preparation of the samples was completed, the wire was replaced following the division established for the various groups.
Brackets of groups 1 (No MRI - No wire), 2 (1.5T MRI – No wire) and 7 (1.5T MRI – No wire) served as control groups and no wire was secured. In the other groups (3 to 6

and 8 to 11) different wires were tested (corresponding to the various materials and dimensions mostly used in orthodontics): stainless steel (stainless steel wire, Ormco, Glendora, CA, USA) and nickel titanium (nickel titanium wire, Ormco, Glendora, CA, USA) alloys in two different shapes: round (0.014 inch) and rectangular (0.019x0.025 inch). Wires were secured in bracket slots with elastomeric ligatures (elastomeric ligatures, Leone, Sesto Fiorentino, Italy).
Specimens were then stored in physiological solution.

3.2. Temperature test and MRI.
Specimens were left at room temperature for 12 hours. For each tooth, the temperature of the bracket and the wire was measured in Celsius degrees with a contact thermometer (PeakTech® Digital Thermometer 5135/5140 Prilf und Messtechnik GmbH, Ahrensburg, Germany). Bracket temperature (Groups 2 to 11) was measured contacting the thermometer probe with upper right brace wing (Figure 22).

Figure 22. Bracket temperature measurement.

Wire temperature (Group 3 to 6 and 8 to 11) was measured contacting the thermometer probe with the vestibular wire surface, 2 mm mesial to bracket slot (Figure 23).

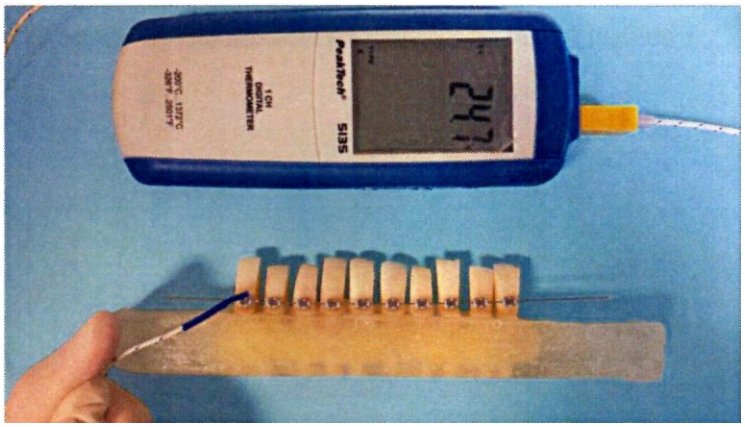

Figure 23. Wire temperature measurement.

Temperature measurements were performed immediately before (T0) and after (T1) MRI exam.

Group 1 served as control and was not submitted to any MRI exam.

Groups 2 to 6 underwent MRI at 1.5T power (Magnetom Symphony Maestro Class 1.5 T, Siemens, Munich, Germany) with the sequences described in Table 2. Different sequences were generated measuring spin–lattice relaxation by using short repetition and echo times (T1) and measuring spin–lattice relaxation by using long repetition and echo times (T2): T2 weighted Turbo Spin Echo in Axial projection (T2W-TSE AXIAL), T2 weighted Turbo Spin Echo in Coronal projection (T2W-TSE CORONAL), T2 FLuid Attenuated Inversion Recovery in axial projection (T2-FLAIR AXIAL) and T1 Volumetric interpolated breath-hold examination in three dimensions fat saturated (T1 VIBE 3D FS). Table 2 reports the main characteristics of the four sequences according to Field of view (FOV), Voxel Size, Slice Thickness, Slices, Time of echo, Repetition time, Scan time and Specific Absorption Rate (SAR) of the whole body.

-	T2W-TSE AXIAL	T2W-TSE CORONAL	T2-FLAIR AXIAL	T1 VIBE 3D FS
FOV (mm)	210x210	200x200	235x185	200x 200
Voxel Size (mm)	0.5x0.5x2.0	0.7x0.5x2.0	1.2x0.7x5.0	1.0x1.0x1.0
Slice Thickness (mm)	2	2	5	1
Slices	24	28	20	128 (slices per slab)
Time of Echo (ms)	84	81	107	2.66
Repetition Time (ms)	3000	3000	9000	6.72
Scan Time (min:s)	6:32	7:20	4:59	6:24
SAR whole body (W/kg)	< 0.5	< 0.5	< 0.5	< 0.5

Table 2. MRI sequences at 1.5T power (Groups 2 to 6).

Groups 7 to 11 underwent MRI at 3T power (Magnetom Verso A Tim System, Siemens, Munich, Germany) with the sequences described in Table 3. The sequences selected were: T2 weighted Turbo Spin Echo in Axial projection (T2W-TSE AXIAL), T2 weighted Turbo Spin Echo in Coronal projection (T2W-TSE CORONAL), T2 FLuid Attenuated Inversion Recovery in axial projection (T2-FLAIR AXIAL), T1 Volumetric interpolated breath-hold examination in three dimensions fat saturated (T1 VIBE 3D FS), T2 weighted two dimensional Fast Low Angle Shot for hemosiderin detection in axial projection (T2W-FL2D HEMO AXIAL), T2 weighted Turbo Inversion Recovery Magnitude in axial projection (T2W-TIRM AXIAL), 2 dimensional echo planar with 5 mm slice diffusion in axial projection (EP2D DIFF 5 mm AXIAL), 2 dimensional echo planar with 3 mm slice diffusion in axial projection (EP2D DIFF 3 mm AXIAL), and Proton Density weighted in axial projection (PDw AXIAL). Table 3 reports the main characteristics of the various sequences according to Field of view (FOV), Voxel Size, Slice Thickness, Slices, Time of echo, Repetition time, Turbo Inversion Recovery, Scan time, and Specific Absorption Rate (SAR) of the whole body.

-	T2W-TSE AXIAL	T2W-TSE CORONAL	T2W-FLAIR AXIAL	T1 VIBE 3D FS	T2W-FL2D HEMO AXIAL	T2W-TIRM AXIAL	EP2D DIFF 5 mm AXIAL	EP2D DIFF 3 mm AXIAL	PDw AXIAL
FOV (mm)	210	200	235	200	210	210	260	190	210
Voxel Size (mm)	0.5x0.5 x2.0	0.7x0.5x2.0	1.2x0.7 x5.0	1.0x1.0 x1.0	0.8x0.5x 3.0	0.7x0.7x 2.0	2.2x2.2x 5.0	2.5x2.5x 3.0	0.8x0.7x 3.0
Slice Thickness (mm)	2	2	5	1	3	2	5	3	3
Slices	25	28	20	128	24	24	15	10	25
Time of Echo (ms)	84	81	108	2.14	19.90	57	75	69	9.1
Repetition Time (ms)	3260	3000	9000	6.72	650	5070	7300	4700	3000
Turbo Inversion Recovery (ms)	-	-	-	-	-	220	220	220	-
Scan Time (min:s)	3:24	2:32	3:18	1:39	3:13	2:23	2:55	1:53	2:53
SAR whole body (W/kg)	< 0.5	< 0.5	< 0.5	< 0.5	< 0.5	< 0.5	< 0.5	< 0.5	< 0.5

Table 3. MRI sequences at 3T Power (Groups 7 to 11).

Total scanning time was approximately 20 minutes for each group.

After MRI and temperature measurement, all the specimens were stored in physiological solution.

3.3. Shear bond strength test.

Adhesion strength was measured with a universal testing machine (Model 3343, Instron, Canton, MA, USA) (Figure 24).

Figure 24. Instron Universal Testing Machine.

Each resin block containing 10 teeth was sectioned in two blocks of 5 teeth in order to allow the insertion in the testing machine. Blocks were included in the mechanic jaw and the shearing force was parallel to bracket base [Scribante et al., 2011]. Each bracket was stressed with an occluso gingival force at a crosshead speed of 1 mm/min [Beltrami et al., 2016] until adhesive failure (Figure 25).

Figure 25. Shear bond strength test. Bracket base was set parallel to shearing force.

Maximum load to debond the appliance was recoded in Newton and subsequently converted into Mega Pascal as a ratio of force on surface area [Sfondrini et al., 2011 A].

3.4. Adhesive remnant index test.

After debonding all the specimens were observed under optical microscopy (Stereomicroscope SR, Zeiss, Oberkochen, Germany). Both enamel and bracket base were evaluated and scored, using a 0-3 scale [Artun and Bergland, 1984]. As showed in Figure 26, this scale is used to define the interface, assigning to each specimen different scores [Sfondrini et al., 2011 B]:

0: no adhesive left on enamel and all the adhesive left on bracket base

1: less than half of the adhesive left on enamel and more than half of the adhesive left on bracket base

2: more than half of the adhesive left on enamel and less than half of the adhesive left on bracket base

3: all the adhesive left on enamel and no adhesive left on bracket base.

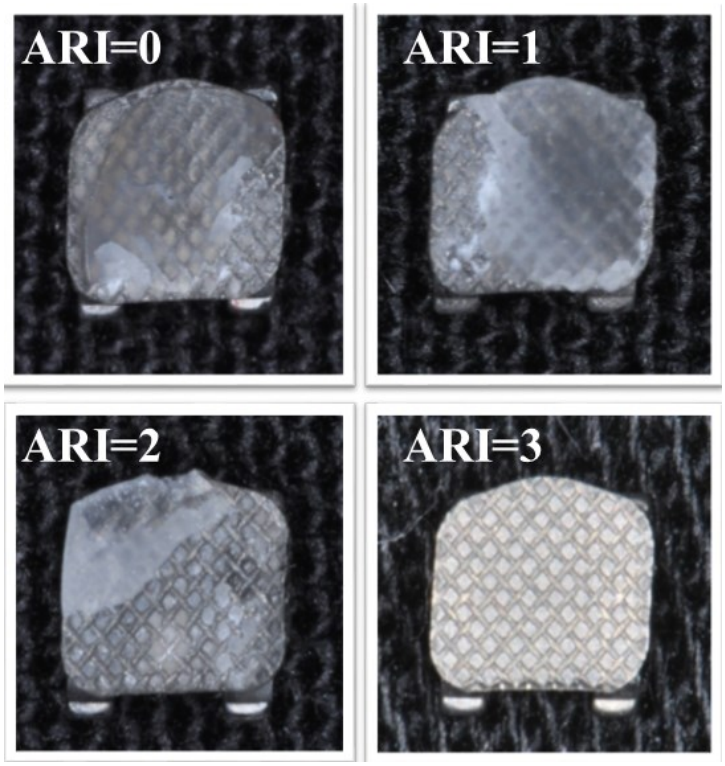

Figure 26. ARI Scores samples. ARI=0 means all the adhesive left on bracket base. ARI=1 means more than half of the adhesive left on bracket base. ARI=2 means less than half of the adhesive left on bracket base. ARI=3 means no adhesive left on bracket base.

4. Statistical analysis.

4. Statistical analysis.

4.1. Summary of the tests used.

Numeric analysis of the data was performed using computer software (R version 3.1.3, R Development Core Team, R Foundation for Statistical Computing, Wien, Austria). Descriptive statistics including mean, standard deviation, minimum, median and maximum values were calculated for all groups.

A linear regression model for bracket temperature, wire temperature and shear bond strength was performed, adding as covariates the wire material, the wire dimension and the MRI power.

Additionally, normality of distributions was calculated with Kolmogorov and Smirnov test. Inferential statistics were performed with ANOVA and Tukey tests for temperatures and shear bond strength values. Fischer test was performed for ARI Scores.

The significance was predetermined at $P<0.05$ for all tests.

4.2. The Software R.

R is a free software environment for statistical computing and graphics. It compiles and runs on a wide variety of UNIX platforms, Windows and MacOS [Kim et al., 2019].

R is a language and environment for statistical computing and graphics. It is a GNU project, which is similar to the S language and environment. It was developed at Bell Laboratories (formerly AT&T, now Lucent Technologies) by John Chambers and colleagues. R can be considered as a different implementation of S. There are some important differences, but much code written for S runs unaltered under R [Brown, 2019].

R provides a wide variety of statistical (linear and nonlinear modelling, classical statistical tests, time-series analysis, classification, clustering) and graphical techniques, and is highly extensible. The S language is often the vehicle of choice for research in statistical methodology, and R provides an Open Source route to participation in that activity. One of R's strengths is the ease with which well-designed publication-quality plots can be produced, including mathematical symbols and formulae where needed.

Great care has been taken over the defaults for the minor design choices in graphics, but the user retains full control [Templ, 2017].

R is available as Free Software under the terms of the Free Software Foundation's GNU General Public License in source code form. It compiles and runs on a wide variety of UNIX platforms and similar systems (including FreeBSD and Linux), Windows and MacOS.

4.3. The R environment.

R is an integrated suite of software facilities for data manipulation, calculation and graphical display. It include an effective data handling and storage facility, a suite of operators for calculations on arrays, in particular matrices, a large, coherent, integrated collection of intermediate tools for data analysis, graphical facilities for data analysis and display either on-screen or on hardcopy, and a well-developed, simple and effective programming language which includes conditionals, loops, user-defined recursive functions and input and output facilities [Wiley and Pace, 2015].

The term "environment" is intended to characterize it as a fully planned and coherent system, rather than an incremental accretion of very specific and inflexible tools, as is frequently the case with other data analysis software.

R, like S, is designed around a true computer language, and it allows users to add additional functionality by defining new functions. Much of the system is itself written in the R dialect of S, which makes it easy for users to follow the algorithmic choices made. For computationally intensive tasks, C, C++ and Fortran code can be linked and called at run time. Advanced users can write C code to manipulate R objects directly [Behr, 2015].

Therefore, it can be considered as an environment within which statistical techniques are implemented. R can be extended (easily) via packages. There are about eight packages supplied with the R distribution and many more are available through the CRAN family of Internet sites covering a very wide range of modern statistics. R has its own LaTeX-like documentation format, which is used to supply comprehensive documentation, both on-line in a number of formats and in hardcopy [Matthews and Farewell, 2015].

4.4. Descriptive Statistics.

Descriptive statistics including mean, standard deviation, minimum, median and maximum values were calculated for all groups.

Statistical analysis in R is performed by using many in-built functions. Most of these functions are part of the R base package. These functions take R vector as an input along with the arguments and give the result.

4.5. Mean.

The mean (average) of the data set was calculated by taking the sum of the values and dividing with the number of values in the data series. The function mean() is used to calculate this in R.

4.6. Standard deviation.

The standard deviation is a measure of the amount of variation or dispersion of a set of values. A low standard deviation indicates that the values tend to be close to the mean (also called the expected value) of the set, while a high standard deviation indicates that the values are spread out over a wider range.

The standard deviation of a random variable, statistical population, data set, or probability distribution is the square root of its variance.

The formula for standard deviation (SD) is:

$$SD = \sqrt{(\sum |x-\mu|^2 / N)}$$

where $\sum$ means "sum of", x is a value in the data set, μ is the mean of the data set, and N is the number of data points in the population.

In the software R the standard deviation is calculated with the formula sd().

4.7. Median.

The median was calculated as the middle value when the data set was ordered from least to greatest. The median() function is used in R to calculate this value.

4.8. Minimum and Maximum.

The minimum is the lower value of a variable, whereas the maximum is the highest value of the variable itself.

The minimum and the maximum of each variable were calculated using the min() or the max() functions. A function called range() would also available, which returns the minimum and maximum in a two element vector.

4.9. Linear regression.

A linear regression model for bracket temperature, wire temperature and shear bond strength was performed, adding as covariates the wire material, the wire dimension and the MRI power.

Linear regression is a statistical model that analyzes the relationship between a response variable (often called y) and one or more variables and their interactions (often called x or explanatory variables). Linear regression is one of the most basic statistical models, its results can be interpreted by almost everyone, and it has been around since the 19th century. Even though it is not as sophisticated as other algorithms like artificial neural networks or random forests, regression is easily readable and it is one of the most used algorithms in medicine [Pardoe, 2013].

Linear regression is used to predict the value of an outcome variable Y based on one or more input predictor variables X. The aim is to establish a linear relationship (a mathematical formula) between the predictor variables and the response variable, so that, the formula can be used to estimate the value of the response Y, when only the predictors (Xs) values are known. Accordingly, the aim of linear regression is to model a continuous variable Y as a mathematical function of one or more X variable(s), so that we can use this regression model to predict the Y when only the X is known. This mathematical equation can be generalized as follows:

$$Y = \beta 1 + \beta 2X + \epsilon$$

where, $\beta 1$ is the intercept and $\beta 2$ is the slope. Collectively, they are called regression coefficients. ϵ is the error term, the part of Y the regression model is unable to explain [Crawley, 2012]. A linear regression can be calculated in R with the command lm. The

command takes the variables in the format: lm([target variable] ~ [predictor variables], data = [data source]).

4.10. Kolmogorov and Smirnov test.

The Kolmogorov–Smirnov test (KS test) is a nonparametric test of the equality of continuous (or discontinuous), one-dimensional probability distributions that can be used to compare a sample with a reference probability distribution (one-sample KS test), or to compare two samples (two-sample KS test). It is named after Andrey Kolmogorov and Nikolai Smirnov. The Kolmogorov–Smirnov statistic quantifies a distance between the empirical distribution function of the sample and the cumulative distribution function of the reference distribution, or between the empirical distribution functions of two samples. The Kolmogorov–Smirnov test can be modified to serve as a goodness of fit test. In the special case of testing for normality of the distribution, samples are standardized and compared with a standard normal distribution. This is equivalent to setting the mean and variance of the reference distribution equal to the sample estimates, and it is known that using these to define the specific reference distribution changes the null distribution of the test statistic.

The Kolmogorov-Smirnov (K-S) test is based on the empirical distribution function (ECDF). Given N ordered data points Y1, Y2, ..., YN, the ECDF is defined as

$$EN=n(i)/N$$

where n(i) is the number of points less than Yi and the Yi are ordered from smallest to largest value. This is a step function that increases by 1/N at the value of each ordered data point.

The Kolmogorov-Smirnov test is defined by:

H0: The data follow a specified distribution

Ha: The data do not follow the specified distribution

Test Statistic: The Kolmogorov-Smirnov test statistic is defined as:

$$D=\max[1\leq i\leq N] (F(Yi) - (i-1) / N , i/N-F(Yi))$$

where F is the theoretical cumulative distribution of the distribution being tested which must be a continuous distribution (i.e., no discrete distributions such as the binomial or Poisson), and it must be fully specified (i.e., the location, scale, and shape parameters cannot be estimated from the data).

The hypothesis regarding the distributional form is rejected if the test statistic, D, is greater than the critical value obtained from a table. There are several variations of these tables in the literature that use somewhat different scaling for the KS test statistic and critical regions. These alternative formulations should be equivalent, but it is necessary to ensure that the test statistic is calculated in a way that is consistent with how the critical values were tabulated.

In the software R this test is performed with Lilliefors (Kolmogorov-Smirnov) Test For Normality. This test is an empirical distribution function omnibus test for the composite hypothesis of normality. The test statistic is the maximal absolute difference between empirical and hypothetical cumulative distribution function. Its formula in the software is lillie.test(x).

4.11. ANOVA (Analysis of variance).

Analysis of variance (ANOVA) is a collection of statistical models and their associated estimation procedures (such as the "variation" among and between groups) used to analyze the differences among group means in a sample. ANOVA was developed by statistician and evolutionary biologist Ronald Fisher. The ANOVA is based on the law of total variance, where the observed variance in a particular variable is partitioned into components attributable to different sources of variation. In its simplest form, ANOVA provides a statistical test of whether two or more population means are equal, and therefore generalizes the t-test beyond two means [Matthews and Farewell, 2015].

There are three classes of models used in the analysis of variance: fixed, random and mixed effect models.

The fixed-effects model (class I) of analysis of variance applies to situations in which the experimenter applies one or more treatments to the subjects of the experiment to see whether the response variable values change. This allows the experimenter to estimate the ranges of response variable values that the treatment would generate in the population as a whole.

Random-effects model (class II) is used when the treatments are not fixed. This occurs when the various factor levels are sampled from a larger population. Because the levels themselves are random variables, some assumptions and the method of contrasting the treatments (a multi-variable generalization of simple differences) differ from the fixed-effects model.

A mixed-effects model (class III) contains experimental factors of both fixed and random-effects types, with appropriately different interpretations and analysis for the two types.

Defining fixed and random effects has proven elusive, with competing definitions arguably leading toward a linguistic question [Behr, 2015].

The analysis of variance has been studied from several approaches, the most common of which uses a linear model that relates the response to the treatments and blocks. The model is linear in parameters but may be nonlinear across factor levels. Interpretation is easy when data is balanced across factors but much deeper understanding is needed for unbalanced data [Monahan, 2011].

The analysis of variance can be presented in terms of a linear model, which makes the following assumptions about the probability distribution of the responses:

Independence of observations – this is an assumption of the model that simplifies the statistical analysis.

Normality – the distributions of the residuals are normal.

Equality (or "homogeneity") of variances, called homoscedasticity — the variance of data in groups should be the same.

ANOVA in R primarily provides evidence of the existence of the mean equality between the groups. This statistical method is an extension of the t-test. It is used in a situation where the factor variable has more than one group. This test gives evidence whether the H0 hypothesis can be accepted or rejected. The H0 hypothesis implies that there is not enough evidence to prove the mean of the group (factor) are different from another. This test is similar to the t-test, although ANOVA test is recommended in situation with more than 2 groups [Ekstrøm and Sørensen, 2010].

The assumptions of ANOVA test are that each factor is randomly sampled, independent and comes from a normally distributed population with unknown but equal variances. The F-statistic is used to test if the data are from significantly different populations (i.e.,

different sample means). To compute the F-statistic, it is needed the division of the between-group variability over the within-group variability.

The between-group variability reflects the differences between the groups inside all of the population.

The within group variability considers the difference between the groups. The variation comes from the individual observations; some points might be very different from the group means. The within group variability picks up this effect and refer to the sampling error.

ANOVA test can be performed in two ways. One-way or two-way refers to the number of independent variables (IVs) in the Analysis of Variance test.

One-way has one independent variable (with 2 levels). Two-way has two independent variables (it can have multiple levels). Additionally, Two-way tests can be with or without replication [Sawitzki, 2009].

A one way ANOVA is used to compare two means from two independent (unrelated) groups using the F-distribution. The null hypothesis for the test is that the two means are equal. Therefore, a significant result means that the two means are unequal. A one way ANOVA tells that at least two groups were different from each other. However, it does not tell which groups were different. If test returns a significant f-statistic, an ad hoc test is needed to tell exactly which groups had a difference in means.

A Two Way ANOVA is an extension of the One Way ANOVA. With a One Way, one independent variable affects a dependent variable. With a Two Way ANOVA, there are two independents. A two way ANOVA is used when one measurement variable (i.e. a quantitative variable) and two nominal variables are present in the study. The results of a Two Way ANOVA calculate a main effect and an interaction effect. The main effect is similar to a One Way ANOVA: each factor's effect is considered separately. With the interaction effect, all factors are considered at the same time. Interaction effects between factors are easier to test if there is more than one observation in each cell [Cohen and Cohen, 2008].

Assumptions for Two Way ANOVA are that the population must be close to a normal distribution; samples must be independent; population variances must be equal; groups must have equal sample sizes.

Repeated measures ANOVA is almost the same as one-way ANOVA, with one main difference: the groups tested are related and not independent. It is called repeated measures because the same group of participants is being measured over and over again. Repeated measures ANOVA is similar to a simple multivariate design. In both tests, the same participants are measured repeatedly. However, with repeated measures the same characteristic is measured with a different condition [Miller, 1997].

When data are collected from the same participants over a period of time, individual differences (a source of between group differences) are reduced or eliminated. Testing is more powerful because the sample size is not divided between groups. The test can be economical, as the same participants are used.

The assumptions for Repeated Measures ANOVA are that there must be one independent variable and one dependent variable; the dependent variable must be continuous, on an interval scale or a ratio scale; the independent variable must be categorical, either on the nominal scale or on ordinal scale. Ideally, levels of dependence between pairs of groups is equal ("sphericity"). Corrections are possible if this assumption is violated [Blokdyk, 2018].

R Software performs ANOVA test with the function aov().

4.12. Pairwise comparison: Tukey test.

ANOVA test does not inform which group has a different mean. Instead, Tukey test can be performed.

Tukey's range test, also known as the Tukey's test, Tukey method, Tukey's honest significance test, or Tukey's HSD (honestly significant difference) test, is a single-step multiple comparison procedure and statistical test. It can be used to find means that are significantly different from each other. It compares all possible pairs of means, and is based on a studentized range distribution (q) (this distribution is similar to the distribution of t from the t-test). Tukey's test compares the means of every treatment to the means of every other treatment; that is, it applies simultaneously to the set of all pairwise comparisons and identifies any difference between two means that is greater than the expected standard error. The confidence coefficient for the set, when all sample sizes are equal, is exactly $1 - \alpha$ for any $0 \leq \alpha \leq 1$. For unequal sample sizes, the

confidence coefficient is greater than $1 - \alpha$, so this method is conservative when there are unequal sample sizes.

R software calculates Tukey test with the function TukeyHSD().

4.13. Fisher exact test.

Fisher's exact test is a statistical significance test used in the analysis of contingency tables. Although in practice it is employed when sample sizes are small, it is valid for all sample sizes. The test is useful for categorical data that result from classifying objects in two different ways; it is used to examine the significance of the association (contingency) between the two kinds of classification.

The Software R performs this test with the function fisher.test().

4.14. P values.

The p-value or probability value is the probability of obtaining test results at least as extreme as the results actually observed during the test, assuming that the null hypothesis is correct

The p-value is used in the context of null hypothesis testing in order to quantify the idea of statistical significance of evidence. Null hypothesis testing is a reductio ad absurdum argument adapted to statistics. In essence, a claim is assumed valid if its counter-claim is improbable.

The p-value is defined as the probability, under the null hypothesis H0 as opposed to HA, denoting the alternative hypothesis, about the unknown distribution F of the random variable X, for the variate to be observed as a value equal to or more extreme than the value observed. If x is the observed value, then the "equal to or more extreme than what was actually observed" can mean $X \geq x$ (right-tail event), $X \leq x$ (left-tail event) or the event giving the smallest probability among $X \geq x$ and $X \leq x$ (double-tailed event). Thus, the p-value is given by

$\Pr (X \geq x \mid H)$

$\Pr (X \leq x \mid H)$

$2 \min \{\Pr (X \leq x \mid H), \Pr (X \geq x \mid H) \}$

The smaller the p-value, the higher the significance because it tells the investigator that the hypothesis under consideration may not adequately explain the observation. The

null hypothesis H is rejected if any of these probabilities is less than or equal to a small, fixed but arbitrarily pre-defined threshold value α, which is referred to as the level of significance. Unlike the p-value, the α level is not derived from any observational data and does not depend on the underlying hypothesis. The value of α is instead set by the researcher before examining the data. The setting of α is arbitrary. By convention, α is commonly set to 0.05, 0.01, 0.005, or 0.001.

When a hypothesis test is performed, a p-value helps in determining the significance of the results. Hypothesis tests are used to test the validity of a claim that is made about a population. This claim on trial, in essence, is called the null hypothesis.

The alternative hypothesis is the one, which would be true if the null hypothesis is concluded to be untrue. All hypothesis tests use a p-value to weigh the strength of the evidence [Panagiotakos, 2008].

The p-value is a number between 0 and 1 and interpreted in the following way:

A small p-value (typically ≤ 0.05) indicates strong evidence against the null hypothesis, so the null hypothesis can be rejected.

A large p-value (> 0.05) indicates weak evidence against the null hypothesis, so the null hypothesis cannot be rejected.

P-values very close to the cutoff (0.05) are considered to be marginal (could go either way).

Accordingly, in the present report the significance was predetermined at $P<0.05$ for all tests.

4.15. Statistical Analysis on the R software.

Below is the R script (and the relative answers on the program console) of the statistical analysis performed in the present report.

```
R version 3.2.3 (2015-12-10) -- "Wooden Christmas-Tree"
Copyright (C) 2015 The R Foundation for Statistical Computing
Platform: i386-w64-mingw32/i386 (32-bit)

> #Commented Statistical Analysis
>
> #Libraries loading:
> library(MASS)
> library(plotrix)
> library(nortest)
>
> #Dataset loading:
> data<-read.csv2("mr.csv",header=T,dec=",",na.string="")
>
> #Dataset structure analysis
> str(data)
'data.frame':   220 obs. of  8 variables:
 $ group   : int  1 1 1 1 1 1 1 1 1 1 ...
 $ mpa     : num  18.5 24.2 24.6 30.1 33.1 ...
 $ temp.w  : num  NA NA NA NA NA NA NA NA NA NA ...
 $ temp.b  : num  -0.2 0.1 -0.3 0.1 -0.1 -0.7 0 0 0 0 ...
 $ size    : int  0 0 0 0 0 0 0 0 0 0 ...
 $ material: Factor w/ 3 levels "NiTi","no.wire",..: 2 2 2 2 2 2 2 2 2 2 ...
 $ power   : num  0 0 0 0 0 0 0 0 0 0 ...
 $ ari     : int  1 0 1 1 1 2 1 0 3 1 ...
> colnames(data)
[1] "group"    "mpa"      "temp.w"   "temp.b"   "size"     "material" "power"    "ari"
> dim(data)
[1] 220   8
```

```
> summary(data)
     group             mpa                  temp.w               temp.b
size           material      power            ari
 Min.    : 1   Min.    :12.04   Min.    :0.000   Min.    :-1.0000   Min.
:   0.0   NiTi   :80   Min.   :0.000   Min.   :0.0000
 1st Qu.: 3   1st Qu.:21.12   1st Qu.:0.500   1st Qu.: 0.1000   1st
Qu.:   0.0   no.wire:60   1st Qu.:1.500   1st Qu.:0.0000
 Median : 6   Median :24.70   Median :1.100   Median : 0.7000   Median
:  14.0   SS     :80   Median :1.500   Median :1.0000
 Mean   : 6   Mean   :24.67   Mean   :1.153   Mean   : 0.9327   Mean
: 705.1                Mean   :2.045   Mean   :0.6091
 3rd Qu.: 9   3rd Qu.:27.82   3rd Qu.:1.600   3rd Qu.: 1.6000   3rd
Qu.:1925.0                3rd Qu.:3.000   3rd Qu.:1.0000
 Max.   :11   Max.   :35.43   Max.   :2.900   Max.   : 3.8000   Max.
:1925.0                Max.   :3.000   Max.   :3.0000
                            NA's   :60
> head (data)
  group   mpa temp.w temp.b size material power ari
1     1 18.53     NA   -0.2    0  no.wire     0   1
2     1 24.21     NA    0.1    0  no.wire     0   0
3     1 24.65     NA   -0.3    0  no.wire     0   1
4     1 30.06     NA    0.1    0  no.wire     0   1
5     1 33.11     NA   -0.1    0  no.wire     0   1
6     1 25.18     NA   -0.7    0  no.wire     0   2
> attach (data)
>
> #The dataset has 221 rows and 8 columns.
> #The experimentation takes into consideration different materials.
> #Orthodontic brackets were tested with or without orthodontic wires.
>  #Wires presented different sizes (size): 0.014 inches and
0.019x0.025 inches.
> #Wires were made with different materials (material): stainless
steel and nickel-titanium.
> #Appliances have been tested with no magnetic field or with magnetic
fields at 2 different powers (power): 1.5 Tesla and 3 Tesla.
> #Data obtained were connected to the measurement of the temperature
of brackets and wires, shear bond strength of orthodontic brackets and
adhesive remnant index scores for each of the 11 goups tested.
> #Variables analyzed were:
```

```
> #-differences of the temperatures of the brackets in Calsius degrees
(temp.b),
> #-differences of the temperatures of the wires in Celsius degrees
(temp.w),
> #-bond strength values in Megapascal(mpa),
> #-adhesive remnant index scores (ari).
>
>
>
>
>
> ################################################
>
>
>
>
>
> ###Analysis of the temperatures of the brackets (temp.b) in the
various groups.
>
> #Descriptive statistics (mean, standard deviation, minimum, median
and maximum values) are calculated for each group.
> mean(temp.b[group=="1"])
[1] -0.105
> sd(temp.b[group=="1"])
[1] 0.2163696
> min(temp.b[group=="1"])
[1] -0.7
> median(temp.b[group=="1"])
[1] 0
> max(temp.b[group=="1"])
[1] 0.1
> mean(temp.b[group=="2"])
[1] 0.105
> sd(temp.b[group=="2"])
[1] 0.3590558
> min(temp.b[group=="2"])
[1] -1
> median(temp.b[group=="2"])
```

```
[1] 0.1
> max(temp.b[group=="2"])
[1] 0.6
> mean(temp.b[group=="3"])
[1] 1.195
> sd(temp.b[group=="3"])
[1] 0.3734265
> min(temp.b[group=="3"])
[1] 0.5
> median(temp.b[group=="3"])
[1] 1.15
> max(temp.b[group=="3"])
[1] 1.9
> mean(temp.b[group=="4"])
[1] 2.155
> sd(temp.b[group=="4"])
[1] 0.5491381
> min(temp.b[group=="4"])
[1] 1.3
> median(temp.b[group=="4"])
[1] 2.1
> max(temp.b[group=="4"])
[1] 3.8
> mean(temp.b[group=="5"])
[1] 0.05
> sd(temp.b[group=="5"])
[1] 0.4406932
> min(temp.b[group=="5"])
[1] -0.8
> median(temp.b[group=="5"])
[1] 0
> max(temp.b[group=="5"])
[1] 0.9
> mean(temp.b[group=="6"])
[1] 0.09
> sd(temp.b[group=="6"])
[1] 0.4024922
> min(temp.b[group=="6"])
[1] -0.5
```

```
> median(temp.b[group=="6"])
[1] 0
> max(temp.b[group=="6"])
[1] 1
> mean(temp.b[group=="7"])
[1] 0.97
> sd(temp.b[group=="7"])
[1] 0.6233188
> min(temp.b[group=="7"])
[1] 0
> median(temp.b[group=="7"])
[1] 1
> max(temp.b[group=="7"])
[1] 2
> mean(temp.b[group=="8"])
[1] 0.69
> sd(temp.b[group=="8"])
[1] 0.4423621
> min(temp.b[group=="8"])
[1] 0.1
> median(temp.b[group=="8"])
[1] 0.55
> max(temp.b[group=="8"])
[1] 1.6
> mean(temp.b[group=="9"])
[1] 1.94
> sd(temp.b[group=="9"])
[1] 0.5072112
> min(temp.b[group=="9"])
[1] 1.2
> median(temp.b[group=="9"])
[1] 1.9
> max(temp.b[group=="9"])
[1] 2.8
> mean(temp.b[group=="10"])
[1] 0.775
> sd(temp.b[group=="10"])
[1] 0.5169496
> min(temp.b[group=="10"])
```

```
[1] 0.3
> median(temp.b[group=="10"])
[1] 0.8
> max(temp.b[group=="10"])
[1] 2.4
> mean(temp.b[group=="11"])
[1] 2.395
> sd(temp.b[group=="11"])
[1] 0.8475817
> min(temp.b[group=="11"])
[1] 0.5
> median(temp.b[group=="11"])
[1] 2.6
> max(temp.b[group=="11"])
[1] 3.7
>
> #Descriptive statistics (mean, standard deviation, minimum, median
and maximum values) are calculated for each wire size (no wire -
0.014" - 0.019"x0.025").
> mean(temp.b[size=="0"])
[1] 0.3233333
> sd(temp.b[size=="0"])
[1] 0.6338921
> min(temp.b[size=="0"])
[1] -1
> median(temp.b[size=="0"])
[1] 0.1
> max(temp.b[size=="0"])
[1] 2
> mean(temp.b[size=="14"])
[1] 0.6775
> sd(temp.b[size=="14"])
[1] 0.6012592
> min(temp.b[size=="14"])
[1] -0.8
> median(temp.b[size=="14"])
[1] 0.7
> max(temp.b[size=="14"])
[1] 2.4
```

```
> mean(temp.b[size=="1925"])
[1] 1.645
> sd(temp.b[size=="1925"])
[1] 1.090221
> min(temp.b[size=="1925"])
[1] -0.5
> median(temp.b[size=="1925"])
[1] 1.9
> max(temp.b[size=="1925"])
[1] 3.8
>
> #Descriptive statistics (mean, standard deviation, minimum, median
and maximum values) are calculated for each wire material (no wire -
SS - NiTi).
> mean(temp.b[material=="no.wire"])
[1] 0.3233333
> sd(temp.b[material=="no.wire"])
[1] 0.6338921
> min(temp.b[material=="no.wire"])
[1] -1
> median(temp.b[material=="no.wire"])
[1] 0.1
> max(temp.b[material=="no.wire"])
[1] 2
> mean(temp.b[material=="SS"])
[1] 1.495
> sd(temp.b[material=="SS"])
[1] 0.7498354
> min(temp.b[material=="SS"])
[1] 0.1
> median(temp.b[material=="SS"])
[1] 1.5
> max(temp.b[material=="SS"])
[1] 3.8
> mean(temp.b[material=="NiTi"])
[1] 0.8275
> sd(temp.b[material=="NiTi"])
[1] 1.111844
> min(temp.b[material=="NiTi"])
```

```
[1] -0.8
> median(temp.b[material=="NiTi"])
[1] 0.5
> max(temp.b[material=="NiTi"])
[1] 3.7
>
> #Normality of distributions is tested with Kolmogorov Smirnov test.
> lillie.test(temp.b[size=="0" & material=="no.wire" & power=="0"])

        Lilliefors (Kolmogorov-Smirnov) normality test

data:  temp.b[size == "0" & material == "no.wire" & power == "0"]
D = 0.33626, p-value = 2.097e-06

> lillie.test(temp.b[size=="0" & material=="no.wire" & power=="1.5"])

        Lilliefors (Kolmogorov-Smirnov) normality test

data:  temp.b[size == "0" & material == "no.wire" & power == "1.5"]
D = 0.13498, p-value = 0.4427

> lillie.test(temp.b[size=="14" & material=="SS" & power=="1.5"])

        Lilliefors (Kolmogorov-Smirnov) normality test

data:  temp.b[size == "14" & material == "SS" & power == "1.5"]
D = 0.10703, p-value = 0.7931

> lillie.test(temp.b[size=="1925" & material=="SS" & power=="1.5"])

        Lilliefors (Kolmogorov-Smirnov) normality test

data:  temp.b[size == "1925" & material == "SS" & power == "1.5"]
D = 0.12774, p-value = 0.5327

> lillie.test(temp.b[size=="14" & material=="NiTi" & power=="1.5"])

        Lilliefors (Kolmogorov-Smirnov) normality test
```

```
data:  temp.b[size == "14" & material == "NiTi" & power == "1.5"]
D = 0.20483, p-value = 0.02749

> lillie.test(temp.b[size=="1925" & material=="NiTi" & power=="1.5"])

        Lilliefors (Kolmogorov-Smirnov) normality test

data:  temp.b[size == "1925" & material == "NiTi" & power == "1.5"]
D = 0.18847, p-value = 0.06083

> lillie.test(temp.b[size=="0" & material=="no.wire" & power=="3"])

        Lilliefors (Kolmogorov-Smirnov) normality test

data:  temp.b[size == "0" & material == "no.wire" & power == "3"]
D = 0.11919, p-value = 0.6434

> lillie.test(temp.b[size=="14" & material=="SS" & power=="3"])

        Lilliefors (Kolmogorov-Smirnov) normality test

data:  temp.b[size == "14" & material == "SS" & power == "3"]
D = 0.18061, p-value = 0.08641

> lillie.test(temp.b[size=="1925" & material=="SS" & power=="3"])

        Lilliefors (Kolmogorov-Smirnov) normality test

data:  temp.b[size == "1925" & material == "SS" & power == "3"]
D = 0.15716, p-value = 0.2189

> lillie.test(temp.b[size=="14" & material=="NiTi" & power=="3"])

        Lilliefors (Kolmogorov-Smirnov) normality test

data:  temp.b[size == "14" & material == "NiTi" & power == "3"]
D = 0.17909, p-value = 0.09228

> lillie.test(temp.b[size=="1925" & material=="NiTi" & power=="3"])
```

```
        Lilliefors (Kolmogorov-Smirnov) normality test

data:  temp.b[size == "1925" & material == "NiTi" & power == "3"]
D = 0.14052, p-value = 0.3782

> #Kolmogorov Smirnov is mostly not significant, therefore data follow
normal distributions (gaussian).
>
> #ANOVA test is applied.
> total<-paste(size,material,power)
> table(total)
total
  0 no.wire 0 0 no.wire 1.5   0 no.wire 3   14 NiTi 1.5     14 NiTi 3
14 SS 1.5         14 SS 3 1925 NiTi 1.5    1925 NiTi 3    1925 SS 1.5
1925 SS 3
           20             20             20             20             20
20                20                20                20                20
20
> anova(lm(temp.b~total))
Analysis of Variance Table

Response: temp.b
           Df  Sum Sq Mean Sq F value    Pr(>F)
total      10 161.043 16.1043  63.266 < 2.2e-16 ***
Residuals 209  53.201  0.2546
---
Signif. codes:  0 ‘***’ 0.001 ‘**’ 0.01 ‘*’ 0.05 ‘.’ 0.1 ‘ ’ 1
> #Analysis of variance shows a significant result (P<0.05).
>
> #A Tukey post hoc test is performed for pairwise comparisons.
> model<-aov(temp.b~total)
> TukeyHSD(model)
  Tukey multiple comparisons of means
    95% family-wise confidence level

Fit: aov(formula = temp.b ~ total)

$total
```

	diff	lwr	upr	p adj
0 no.wire 1.5-0 no.wire 0	0.210	-0.30928496	0.72928496	0.9651231
0 no.wire 3-0 no.wire 0	1.075	0.55571504	1.59428496	0.0000000
14 NiTi 1.5-0 no.wire 0	0.155	-0.36428496	0.67428496	0.9965132
14 NiTi 3-0 no.wire 0	0.880	0.36071504	1.39928496	0.0000055
14 SS 1.5-0 no.wire 0	1.300	0.78071504	1.81928496	0.0000000
14 SS 3-0 no.wire 0	0.795	0.27571504	1.31428496	0.0000691
1925 NiTi 1.5-0 no.wire 0	0.195	-0.32428496	0.71428496	0.9793412
1925 NiTi 3-0 no.wire 0	2.500	1.98071504	3.01928496	0.0000000
1925 SS 1.5-0 no.wire 0	2.260	1.74071504	2.77928496	0.0000000
1925 SS 3-0 no.wire 0	2.045	1.52571504	2.56428496	0.0000000
0 no.wire 3-0 no.wire 1.5	0.865	0.34571504	1.38428496	0.0000087
14 NiTi 1.5-0 no.wire 1.5	-0.055	-0.57428496	0.46428496	0.9999998
14 NiTi 3-0 no.wire 1.5	0.670	0.15071504	1.18928496	0.0019295
14 SS 1.5-0 no.wire 1.5	1.090	0.57071504	1.60928496	0.0000000
14 SS 3-0 no.wire 1.5	0.585	0.06571504	1.10428496	0.0135817
1925 NiTi 1.5-0 no.wire 1.5	-0.015	-0.53428496	0.50428496	1.0000000
1925 NiTi 3-0 no.wire 1.5	2.290	1.77071504	2.80928496	0.0000000
1925 SS 1.5-0 no.wire 1.5	2.050	1.53071504	2.56928496	0.0000000
1925 SS 3-0 no.wire 1.5	1.835	1.31571504	2.35428496	0.0000000
14 NiTi 1.5-0 no.wire 3	-0.920	-1.43928496	-0.40071504	0.0000016
14 NiTi 3-0 no.wire 3	-0.195	-0.71428496	0.32428496	0.9793412
14 SS 1.5-0 no.wire 3	0.225	-0.29428496	0.74428496	0.9447037
14 SS 3-0 no.wire 3	-0.280	-0.79928496	0.23928496	0.8047519
1925 NiTi 1.5-0 no.wire 3	-0.880	-1.39928496	-0.36071504	0.0000055
1925 NiTi 3-0 no.wire 3	1.425	0.90571504	1.94428496	0.0000000
1925 SS 1.5-0 no.wire 3	1.185	0.66571504	1.70428496	0.0000000
1925 SS 3-0 no.wire 3	0.970	0.45071504	1.48928496	0.0000003
14 NiTi 3-14 NiTi 1.5	0.725	0.20571504	1.24428496	0.0004744
14 SS 1.5-14 NiTi 1.5	1.145	0.62571504	1.66428496	0.0000000
14 SS 3-14 NiTi 1.5	0.640	0.12071504	1.15928496	0.0039654
1925 NiTi 1.5-14 NiTi 1.5	0.040	-0.47928496	0.55928496	1.0000000
1925 NiTi 3-14 NiTi 1.5	2.345	1.82571504	2.86428496	0.0000000
1925 SS 1.5-14 NiTi 1.5	2.105	1.58571504	2.62428496	0.0000000
1925 SS 3-14 NiTi 1.5	1.890	1.37071504	2.40928496	0.0000000
14 SS 1.5-14 NiTi 3	0.420	-0.09928496	0.93928496	0.2391110
14 SS 3-14 NiTi 3	-0.085	-0.60428496	0.43428496	0.9999836
1925 NiTi 1.5-14 NiTi 3	-0.685	-1.20428496	-0.16571504	0.0013297
1925 NiTi 3-14 NiTi 3	1.620	1.10071504	2.13928496	0.0000000

```
1925 SS 1.5-14 NiTi 3        1.380  0.86071504  1.89928496 0.0000000
1925 SS 3-14 NiTi 3          1.165  0.64571504  1.68428496 0.0000000
14 SS 3-14 SS 1.5           -0.505 -1.02428496  0.01428496 0.0646405
1925 NiTi 1.5-14 SS 1.5     -1.105 -1.62428496 -0.58571504 0.0000000
1925 NiTi 3-14 SS 1.5        1.200  0.68071504  1.71928496 0.0000000
1925 SS 1.5-14 SS 1.5        0.960  0.44071504  1.47928496 0.0000004
1925 SS 3-14 SS 1.5          0.745  0.22571504  1.26428496 0.0002779
1925 NiTi 1.5-14 SS 3       -0.600 -1.11928496 -0.08071504 0.0098254
1925 NiTi 3-14 SS 3          1.705  1.18571504  2.22428496 0.0000000
1925 SS 1.5-14 SS 3          1.465  0.94571504  1.98428496 0.0000000
1925 SS 3-14 SS 3            1.250  0.73071504  1.76928496 0.0000000
1925 NiTi 3-1925 NiTi 1.5    2.305  1.78571504  2.82428496 0.0000000
1925 SS 1.5-1925 NiTi 1.5    2.065  1.54571504  2.58428496 0.0000000
1925 SS 3-1925 NiTi 1.5      1.850  1.33071504  2.36928496 0.0000000
1925 SS 1.5-1925 NiTi 3     -0.240 -0.75928496  0.27928496 0.9170492
1925 SS 3-1925 NiTi 3       -0.455 -0.97428496  0.06428496 0.1463540
1925 SS 3-1925 SS 1.5       -0.215 -0.73428496  0.30428496 0.9590630

> #The significance of the comparisons of all groups each other is
recorded.
>
> #A box plot is drawn, representing the results for each group.
> boxplot(temp.b~group)
> title(ylab="Bracket temperature variation (°C)")
> title(xlab="Groups")
>
> #A box plot is drawn, representing the results for each magnetic
field power.
> boxplot(temp.b~power)
> title(ylab="Bracket temperature variation (°C)")
> title(xlab="MRI Power (T)")
>
> #A box plot is drawn, representing the results for each wire size.
> boxplot(temp.b~size)
> title(ylab="Bracket temperature variation (°C)")
> title(xlab="Wire Size")
>
> #A box plot is drawn, representing the results for each wire
material.
```

```
> boxplot(temp.b~material)
> title(ylab="Bracket temperature variation (°C)")
> title(xlab="Wire Material")
>
> #Linear regressions.
> #Linear regression with family=gaussian and link=identity parameters
are calculated.
>
> #The effect of wire material on temperature of the bracket is
tested.
> linearmodel<-glm(temp.b~material,family=gaussian(link="identity"))
> summary(linearmodel)

Call:
glm(formula = temp.b ~ material, family = gaussian(link = "identity"))

Deviance Residuals:
    Min       1Q   Median       3Q      Max
-1.6275  -0.5444  -0.2092   0.4050   2.8725

Coefficients:
                Estimate Std. Error t value Pr(>|t|)
(Intercept)      0.82750    0.09772   8.468 3.77e-15 ***
materialno.wire -0.50417    0.14927  -3.377 0.000867 ***
materialSS       0.66750    0.13820   4.830 2.58e-06 ***
---
Signif. codes:  0 ‘***’ 0.001 ‘**’ 0.01 ‘*’ 0.05 ‘.’ 0.1 ‘ ’ 1

(Dispersion parameter for gaussian family taken to be 0.7639854)

    Null deviance: 214.24  on 219  degrees of freedom
Residual deviance: 165.78  on 217  degrees of freedom
AIC: 570.09

Number of Fisher Scoring iterations: 2

> confint(linearmodel)
Waiting for profiling to be done...
                     2.5 %     97.5 %
```

```
(Intercept)      0.6359661  1.0190339
materialno.wire -0.7967395 -0.2115938
materialSS       0.3966302  0.9383698
> #P value is highly significant. The temperature variations of the brackets (temp.b) are significantly influenced by wire materials (material).
>
> #The effect of wire size on temperature of the bracket is tested.
> linearmodel2<-glm(temp.b~size,family=gaussian(link="identity"))
> summary(linearmodel2)

Call:
glm(formula = temp.b ~ size, family = gaussian(link = "identity"))

Deviance Residuals:
    Min       1Q   Median       3Q      Max
-2.1461  -0.5204  -0.0286   0.5714   2.1539

Coefficients:
             Estimate Std. Error t value Pr(>|t|)
(Intercept) 0.5204174  0.0704620   7.386 3.18e-12 ***
size        0.0005848  0.0000607   9.634  < 2e-16 ***
---
Signif. codes:  0 ‘***’ 0.001 ‘**’ 0.01 ‘*’ 0.05 ‘.’ 0.1 ‘ ’ 1

(Dispersion parameter for gaussian family taken to be 0.6893076)

    Null deviance: 214.24  on 219  degrees of freedom
Residual deviance: 150.27  on 218  degrees of freedom
AIC: 546.47

Number of Fisher Scoring iterations: 2

> confint(linearmodel2)
Waiting for profiling to be done...
                   2.5 %       97.5 %
(Intercept) 0.3823144715 0.6585203428
size        0.0004657941 0.0007037284
```

```
> #P value is highly significant. The temperature variations of the
brackets (temp.b) are significantly influenced by wire sizes (size).
>
> #The effect of MRI power on temperature of the bracket is tested.
> linearmodel3<-glm(temp.b~power,family=gaussian(link="identity"))
> summary(linearmodel3)

Call:
glm(formula = temp.b ~ power, family = gaussian(link = "identity"))

Deviance Residuals:
    Min       1Q   Median       3Q      Max
-1.6812  -0.6812  -0.1729   0.6188   3.1188

Coefficients:
            Estimate Std. Error t value Pr(>|t|)
(Intercept) -0.01050    0.13993  -0.075     0.94
power        0.46113    0.06188   7.452 2.13e-12 ***
---
Signif. codes:  0 ‘***’ 0.001 ‘**’ 0.01 ‘*’ 0.05 ‘.’ 0.1 ‘ ’ 1

(Dispersion parameter for gaussian family taken to be 0.7832523)

    Null deviance: 214.24  on 219  degrees of freedom
Residual deviance: 170.75  on 218  degrees of freedom
AIC: 574.58

Number of Fisher Scoring iterations: 2

> confint(linearmodel3)
Waiting for profiling to be done...
                 2.5 %    97.5 %
(Intercept) -0.2847641 0.2637641
power        0.3398492 0.5824175
> #P value is highly significant. The temperature variations of the
brackets (temp.b) are significantly influenced by MRI power (power).
>
> #The effect of temperature of the wire on temperature of the bracket
is tested.
```

```
> linearmodel4<-glm(temp.b~temp.w,family=gaussian(link="identity"))
> summary(linearmodel4)

Call:
glm(formula = temp.b ~ temp.w, family = gaussian(link = "identity"))

Deviance Residuals:
     Min        1Q    Median        3Q       Max
-2.34194  -0.49286  -0.02792   0.49545   2.28610

Coefficients:
            Estimate Std. Error t value Pr(>|t|)
(Intercept) -0.01883    0.10961  -0.172    0.864
temp.w       1.02337    0.08157  12.547   <2e-16 ***
---
Signif. codes:  0 ‘***’ 0.001 ‘**’ 0.01 ‘*’ 0.05 ‘.’ 0.1 ‘ ’ 1

(Dispersion parameter for gaussian family taken to be 0.5069482)

    Null deviance: 159.900  on 159  degrees of freedom
Residual deviance:  80.098  on 158  degrees of freedom
  (60 observations deleted due to missingness)
AIC: 349.35

Number of Fisher Scoring iterations: 2

> confint(linearmodel4)
Waiting for profiling to be done...
                2.5 %    97.5 %
(Intercept) -0.2336628 0.1960103
temp.w       0.8635061 1.1832386
> #P value is highly significant. The temperature variations of the
brackets (temp.b) are significantly influenced by the temperature
variations of the wires (temp.w).
>
>
>
>
>
```

```
> ################################################
>
>
>
>
>
> ###Analysis of the temperatures of the wires (temp.w) in the various
groups.
>
> #Descriptive statistics (mean, standard deviation, minimum, median
and maximum values) are calculated for each group
> mean(temp.w[group=="1"])
[1] NA
> sd(temp.w[group=="1"])
[1] NA
> min(temp.w[group=="1"])
[1] NA
> median(temp.w[group=="1"])
[1] NA
> max(temp.w[group=="1"])
[1] NA
> mean(temp.w[group=="2"])
[1] NA
> sd(temp.w[group=="2"])
[1] NA
> min(temp.w[group=="2"])
[1] NA
> median(temp.w[group=="2"])
[1] NA
> max(temp.w[group=="2"])
[1] NA
> mean(temp.w[group=="3"])
[1] 1.015
> sd(temp.w[group=="3"])
[1] 0.2680829
> min(temp.w[group=="3"])
[1] 0.5
> median(temp.w[group=="3"])
[1] 1
```

```
> max(temp.w[group=="3"])
[1] 1.7
> mean(temp.w[group=="4"])
[1] 1.69
> sd(temp.w[group=="4"])
[1] 0.5919637
> min(temp.w[group=="4"])
[1] 0.6
> median(temp.w[group=="4"])
[1] 1.8
> max(temp.w[group=="4"])
[1] 2.8
> mean(temp.w[group=="5"])
[1] 0.42
> sd(temp.w[group=="5"])
[1] 0.1056309
> min(temp.w[group=="5"])
[1] 0.2
> median(temp.w[group=="5"])
[1] 0.5
> max(temp.w[group=="5"])
[1] 0.5
> mean(temp.w[group=="6"])
[1] 0.39
> sd(temp.w[group=="6"])
[1] 0.1410487
> min(temp.w[group=="6"])
[1] 0.1
> median(temp.w[group=="6"])
[1] 0.5
> max(temp.w[group=="6"])
[1] 0.5
> mean(temp.w[group=="7"])
[1] NA
> sd(temp.w[group=="7"])
[1] NA
> min(temp.w[group=="7"])
[1] NA
> median(temp.w[group=="7"])
```

```
[1] NA
> max(temp.w[group=="7"])
[1] NA
> mean(temp.w[group=="8"])
[1] 1.26
> sd(temp.w[group=="8"])
[1] 0.4417668
> min(temp.w[group=="8"])
[1] 0.5
> median(temp.w[group=="8"])
[1] 1.2
> max(temp.w[group=="8"])
[1] 2.2
> mean(temp.w[group=="9"])
[1] 1.74
> sd(temp.w[group=="9"])
[1] 0.6443275
> min(temp.w[group=="9"])
[1] 0
> median(temp.w[group=="9"])
[1] 1.6
> max(temp.w[group=="9"])
[1] 2.5
> mean(temp.w[group=="10"])
[1] 1.065
> sd(temp.w[group=="10"])
[1] 0.6792217
> min(temp.w[group=="10"])
[1] 0.1
> median(temp.w[group=="10"])
[1] 1.25
> max(temp.w[group=="10"])
[1] 2.6
> mean(temp.w[group=="11"])
[1] 1.645
> sd(temp.w[group=="11"])
[1] 0.5880163
> min(temp.w[group=="11"])
[1] 0.8
```

```
> median(temp.w[group=="11"])
[1] 1.4
> max(temp.w[group=="11"])
[1] 2.9
>
> #Groups 1, 2 e 7 reported the result "NA" as wires were not inserted
in the specimens. Only brackets were tested.
> #Group 1 served as control (No wires, No MRI).
> #Groups 2 and 7 were tested with no wires and after 1.5 T and 3 T
MRI powers respectively.
>
> #Descriptive statistics (mean, standard deviation, minimum, median
and maximum values) are calculated for each wire size (no wire -
0.014" - 0.019"x0.025").
> mean(temp.w[size=="0"])
[1] NA
> sd(temp.w[size=="0"])
[1] NA
> min(temp.w[size=="0"])
[1] NA
> median(temp.w[size=="0"])
[1] NA
> max(temp.w[size=="0"])
[1] NA
> mean(temp.w[size=="14"])
[1] 0.94
> sd(temp.w[size=="14"])
[1] 0.5268968
> min(temp.w[size=="14"])
[1] 0.1
> median(temp.w[size=="14"])
[1] 1
> max(temp.w[size=="14"])
[1] 2.6
> mean(temp.w[size=="1925"])
[1] 1.36625
> sd(temp.w[size=="1925"])
[1] 0.7713122
> min(temp.w[size=="1925"])
```

```
[1] 0
> median(temp.w[size=="1925"])
[1] 1.4
> max(temp.w[size=="1925"])
[1] 2.9
>
> #Descriptive statistics (mean, standard deviation, minimum, median and maximum values) are calculated for each wire material (no wire - SS - NiTi).
> mean(temp.w[material=="no.wire"])
[1] NA
> sd(temp.w[material=="no.wire"])
[1] NA
> min(temp.w[material=="no.wire"])
[1] NA
> median(temp.w[material=="no.wire"])
[1] NA
> max(temp.w[material=="no.wire"])
[1] NA
> mean(temp.w[material=="SS"])
[1] 1.42625
> sd(temp.w[material=="SS"])
[1] 0.5836905
> min(temp.w[material=="SS"])
[1] 0
> median(temp.w[material=="SS"])
[1] 1.4
> max(temp.w[material=="SS"])
[1] 2.8
> mean(temp.w[material=="NiTi"])
[1] 0.88
> sd(temp.w[material=="NiTi"])
[1] 0.6875751
> min(temp.w[material=="NiTi"])
[1] 0.1
> median(temp.w[material=="NiTi"])
[1] 0.5
> max(temp.w[material=="NiTi"])
[1] 2.9
```

```
>
> #Groups 1, 2 e 7 (no.wire) reported the result "NA" as wires were
not inserted in the specimens. Only brackets were tested.
> #Group 1 served as control (No wires, No MRI).
> #Groups 2 and 7 were tested with no wires and after 1.5 T and 3 T
MRI powers respectively.
>
> #Normality of distributions is tested with Kolmogorov Smirnov test.
> lillie.test(temp.w[size=="14" & material=="SS" & power=="1.5"])

        Lilliefors (Kolmogorov-Smirnov) normality test

data:  temp.w[size == "14" & material == "SS" & power == "1.5"]
D = 0.27769, p-value = 0.0002836

> lillie.test(temp.w[size=="1925" & material=="SS" & power=="1.5"])

        Lilliefors (Kolmogorov-Smirnov) normality test

data:  temp.w[size == "1925" & material == "SS" & power == "1.5"]
D = 0.27371, p-value = 0.0003805

> lillie.test(temp.w[size=="14" & material=="NiTi" & power=="1.5"])

        Lilliefors (Kolmogorov-Smirnov) normality test

data:  temp.w[size == "14" & material == "NiTi" & power == "1.5"]
D = 0.37558, p-value = 4.207e-08

> lillie.test(temp.w[size=="1925" & material=="NiTi" & power=="1.5"])

        Lilliefors (Kolmogorov-Smirnov) normality test

data:  temp.w[size == "1925" & material == "NiTi" & power == "1.5"]
D = 0.33227, p-value = 3.034e-06

> lillie.test(temp.w[size=="14" & material=="SS" & power=="3"])

        Lilliefors (Kolmogorov-Smirnov) normality test
```

```
data:  temp.w[size == "14" & material == "SS" & power == "3"]
D = 0.10402, p-value = 0.8257

> lillie.test(temp.w[size=="1925" & material=="SS" & power=="3"])

        Lilliefors (Kolmogorov-Smirnov) normality test

data:  temp.w[size == "1925" & material == "SS" & power == "3"]
D = 0.13601, p-value = 0.4304

> lillie.test(temp.w[size=="14" & material=="NiTi" & power=="3"])

        Lilliefors (Kolmogorov-Smirnov) normality test

data:  temp.w[size == "14" & material == "NiTi" & power == "3"]
D = 0.13623, p-value = 0.4277

> lillie.test(temp.w[size=="1925" & material=="NiTi" & power=="3"])

        Lilliefors (Kolmogorov-Smirnov) normality test

data:  temp.w[size == "1925" & material == "NiTi" & power == "3"]
D = 0.21153, p-value = 0.01938

> #Kolmogorov Smirnov is mostly not significant, therefore data follow
normal distributions (gaussian).
>
> #ANOVA test is applied.
> total<-paste(size,material,power)
> table(total)
total
  0 no.wire 0 0 no.wire 1.5   0 no.wire 3   14 NiTi 1.5     14 NiTi 3
14 SS 1.5         14 SS 3 1925 NiTi 1.5    1925 NiTi 3    1925 SS 1.5
1925 SS 3
          20            20            20            20            20
20              20              20              20              20
20
> anova(lm(temp.w~total))
```

```
Analysis of Variance Table

Response: temp.w
           Df Sum Sq Mean Sq F value    Pr(>F)
total       7 40.654  5.8077  24.836 < 2.2e-16 ***
Residuals 152 35.544  0.2338
---
Signif. codes:  0 ‘***’ 0.001 ‘**’ 0.01 ‘*’ 0.05 ‘.’ 0.1 ‘ ’ 1
> #Analysis of variance shows a significant result (P<0.05).
>
> #A Tukey post hoc test is performed for pairwise comparisons.
> model<-aov(temp.w~total)
> TukeyHSD(model)
  Tukey multiple comparisons of means
    95% family-wise confidence level

Fit: aov(formula = temp.w ~ total)

$total
                             diff          lwr         upr     p adj
14 NiTi 3-14 NiTi 1.5       0.645  0.174982128  1.1150179 0.0010782
14 SS 1.5-14 NiTi 1.5       0.595  0.124982128  1.0650179 0.0036440
14 SS 3-14 NiTi 1.5         0.840  0.369982128  1.3100179 0.0000045
1925 NiTi 1.5-14 NiTi 1.5  -0.030 -0.500017872  0.4400179 0.9999994
1925 NiTi 3-14 NiTi 1.5     1.225  0.754982128  1.6950179 0.0000000
1925 SS 1.5-14 NiTi 1.5     1.270  0.799982128  1.7400179 0.0000000
1925 SS 3-14 NiTi 1.5       1.320  0.849982128  1.7900179 0.0000000
14 SS 1.5-14 NiTi 3        -0.050 -0.520017872  0.4200179 0.9999799
14 SS 3-14 NiTi 3           0.195 -0.275017872  0.6650179 0.9066578
1925 NiTi 1.5-14 NiTi 3    -0.675 -1.145017872 -0.2049821 0.0004985
1925 NiTi 3-14 NiTi 3       0.580  0.109982128  1.0500179 0.0051596
1925 SS 1.5-14 NiTi 3       0.625  0.154982128  1.0950179 0.0017734
1925 SS 3-14 NiTi 3         0.675  0.204982128  1.1450179 0.0004985
14 SS 3-14 SS 1.5           0.245 -0.225017872  0.7150179 0.7483754
1925 NiTi 1.5-14 SS 1.5    -0.625 -1.095017872 -0.1549821 0.0017734
1925 NiTi 3-14 SS 1.5       0.630  0.159982128  1.1000179 0.0015680
1925 SS 1.5-14 SS 1.5       0.675  0.204982128  1.1450179 0.0004985
1925 SS 3-14 SS 1.5         0.725  0.254982128  1.1950179 0.0001294
1925 NiTi 1.5-14 SS 3      -0.870 -1.340017872 -0.3999821 0.0000018
```

```
1925 NiTi 3-14 SS 3        0.385 -0.085017872  0.8550179 0.1960466
1925 SS 1.5-14 SS 3        0.430 -0.040017872  0.9000179 0.0996802
1925 SS 3-14 SS 3          0.480  0.009982128  0.9500179 0.0415867
1925 NiTi 3-1925 NiTi 1.5  1.255  0.784982128  1.7250179 0.0000000
1925 SS 1.5-1925 NiTi 1.5  1.300  0.829982128  1.7700179 0.0000000
1925 SS 3-1925 NiTi 1.5    1.350  0.879982128  1.8200179 0.0000000
1925 SS 1.5-1925 NiTi 3    0.045 -0.425017872  0.5150179 0.9999903
1925 SS 3-1925 NiTi 3      0.095 -0.375017872  0.5650179 0.9985442
1925 SS 3-1925 SS 1.5      0.050 -0.420017872  0.5200179 0.9999799

> #The significance of the comparisons of all groups each other is
recorded.
>
> #A box plot is drawn, representing the results for each group.
> boxplot(temp.w~group)
> title(ylab="Wire temperature variation (°C)")
> title(xlab="Groups")
>
> #A box plot is drawn, representing the results for each magnetic
field power.
> boxplot(temp.w~power)
> title(ylab="Wire temperature variation (°C)")
> title(xlab="MRI Power (T)")
>
> #A box plot is drawn, representing the results for each wire size.
> boxplot(temp.w~size)
> title(ylab="Wire temperature variation (°C)")
> title(xlab="Wire Size")
>
> #A box plot is drawn, representing the results for each wire
material.
> boxplot(temp.w~material)
> title(ylab="Wire temperature variation (°C)")
> title(xlab="Wire Material")
>
> #Linear regressions.
> #Linear regression with family=gaussian and link=identity parameters
are calculated.
>
```

```
> #The effect of wire material on temperature of the wire is tested.
> linearmodel<-glm(temp.w~material,family=gaussian(link="identity"))
> summary(linearmodel)

Call:
glm(formula = temp.w ~ material, family = gaussian(link = "identity"))

Deviance Residuals:
    Min       1Q   Median       3Q      Max
-1.4263  -0.4263  -0.2263   0.3853   2.0200

Coefficients:
            Estimate Std. Error t value Pr(>|t|)
(Intercept)   0.8800     0.0713  12.342  < 2e-16 ***
materialSS    0.5463     0.1008   5.417 2.22e-07 ***
---
Signif. codes:  0 ‘***’ 0.001 ‘**’ 0.01 ‘*’ 0.05 ‘.’ 0.1 ‘ ’ 1

(Dispersion parameter for gaussian family taken to be 0.4067271)

    Null deviance: 76.198  on 159  degrees of freedom
Residual deviance: 64.263  on 158  degrees of freedom
  (60 observations deleted due to missingness)
AIC: 314.11

Number of Fisher Scoring iterations: 2

> confint(linearmodel)
Waiting for profiling to be done...
                2.5 %    97.5 %
(Intercept) 0.7402491 1.0197509
materialSS  0.3486124 0.7438876
> #P value is highly significant. The temperature variations of the
wires   (temp.w)   are   significantly   influenced   by   wire   materials
(material).
>
> #The effect of wire size on temperature of the wire is tested.
> linearmodel2<-glm(temp.w~size,family=gaussian(link="identity"))
> summary(linearmodel2)
```

```
Call:
glm(formula = temp.w ~ size, family = gaussian(link = "identity"))

Deviance Residuals:
     Min        1Q    Median        3Q       Max
-1.36625  -0.46625   0.03375   0.43375   1.66000

Coefficients:
             Estimate Std. Error t value Pr(>|t|)
(Intercept) 9.369e-01  7.439e-02  12.594  < 2e-16 ***
size        2.231e-04  5.465e-05   4.081 7.09e-05 ***
---
Signif. codes:  0 ‘***’ 0.001 ‘**’ 0.01 ‘*’ 0.05 ‘.’ 0.1 ‘ ’ 1

(Dispersion parameter for gaussian family taken to be 0.4362714)

    Null deviance: 76.198  on 159  degrees of freedom
Residual deviance: 68.931  on 158  degrees of freedom
  (60 observations deleted due to missingness)
AIC: 325.33

Number of Fisher Scoring iterations: 2

> confint(linearmodel2)
Waiting for profiling to be done...
                   2.5 %       97.5 %
(Intercept) 0.7910754571 1.0826791216
size        0.0001159393 0.0003301622
> #P value is highly significant. The temperature variations of the
wires (temp.w) are significantly influenced by wire sizes (size).
>
> #The effect of MRI power on temperature of the wire is tested.
> linearmodel3<-glm(temp.w~power,family=gaussian(link="identity"))
> summary(linearmodel3)

Call:
glm(formula = temp.w ~ power, family = gaussian(link = "identity"))
```

```
Deviance Residuals:
    Min       1Q   Median       3Q      Max
-1.4275  -0.3787  -0.0275   0.2847   1.9212

Coefficients:
            Estimate Std. Error t value Pr(>|t|)
(Intercept)  0.33000    0.15930   2.072   0.0399 *
power        0.36583    0.06717   5.447 1.93e-07 ***
---
Signif. codes:  0 ‘***’ 0.001 ‘**’ 0.01 ‘*’ 0.05 ‘.’ 0.1 ‘ ’ 1

(Dispersion parameter for gaussian family taken to be 0.406034)

    Null deviance: 76.198  on 159  degrees of freedom
Residual deviance: 64.153  on 158  degrees of freedom
  (60 observations deleted due to missingness)
AIC: 313.84

Number of Fisher Scoring iterations: 2

> confint(linearmodel3)
Waiting for profiling to be done...
                2.5 %    97.5 %
(Intercept) 0.01777382 0.6422262
power       0.23418722 0.4974794
> #P value is highly significant. The temperature variations of the
wires (temp.w) are significantly influenced by MRI power (power).
>
> #The effect of temperature of the bracket on temperature of the wire
is tested.
> linearmodel4<-glm(temp.w~temp.b,family=gaussian(link="identity"))
> summary(linearmodel4)

Call:
glm(formula = temp.w ~ temp.b, family = gaussian(link = "identity"))

Deviance Residuals:
     Min        1Q    Median        3Q       Max
-1.26956  -0.30908  -0.08188   0.29633   1.86689
```

```
Coefficients:
            Estimate Std. Error t value Pr(>|t|)
(Intercept)  0.58681    0.05956   9.853   <2e-16 ***
temp.b       0.48768    0.03887  12.547   <2e-16 ***
---
Signif. codes:  0 ‘***’ 0.001 ‘**’ 0.01 ‘*’ 0.05 ‘.’ 0.1 ‘ ’ 1

(Dispersion parameter for gaussian family taken to be 0.2415805)

    Null deviance: 76.198  on 159  degrees of freedom
Residual deviance: 38.170  on 158  degrees of freedom
  (60 observations deleted due to missingness)
AIC: 230.76

Number of Fisher Scoring iterations: 2

> confint(linearmodel4)
Waiting for profiling to be done...
                2.5 %    97.5 %
(Intercept) 0.4700778 0.7035432
temp.b      0.4114942 0.5638591
> #P value is highly significant. The temperature variations of the
wires (temp.w) are significantly influenced by the temperature
variations of the brackets (temp.b).
>
>
>
>
>
> ################################################
>
>
>
>
>
> ###Analysis of the temperatures of the shear bond strength values
(mpa) in the various groups.
>
```

```
> #Descriptive statistics (mean, standard deviation, minimum, median
and maximum values) are calculated for each group
>
> mean(mpa[size=="0" & material=="no.wire" & power=="0"])
[1] 26.4525
> sd(mpa[size=="0" & material=="no.wire" & power=="0"])
[1] 4.637291
> min(mpa[size=="0" & material=="no.wire" & power=="0"])
[1] 18.44
> median(mpa[size=="0" & material=="no.wire" & power=="0"])
[1] 25.26
> max(mpa[size=="0" & material=="no.wire" & power=="0"])
[1] 33.44
> mean(mpa[size=="0" & material=="no.wire" & power=="1.5"])
[1] 25.067
> sd(mpa[size=="0" & material=="no.wire" & power=="1.5"])
[1] 4.358841
> min(mpa[size=="0" & material=="no.wire" & power=="1.5"])
[1] 16.35
> median(mpa[size=="0" & material=="no.wire" & power=="1.5"])
[1] 25.13
> max(mpa[size=="0" & material=="no.wire" & power=="1.5"])
[1] 33.29
> mean(mpa[size=="14" & material=="SS" & power=="1.5"])
[1] 24.908
> sd(mpa[size=="14" & material=="SS" & power=="1.5"])
[1] 3.562739
> min(mpa[size=="14" & material=="SS" & power=="1.5"])
[1] 18.02
> median(mpa[size=="14" & material=="SS" & power=="1.5"])
[1] 24.64
> max(mpa[size=="14" & material=="SS" & power=="1.5"])
[1] 33.81
> mean(mpa[size=="1925" & material=="SS" & power=="1.5"])
[1] 24.491
> sd(mpa[size=="1925" & material=="SS" & power=="1.5"])
[1] 4.303338
> min(mpa[size=="1925" & material=="SS" & power=="1.5"])
[1] 18.23
```

```
> median(mpa[size=="1925" & material=="SS" & power=="1.5"])
[1] 24.85
> max(mpa[size=="1925" & material=="SS" & power=="1.5"])
[1] 31.99
> mean(mpa[size=="14" & material=="NiTi" & power=="1.5"])
[1] 23.3335
> sd(mpa[size=="14" & material=="NiTi" & power=="1.5"])
[1] 4.784804
> min(mpa[size=="14" & material=="NiTi" & power=="1.5"])
[1] 15.98
> median(mpa[size=="14" & material=="NiTi" & power=="1.5"])
[1] 23.015
> max(mpa[size=="14" & material=="NiTi" & power=="1.5"])
[1] 31.07
> mean(mpa[size=="1925" & material=="NiTi" & power=="1.5"])
[1] 25.2945
> sd(mpa[size=="1925" & material=="NiTi" & power=="1.5"])
[1] 5.143565
> mean(mpa[size=="1925" & material=="NiTi" & power=="1.5"])
[1] 25.2945
> median(mpa[size=="1925" & material=="NiTi" & power=="1.5"])
[1] 24.685
> max(mpa[size=="1925" & material=="NiTi" & power=="1.5"])
[1] 35.43
> mean(mpa[size=="0" & material=="no.wire" & power=="3"])
[1] 24.388
> sd(mpa[size=="0" & material=="no.wire" & power=="3"])
[1] 5.55665
> min(mpa[size=="0" & material=="no.wire" & power=="3"])
[1] 14.76
> median(mpa[size=="0" & material=="no.wire" & power=="3"])
[1] 24.68
> max(mpa[size=="0" & material=="no.wire" & power=="3"])
[1] 33.95
> mean(mpa[size=="14" & material=="SS" & power=="3"])
[1] 24.2105
> sd(mpa[size=="14" & material=="SS" & power=="3"])
[1] 4.708955
> min(mpa[size=="14" & material=="SS" & power=="3"])
```

```
[1] 16.2
> median(mpa[size=="14" & material=="SS" & power=="3"])
[1] 24.005
> max(mpa[size=="14" & material=="SS" & power=="3"])
[1] 34.62
> mean(mpa[size=="1925" & material=="SS" & power=="3"])
[1] 24.5095
> sd(mpa[size=="1925" & material=="SS" & power=="3"])
[1] 5.523557
> min(mpa[size=="1925" & material=="SS" & power=="3"])
[1] 12.04
> median(mpa[size=="1925" & material=="SS" & power=="3"])
[1] 24.52
> max(mpa[size=="1925" & material=="SS" & power=="3"])
[1] 33.13
> mean(mpa[size=="14" & material=="NiTi" & power=="3"])
[1] 24.3815
> sd(mpa[size=="14" & material=="NiTi" & power=="3"])
[1] 5.438834
> min(mpa[size=="14" & material=="NiTi" & power=="3"])
[1] 14.18
> median(mpa[size=="14" & material=="NiTi" & power=="3"])
[1] 23.815
> max(mpa[size=="14" & material=="NiTi" & power=="3"])
[1] 34.83
> mean(mpa[size=="1925" & material=="NiTi" & power=="3"])
[1] 24.338
> sd(mpa[size=="1925" & material=="NiTi" & power=="3"])
[1] 5.240093
> min(mpa[size=="1925" & material=="NiTi" & power=="3"])
[1] 14.94
> median(mpa[size=="1925" & material=="NiTi" & power=="3"])
[1] 24.77
> max(mpa[size=="1925" & material=="NiTi" & power=="3"])
[1] 31.85
>
> #Descriptive statistics (mean, standard deviation, minimum, median
and maximum values) are calculated for each wire size (no wire -
0.014" - 0.019"x0.025").
```

```
> mean(mpa[size=="0"])
[1] 25.3025
> sd(mpa[size=="0"])
[1] 4.872113
> min(mpa[size=="0"])
[1] 14.76
> median(mpa[size=="0"])
[1] 25.12
> max(mpa[size=="0"])
[1] 33.95
> mean(mpa[size=="14"])
[1] 24.20838
> sd(mpa[size=="14"])
[1] 4.618629
> min(mpa[size=="14"])
[1] 14.18
> median(mpa[size=="14"])
[1] 24.035
> max(mpa[size=="14"])
[1] 34.83
> mean(mpa[size=="1925"])
[1] 24.65825
> sd(mpa[size=="1925"])
[1] 4.989953
> min(mpa[size=="1925"])
[1] 12.04
> median(mpa[size=="1925"])
[1] 24.75
> max(mpa[size=="1925"])
[1] 35.43
>
> #Descriptive statistics (mean, standard deviation, minimum, median
and maximum values) are calculated for each wire material (no wire -
SS - NiTi).
> mean(mpa[material=="no.wire"])
[1] 25.3025
> sd(mpa[material=="no.wire"])
[1] 4.872113
> min(mpa[material=="no.wire"])
```

```
[1] 14.76
> median(mpa[material=="no.wire"])
[1] 25.12
> max(mpa[material=="no.wire"])
[1] 33.95
> mean(mpa[material=="SS"])
[1] 24.52975
> sd(mpa[material=="SS"])
[1] 4.498885
> min(mpa[material=="SS"])
[1] 12.04
> median(mpa[material=="SS"])
[1] 24.675
> max(mpa[material=="SS"])
[1] 34.62
> mean(mpa[material=="NiTi"])
[1] 24.33687
> sd(mpa[material=="NiTi"])
[1] 5.106372
> min(mpa[material=="NiTi"])
[1] 14.18
> median(mpa[material=="NiTi"])
[1] 24.39
> max(mpa[material=="NiTi"])
[1] 35.43
>
> #Normality of distributions is tested with Kolmogorov Smirnov test.
> lillie.test(mpa[size=="0" & material=="no.wire" & power=="0"])

        Lilliefors (Kolmogorov-Smirnov) normality test

data:  mpa[size == "0" & material == "no.wire" & power == "0"]
D = 0.17124, p-value = 0.1292

> lillie.test(mpa[size=="0" & material=="no.wire" & power=="1.5"])

        Lilliefors (Kolmogorov-Smirnov) normality test

data:  mpa[size == "0" & material == "no.wire" & power == "1.5"]
```

```
D = 0.11347, p-value = 0.7166

> lillie.test(mpa[size=="14" & material=="SS" & power=="1.5"])

        Lilliefors (Kolmogorov-Smirnov) normality test

data:  mpa[size == "14" & material == "SS" & power == "1.5"]
D = 0.15768, p-value = 0.2149

> lillie.test(mpa[size=="1925" & material=="SS" & power=="1.5"])

        Lilliefors (Kolmogorov-Smirnov) normality test

data:  mpa[size == "1925" & material == "SS" & power == "1.5"]
D = 0.13261, p-value = 0.4716

> lillie.test(mpa[size=="14" & material=="NiTi" & power=="1.5"])

        Lilliefors (Kolmogorov-Smirnov) normality test

data:  mpa[size == "14" & material == "NiTi" & power == "1.5"]
D = 0.10414, p-value = 0.8245

> lillie.test(mpa[size=="1925" & material=="NiTi" & power=="1.5"])

        Lilliefors (Kolmogorov-Smirnov) normality test

data:  mpa[size == "1925" & material == "NiTi" & power == "1.5"]
D = 0.16781, p-value = 0.1474

> lillie.test(mpa[size=="0" & material=="no.wire" & power=="3"])

        Lilliefors (Kolmogorov-Smirnov) normality test

data:  mpa[size == "0" & material == "no.wire" & power == "3"]
D = 0.12933, p-value = 0.5125

> lillie.test(mpa[size=="14" & material=="SS" & power=="3"])
```

```
        Lilliefors (Kolmogorov-Smirnov) normality test

data:  mpa[size == "14" & material == "SS" & power == "3"]
D = 0.15444, p-value = 0.241

> lillie.test(mpa[size=="1925" & material=="SS" & power=="3"])

        Lilliefors (Kolmogorov-Smirnov) normality test

data:  mpa[size == "1925" & material == "SS" & power == "3"]
D = 0.16616, p-value = 0.157

> lillie.test(mpa[size=="14" & material=="NiTi" & power=="3"])

        Lilliefors (Kolmogorov-Smirnov) normality test

data:  mpa[size == "14" & material == "NiTi" & power == "3"]
D = 0.097176, p-value = 0.8899

> lillie.test(mpa[size=="1925" & material=="NiTi" & power=="3"])

        Lilliefors (Kolmogorov-Smirnov) normality test

data:  mpa[size == "1925" & material == "NiTi" & power == "3"]
D = 0.16107, p-value = 0.1899

> #Kolmogorov Smirnov is mostly not significant, therefore data follow
normal distributions (gaussian).
>
> #ANOVA test is applied.
> total<-paste(size,material,power)
> table(total)
total
  0 no.wire 0 0 no.wire 1.5   0 no.wire 3   14 NiTi 1.5     14 NiTi 3
14 SS 1.5         14 SS 3 1925 NiTi 1.5    1925 NiTi 3    1925 SS 1.5
1925 SS 3
          20            20            20            20            20
20               20               20               20               20
20
```

```
> anova(lm(mpa~total))
Analysis of Variance Table

Response: mpa
           Df Sum Sq Mean Sq F value Pr(>F)
total      10  122.2  12.219  0.5137 0.8795
Residuals 209 4971.7  23.788
> #Analysis of variance shows a not significant result (P>0.05). No
post hoc test is performed.
>
> #A box plot is drawn, representing the results for each group.
> boxplot(mpa~group)
> title(ylab="Shear bond strength (MPa)")
> title(xlab="Groups")
>
> #A box plot is drawn, representing the results for each magnetic
field power.
> boxplot(mpa~power)
> title(ylab="Shear bond strength (MPa)")
> title(xlab="MRI Power (T)")
>
> #A box plot is drawn, representing the results for each wire size.
> boxplot(mpa~size)
> title(ylab="Shear bond strength (MPa)")
> title(xlab="Wire Size")
>
> #A box plot is drawn, representing the results for each wire
material.
> boxplot(mpa~material)
> title(ylab="Shear bond strength (MPa)")
> title(xlab="Wire Material")
>
> #Linear regressions.
> #Linear regression with family=gaussian and link=identity parameters
are calculated.
>
> #The effect of wire material on shear bond strength is tested.
> linearmodel<-glm(mpa~material,family=gaussian(link="identity"))
> summary(linearmodel)
```

```
Call:
glm(formula = mpa ~ material, family = gaussian(link = "identity"))

Deviance Residuals:
     Min        1Q    Median        3Q       Max
-12.4898   -3.2798    0.0267    3.1806   11.0931

Coefficients:
                Estimate Std. Error t value Pr(>|t|)
(Intercept)      24.3369     0.5399  45.081   <2e-16 ***
materialno.wire   0.9656     0.8246   1.171    0.243
materialSS        0.1929     0.7635   0.253    0.801
---
Signif. codes:  0 ‘***’ 0.001 ‘**’ 0.01 ‘*’ 0.05 ‘.’ 0.1 ‘ ’ 1

(Dispersion parameter for gaussian family taken to be 23.31519)

    Null deviance: 5093.9  on 219  degrees of freedom
Residual deviance: 5059.4  on 217  degrees of freedom
AIC: 1322.1

Number of Fisher Scoring iterations: 2

> confint(linearmodel)
Waiting for profiling to be done...
                     2.5 %    97.5 %
(Intercept)     23.2787850 25.394965
materialno.wire -0.6506342  2.581884
materialSS      -1.3034903  1.689240
> #P value is not significant. The shear bond strength values (mpa)
are not significantly influenced by wire materials (material).
>
> #The effect of wire size on shear bond strength is tested.
> linearmodel2<-glm(mpa~size,family=gaussian(link="identity"))
> summary(linearmodel2)

Call:
glm(formula = mpa ~ size, family = gaussian(link = "identity"))
```

```
Deviance Residuals:
    Min       1Q   Median       3Q      Max
-12.615   -3.538    0.033    3.149   10.775

Coefficients:
             Estimate Std. Error t value Pr(>|t|)
(Intercept)  2.468e+01  4.102e-01  60.158   <2e-16 ***
size        -1.274e-05  3.534e-04  -0.036    0.971
---
Signif. codes:  0 ‘***’ 0.001 ‘**’ 0.01 ‘*’ 0.05 ‘.’ 0.1 ‘ ’ 1

(Dispersion parameter for gaussian family taken to be 23.36615)

    Null deviance: 5093.9  on 219  degrees of freedom
Residual deviance: 5093.8  on 218  degrees of freedom
AIC: 1321.6

Number of Fisher Scoring iterations: 2

> confint(linearmodel2)
Waiting for profiling to be done...
                    2.5 %       97.5 %
(Intercept) 23.8752812870 2.548341e+01
size        -0.0007053871 6.799138e-04
> #P value is not significant. The shear bond strength values (mpa)
are not significantly influenced by wire sizes (size).
>
> #The effect of MRI power on shear bond strength is tested.
> linearmodel3<-glm(mpa~power,family=gaussian(link="identity"))
> summary(linearmodel3)

Call:
glm(formula = mpa ~ power, family = gaussian(link = "identity"))

Deviance Residuals:
     Min        1Q    Median        3Q       Max
-12.1675   -3.4717   -0.1199    3.2751   10.6225
```

```
Coefficients:
            Estimate Std. Error t value Pr(>|t|)
(Intercept)  25.6623     0.7607  33.736   <2e-16 ***
power        -0.4849     0.3364  -1.442    0.151
---
Signif. codes:  0 ‘***’ 0.001 ‘**’ 0.01 ‘*’ 0.05 ‘.’ 0.1 ‘ ’ 1

(Dispersion parameter for gaussian family taken to be 23.14563)

    Null deviance: 5093.9  on 219  degrees of freedom
Residual deviance: 5045.7  on 218  degrees of freedom
AIC: 1319.5

Number of Fisher Scoring iterations: 2

> confint(linearmodel3)
Waiting for profiling to be done...
                2.5 %     97.5 %
(Intercept) 24.171386 27.1532142
power       -1.144254  0.1743604
> #P value is not significant. The shear bond strength values (mpa)
are not significantly influenced by MRI power (power).
>
> #The effect of temperature of the bracket on shear bond strength is
tested.
> linearmodel4<-glm(mpa~temp.b,family=gaussian(link="identity"))
> summary(linearmodel4)

Call:
glm(formula = mpa ~ temp.b, family = gaussian(link = "identity"))

Deviance Residuals:
     Min        1Q    Median        3Q       Max
-12.5237   -3.3842   -0.0248    3.2485   10.5240

Coefficients:
            Estimate Std. Error t value Pr(>|t|)
(Intercept)  24.8832     0.4479  55.550   <2e-16 ***
temp.b       -0.2282     0.3299  -0.692     0.49
```

```
---
Signif. codes:  0 ‘***’ 0.001 ‘**’ 0.01 ‘*’ 0.05 ‘.’ 0.1 ‘ ’ 1

(Dispersion parameter for gaussian family taken to be 23.31511)

    Null deviance: 5093.9  on 219  degrees of freedom
Residual deviance: 5082.7  on 218  degrees of freedom
AIC: 1321.1

Number of Fisher Scoring iterations: 2

> confint(linearmodel4)
Waiting for profiling to be done...
                2.5 %     97.5 %
(Intercept) 24.0052681 25.7611738
temp.b      -0.8747745  0.4183553
> #P value is not significant. The shear bond strength values (mpa) are not significantly influenced by temperature variations of the brackets (temp.b).
>
> #The effect of temperature of the wire on shear bond strength is tested.
> linearmodel5<-glm(mpa~temp.w,family=gaussian(link="identity"))
> summary(linearmodel5)

Call:
glm(formula = mpa ~ temp.w, family = gaussian(link = "identity"))

Deviance Residuals:
     Min        1Q    Median        3Q       Max
-12.5700   -3.5674    0.0506    3.2105   11.2550

Coefficients:
            Estimate Std. Error t value Pr(>|t|)
(Intercept)  23.9773     0.7398  32.411   <2e-16 ***
temp.w        0.3955     0.5505   0.718    0.474
---
Signif. codes:  0 ‘***’ 0.001 ‘**’ 0.01 ‘*’ 0.05 ‘.’ 0.1 ‘ ’ 1
```

```
(Dispersion parameter for gaussian family taken to be 23.0915)

    Null deviance: 3660.4  on 159  degrees of freedom
Residual deviance: 3648.5  on 158  degrees of freedom
  (60 observations deleted due to missingness)
AIC: 960.36

Number of Fisher Scoring iterations: 2

> confint(linearmodel5)
Waiting for profiling to be done...
                 2.5 %    97.5 %
(Intercept) 22.5273434 25.427240
temp.w      -0.6834841  1.474415
> #P value is not significant. The shear bond strength values (mpa) are not significantly influenced by temperature variations of the wires (temp.w).
>
>
>
>
>
> ################################################
>
>
>
>
>
>  ###Analysis of the adhesive remnant index scores (ari) in the variuous groups
>
> #ARI table is created.
> table(group,ari)
     ari
group  0  1  2  3
   1   3 15  1  1
   2  10  9  1  0
   3  11  6  2  1
   4  11  8  1  0
```

```
   5   9  6  5  0
   6   9  8  3  0
   7  11  9  0  0
   8  11  7  2  0
   9  11  9  0  0
   10 10  9  1  0
   11 12  7  0  1
> tab<-table(ari,group)
> tab
   group
ari  1  2  3  4  5  6  7  8  9 10 11
  0  3 10 11 11  9  9 11 11 11 10 12
  1 15  9  6  8  6  8  9  7  9  9  7
  2  1  1  2  1  5  3  0  2  0  1  0
  3  1  0  1  0  0  0  0  0  0  0  1
> apply(tab,2,sum)
 1  2  3  4  5  6  7  8  9 10 11
20 20 20 20 20 20 20 20 20 20 20
>
> #Percentages are calculated. An histogram is realized.
> tabp<-apply(tab,2,function(x){x/20*100})
>                                                                    xlim<-
barplot(tabp,las=2,legend.text=c("0","1","2","3"),xlim=c(0,14.5))
> title(ylab="Frequency distribution (%)")
>
> #Frequencies are analized with Fisher test.
>
> #ari==0
> M<-rbind(tab[1,],apply(tab,2,sum)-tab[1,])
> simulate.p.value=TRUE
> fisher.test(M, workspace = 2e8)

        Fisher's Exact Test for Count Data

data:  M
p-value = 0.2544
alternative hypothesis: two.sided

> ccb<-combn(1:10,2);ccb
```

```
     [,1] [,2] [,3] [,4] [,5] [,6] [,7] [,8] [,9] [,10] [,11] [,12]
[,13] [,14] [,15] [,16] [,17] [,18] [,19] [,20] [,21] [,22] [,23]
[,24] [,25] [,26] [,27] [,28] [,29] [,30] [,31] [,32] [,33] [,34]
[,35] [,36] [,37] [,38]
[1,]    1    1    1    1    1    1    1    1    1      2      2      2
2      2      2      2      2      3      3      3      3      3      3      3
4      4      4      4      4      4      5      5      5      5      5      6
6      6
[2,]    2    3    4    5    6    7    8    9   10      3      4      5
6      7      8      9     10      4      5      6      7      8      9     10
5      6      7      8      9     10      6      7      8      9     10      7
8      9
     [,39] [,40] [,41] [,42] [,43] [,44] [,45]
[1,]     6     7     7     7     8     8     9
[2,]    10     8     9    10     9    10    10
> for(i in 1:45){
+      print(paste(paste(colnames(M[,c(ccb[1,i],ccb[2,i])]),collapse="-
"),"p=",fisher.test(M[,c(ccb[1,i],ccb[2,i])])$p.value))
+ }
[1] "1-2 p= 0.0407423950249312"
[1] "1-3 p= 0.0187011260426166"
[1] "1-4 p= 0.0187011260426166"
[1] "1-5 p= 0.0823587770195111"
[1] "1-6 p= 0.0823587770195111"
[1] "1-7 p= 0.0187011260426166"
[1] "1-8 p= 0.0187011260426166"
[1] "1-9 p= 0.0187011260426166"
[1] "1-10 p= 0.0407423950249312"
[1] "2-3 p= 1"
[1] "2-4 p= 1"
[1] "2-5 p= 1"
[1] "2-6 p= 1"
[1] "2-7 p= 1"
[1] "2-8 p= 1"
[1] "2-9 p= 1"
[1] "2-10 p= 1"
[1] "3-4 p= 1"
[1] "3-5 p= 0.752371134563909"
[1] "3-6 p= 0.752371134563909"
```

```
[1] "3-7 p= 1"
[1] "3-8 p= 1"
[1] "3-9 p= 1"
[1] "3-10 p= 1"
[1] "4-5 p= 0.752371134563909"
[1] "4-6 p= 0.752371134563909"
[1] "4-7 p= 1"
[1] "4-8 p= 1"
[1] "4-9 p= 1"
[1] "4-10 p= 1"
[1] "5-6 p= 1"
[1] "5-7 p= 0.752371134563909"
[1] "5-8 p= 0.752371134563909"
[1] "5-9 p= 0.752371134563909"
[1] "5-10 p= 1"
[1] "6-7 p= 0.752371134563909"
[1] "6-8 p= 0.752371134563909"
[1] "6-9 p= 0.752371134563909"
[1] "6-10 p= 1"
[1] "7-8 p= 1"
[1] "7-9 p= 1"
[1] "7-10 p= 1"
[1] "8-9 p= 1"
[1] "8-10 p= 1"
[1] "9-10 p= 1"
>
> #Function check:
> fisher.test(M[,c(1,2)])

        Fisher's Exact Test for Count Data

data:  M[, c(1, 2)]
p-value = 0.04074
alternative hypothesis: true odds ratio is not equal to 1
95 percent confidence interval:
 0.02632766 0.94457354
sample estimates:
odds ratio
  0.184812
```

```
> fisher.test(M[,c(1,3)])

        Fisher's Exact Test for Count Data

data:  M[, c(1, 3)]
p-value = 0.0187
alternative hypothesis: true odds ratio is not equal to 1
95 percent confidence interval:
 0.02161473 0.77428598
sample estimates:
odds ratio
 0.1522633

> fisher.test(M[,c(1,4)])

        Fisher's Exact Test for Count Data

data:  M[, c(1, 4)]
p-value = 0.0187
alternative hypothesis: true odds ratio is not equal to 1
95 percent confidence interval:
 0.02161473 0.77428598
sample estimates:
odds ratio
 0.1522633

> fisher.test(M[,c(1,5)])

        Fisher's Exact Test for Count Data

data:  M[, c(1, 5)]
p-value = 0.08236
alternative hypothesis: true odds ratio is not equal to 1
95 percent confidence interval:
 0.03190662 1.16159463
sample estimates:
odds ratio
 0.2244591
```

```
>
> #ari==1
> M<-rbind(tab[2,],apply(tab,2,sum)-tab[2,])
> simulate.p.value=TRUE
> fisher.test(M, workspace = 2e8)

        Fisher's Exact Test for Count Data

data:  M
p-value = 0.2695
alternative hypothesis: two.sided

> ccb<-combn(1:10,2);ccb
     [,1] [,2] [,3] [,4] [,5] [,6] [,7] [,8] [,9] [,10] [,11] [,12]
[,13] [,14] [,15] [,16] [,17] [,18] [,19] [,20] [,21] [,22] [,23]
[,24] [,25] [,26] [,27] [,28] [,29] [,30] [,31] [,32] [,33] [,34]
[,35] [,36] [,37] [,38]
[1,]    1    1    1    1    1    1    1    1    1     2     2     2
2     2     2     2     2     3     3     3     3     3     3     3
4     4     4     4     4     4     5     5     5     5     5     6
6     6
[2,]    2    3    4    5    6    7    8    9   10     3     4     5
6     7     8     9    10     4     5     6     7     8     9    10
5     6     7     8     9    10     6     7     8     9    10     7
8     9
     [,39] [,40] [,41] [,42] [,43] [,44] [,45]
[1,]     6     7     7     7     8     8     9
[2,]    10     8     9    10     9    10    10
> for(i in 1:45){
+      print(paste(paste(colnames(M[,c(ccb[1,i],ccb[2,i])]),collapse="-
"),"p=",fisher.test(M[,c(ccb[1,i],ccb[2,i])])$p.value))
+ }
[1] "1-2 p= 0.105340267965407"
[1] "1-3 p= 0.0103867021988606"
[1] "1-4 p= 0.0535509925943741"
[1] "1-5 p= 0.0103867021988606"
[1] "1-6 p= 0.0535509925943741"
[1] "1-7 p= 0.105340267965407"
```

```
[1] "1-8 p= 0.0248417203778233"
[1] "1-9 p= 0.105340267965407"
[1] "1-10 p= 0.105340267965407"
[1] "2-3 p= 0.514475543396567"
[1] "2-4 p= 1"
[1] "2-5 p= 0.514475543396567"
[1] "2-6 p= 1"
[1] "2-7 p= 1"
[1] "2-8 p= 0.747527282566215"
[1] "2-9 p= 1"
[1] "2-10 p= 1"
[1] "3-4 p= 0.741053623144835"
[1] "3-5 p= 1"
[1] "3-6 p= 0.741053623144835"
[1] "3-7 p= 0.514475543396567"
[1] "3-8 p= 1"
[1] "3-9 p= 0.514475543396567"
[1] "3-10 p= 0.514475543396567"
[1] "4-5 p= 0.741053623144835"
[1] "4-6 p= 1"
[1] "4-7 p= 1"
[1] "4-8 p= 1"
[1] "4-9 p= 1"
[1] "4-10 p= 1"
[1] "5-6 p= 0.741053623144835"
[1] "5-7 p= 0.514475543396567"
[1] "5-8 p= 1"
[1] "5-9 p= 0.514475543396567"
[1] "5-10 p= 0.514475543396567"
[1] "6-7 p= 1"
[1] "6-8 p= 1"
[1] "6-9 p= 1"
[1] "6-10 p= 1"
[1] "7-8 p= 0.747527282566215"
[1] "7-9 p= 1"
[1] "7-10 p= 1"
[1] "8-9 p= 0.747527282566215"
[1] "8-10 p= 0.747527282566215"
[1] "9-10 p= 1"
```

```
>
> #ari==2
> M<-rbind(tab[3,],apply(tab,2,sum)-tab[3,])
> simulate.p.value=TRUE
> fisher.test(M, workspace = 2e8)

        Fisher's Exact Test for Count Data

data:  M
p-value = 0.1091
alternative hypothesis: two.sided

> ccb<-combn(1:10,2);ccb
     [,1] [,2] [,3] [,4] [,5] [,6] [,7] [,8] [,9] [,10] [,11] [,12]
[,13] [,14] [,15] [,16] [,17] [,18] [,19] [,20] [,21] [,22] [,23]
[,24] [,25] [,26] [,27] [,28] [,29] [,30] [,31] [,32] [,33] [,34]
[,35] [,36] [,37] [,38]
[1,]    1    1    1    1    1    1    1    1    1     2     2     2
2     2     2     2     2     3     3     3     3     3     3     3
4     4     4     4     4     4     5     5     5     5     5     6
6     6
[2,]    2    3    4    5    6    7    8    9   10     3     4     5
6     7     8     9    10     4     5     6     7     8     9    10
5     6     7     8     9    10     6     7     8     9    10     7
8     9
     [,39] [,40] [,41] [,42] [,43] [,44] [,45]
[1,]     6     7     7     7     8     8     9
[2,]    10     8     9    10     9    10    10
> for(i in 1:45){
+      print(paste(paste(colnames(M[,c(ccb[1,i],ccb[2,i])]),collapse="-
"),"p=",fisher.test(M[,c(ccb[1,i],ccb[2,i])])$p.value))
+ }
[1] "1-2 p= 1"
[1] "1-3 p= 1"
[1] "1-4 p= 1"
[1] "1-5 p= 0.181764181764182"
[1] "1-6 p= 0.604989604989605"
[1] "1-7 p= 1"
[1] "1-8 p= 1"
```

```
[1] "1-9 p= 1"
[1] "1-10 p= 1"
[1] "2-3 p= 1"
[1] "2-4 p= 1"
[1] "2-5 p= 0.181764181764182"
[1] "2-6 p= 0.604989604989605"
[1] "2-7 p= 1"
[1] "2-8 p= 1"
[1] "2-9 p= 1"
[1] "2-10 p= 1"
[1] "3-4 p= 1"
[1] "3-5 p= 0.407484407484408"
[1] "3-6 p= 1"
[1] "3-7 p= 0.487179487179487"
[1] "3-8 p= 1"
[1] "3-9 p= 0.487179487179487"
[1] "3-10 p= 1"
[1] "4-5 p= 0.181764181764182"
[1] "4-6 p= 0.604989604989605"
[1] "4-7 p= 1"
[1] "4-8 p= 1"
[1] "4-9 p= 1"
[1] "4-10 p= 1"
[1] "5-6 p= 0.694764694764695"
[1] "5-7 p= 0.0471240471240471"
[1] "5-8 p= 0.407484407484408"
[1] "5-9 p= 0.0471240471240471"
[1] "5-10 p= 0.181764181764182"
[1] "6-7 p= 0.230769230769231"
[1] "6-8 p= 1"
[1] "6-9 p= 0.230769230769231"
[1] "6-10 p= 0.604989604989605"
[1] "7-8 p= 0.487179487179487"
[1] "7-9 p= 1"
[1] "7-10 p= 1"
[1] "8-9 p= 0.487179487179487"
[1] "8-10 p= 1"
[1] "9-10 p= 1"
>
```

```
> #ari==3
> M<-rbind(tab[4,],apply(tab,2,sum)-tab[4,])
> simulate.p.value=TRUE
> fisher.test(M, workspace = 2e8)
Errore: cannot allocate vector of size 762.9 Mb
> ccb<-combn(1:10,2);ccb
     [,1] [,2] [,3] [,4] [,5] [,6] [,7] [,8] [,9] [,10] [,11] [,12]
[,13] [,14] [,15] [,16] [,17] [,18] [,19] [,20] [,21] [,22] [,23]
[,24] [,25] [,26] [,27] [,28] [,29] [,30] [,31] [,32] [,33] [,34]
[,35] [,36] [,37] [,38]
[1,]    1    1    1    1    1    1    1    1    1     2     2     2
2     2     2     2     2     3     3     3     3     3     3     3
4     4     4     4     4     4     5     5     5     5     5     6
6     6
[2,]    2    3    4    5    6    7    8    9   10     3     4     5
6     7     8     9    10     4     5     6     7     8     9    10
5     6     7     8     9    10     6     7     8     9    10     7
8     9
     [,39] [,40] [,41] [,42] [,43] [,44] [,45]
[1,]     6     7     7     7     8     8     9
[2,]    10     8     9    10     9    10    10
> for(i in 1:45){
+      print(paste(paste(colnames(M[,c(ccb[1,i],ccb[2,i])]),collapse="-
"),"p=",fisher.test(M[,c(ccb[1,i],ccb[2,i])])$p.value))
+ }
[1] "1-2 p= 1"
[1] "1-3 p= 1"
[1] "1-4 p= 1"
[1] "1-5 p= 1"
[1] "1-6 p= 1"
[1] "1-7 p= 1"
[1] "1-8 p= 1"
[1] "1-9 p= 1"
[1] "1-10 p= 1"
[1] "2-3 p= 1"
[1] "2-4 p= 1"
[1] "2-5 p= 1"
[1] "2-6 p= 1"
[1] "2-7 p= 1"
```

```
[1] "2-8 p= 1"
[1] "2-9 p= 1"
[1] "2-10 p= 1"
[1] "3-4 p= 1"
[1] "3-5 p= 1"
[1] "3-6 p= 1"
[1] "3-7 p= 1"
[1] "3-8 p= 1"
[1] "3-9 p= 1"
[1] "3-10 p= 1"
[1] "4-5 p= 1"
[1] "4-6 p= 1"
[1] "4-7 p= 1"
[1] "4-8 p= 1"
[1] "4-9 p= 1"
[1] "4-10 p= 1"
[1] "5-6 p= 1"
[1] "5-7 p= 1"
[1] "5-8 p= 1"
[1] "5-9 p= 1"
[1] "5-10 p= 1"
[1] "6-7 p= 1"
[1] "6-8 p= 1"
[1] "6-9 p= 1"
[1] "6-10 p= 1"
[1] "7-8 p= 1"
[1] "7-9 p= 1"
[1] "7-10 p= 1"
[1] "8-9 p= 1"
[1] "8-10 p= 1"
[1] "9-10 p= 1"
>
>
>
> detach(data)
>
>
>
```

5. Results.

5. Results.

5.1. Linear regressions.

Linear regression models are shown in Table 4.

Variable	Coefficients	Estimate	Std. Error	t value	Pr(>|t|)	Confidence intervals 2.5 %	97.5 %
Bracket temperature	Intercept	0.88	0.07	12.34	<0.0001	0.74	1.02
	WireMaterial	0.54	0.10	5.41	<0.0001	0.35	0.74
	Intercept	0.94	0.07	12.59	<0.0001	0.79	1.08
	WireSize	0.0002	0.00005	4.08	<0.0001	0.0001	0.0003
	Intercept	0.33	0.16	2.07	0.04	0.02	0.64
	Power	0.37	0.07	5.45	<0.0001	0.23	0.50
Wire Temperature	Intercept	0.88	0.07	12.34	<0.0001	0.74	1.02
	WireMaterial	0.55	0.10	5.42	<0.0001	0.35	0.74
	Intercept	0.94	0.07	12.59	<0.0001	0.79	1.08
	WireSize	0.0002	0.0002	4.08	<0.0001	0.0001	0.0003
	Intercept	0.33	0.16	2.07	0.04	0.02	0.64
	Power	0.37	0.07	5.45	<0.0001	0.23	0.50
Shear Bond Strength	Intercept	24.34	0.54	45.23	<0.0001	23.28	25.39
	WireMaterial	0.19	0.76	0.25	0.8	-1.30	1.68
	Intercept	24.68	0.41	60.16	<0.0001	23.87	25.48
	WireSize	-0.00001	0.0003	-0.04	0.97	-0.0007	0.0007
	Intercept	25.66	0.76	33.74	<0.0001	24.17	27.15
	Power	-0.48	0.34	-1.44	0.15	-1.14	0.17

Table 4. Results of Linear regression models of the different variables (shear bond strength, bracket temperature, wire temperature). Covariates tested were wire material, the wire dimension and the MRI power.

As Showed in Figures 27, 28 and 29, wire temperatures were significantly affected by MRI Power ($P<0.0001$), wire material ($P<0.0001$) and wire size ($P<0.05$).

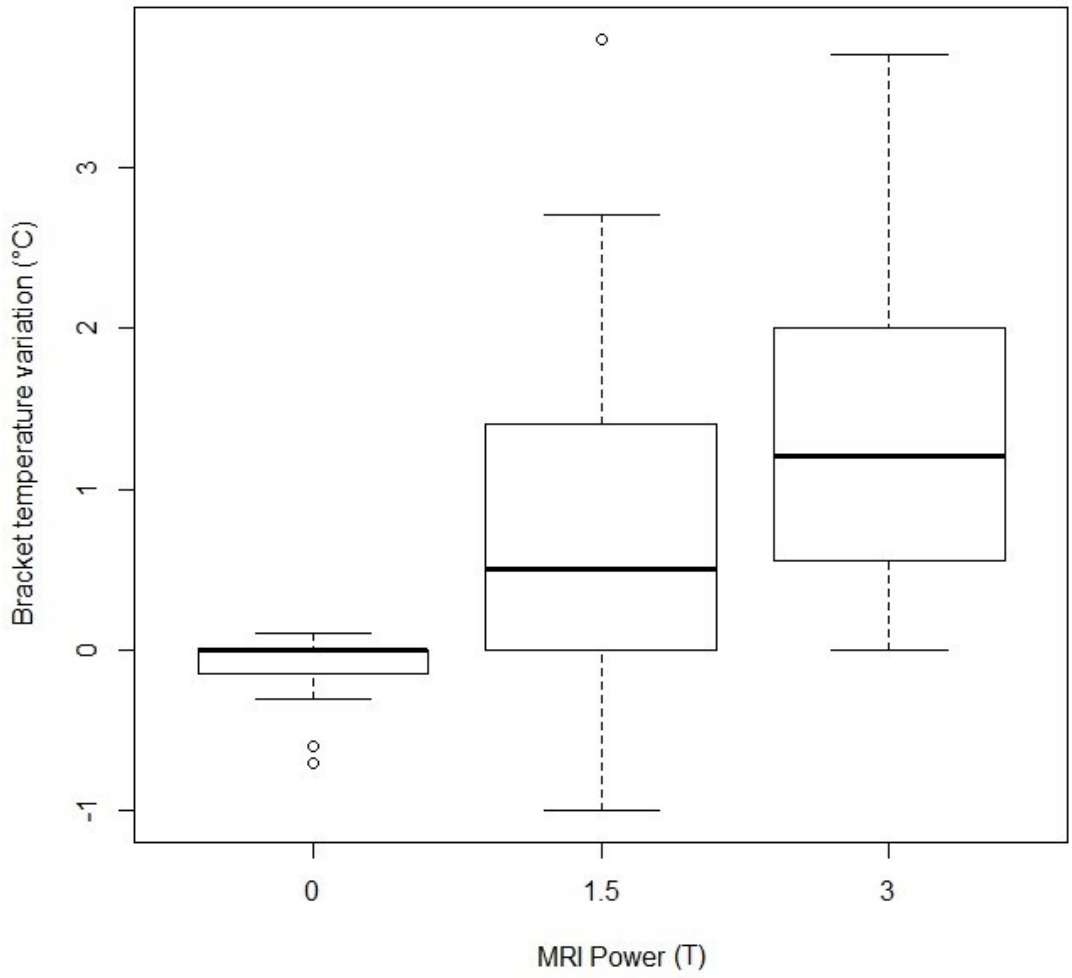

Figure 27. Effect of MRI power on the temperature variation of the bracket.

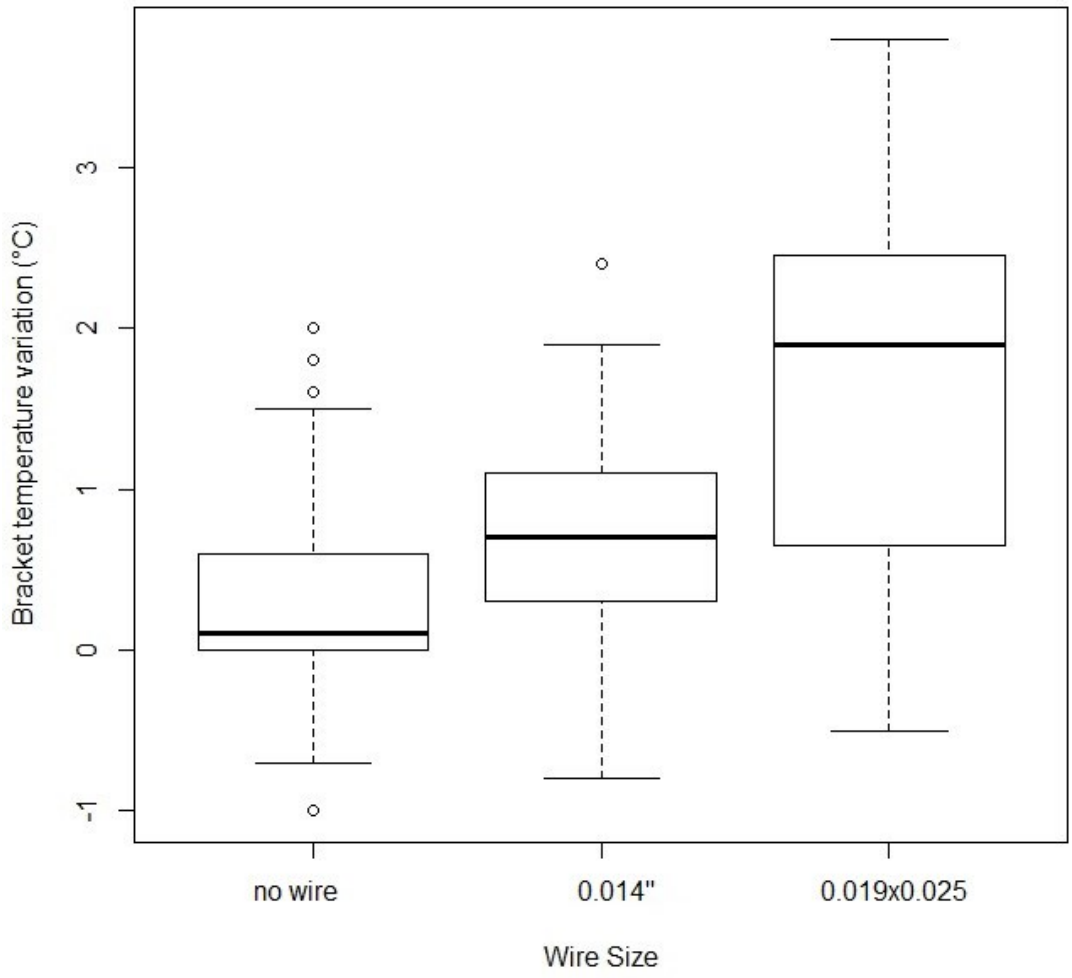

Figure 28. Effect of wire size on the temperature variation of the bracket.

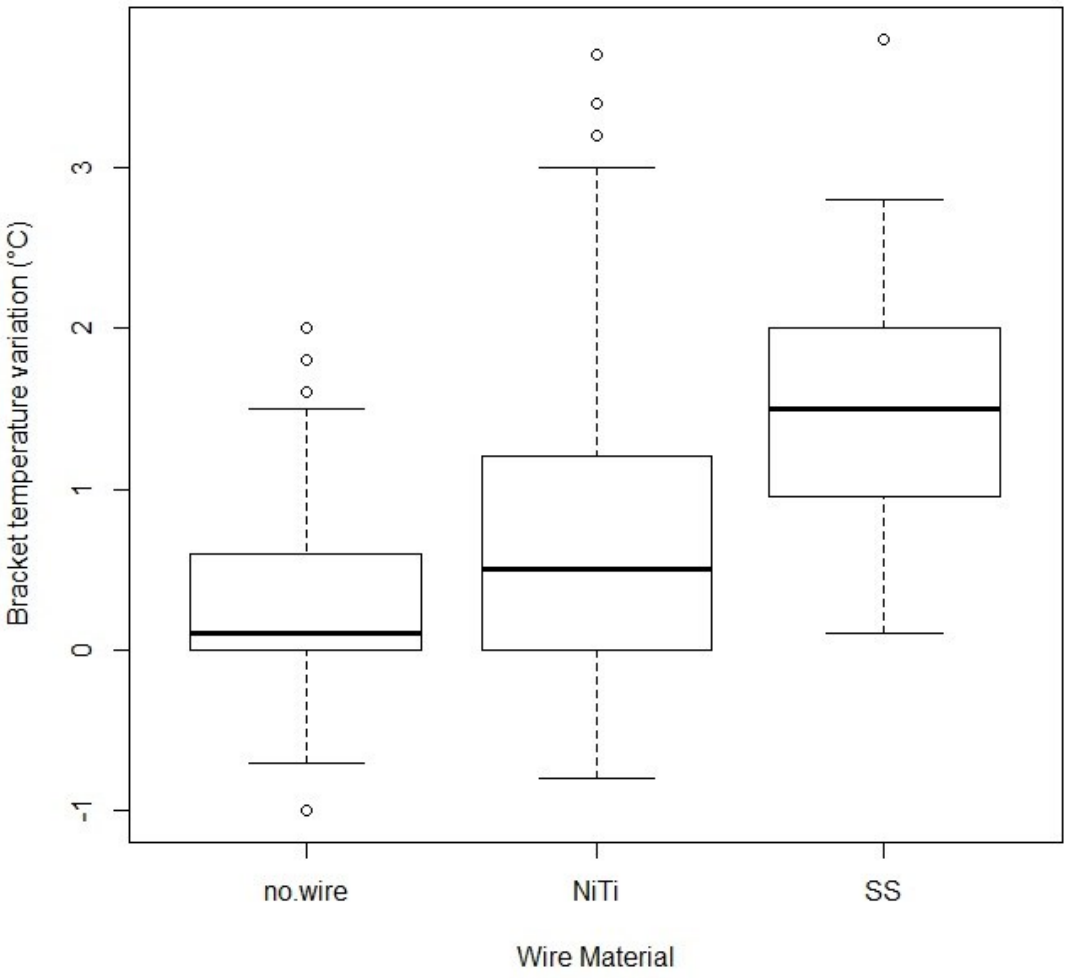

Figure 29. Effect of wire material on the temperature variation of the bracket.

As Showed in Figures 30, 31 and 32, bracket temperatures were significantly affected by MRI Power ($P<0.0001$), wire material ($P<0.0001$) and wire size ($P<0.05$).

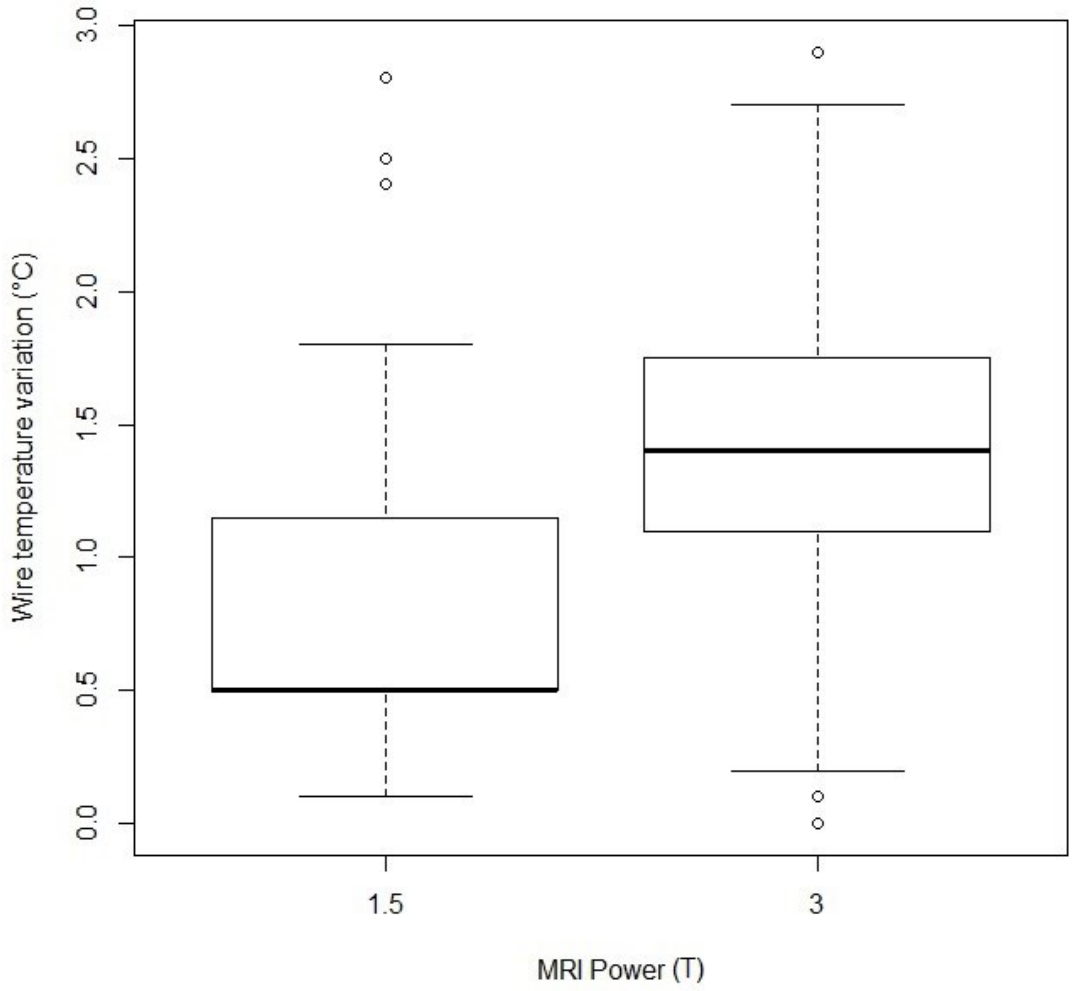

Figure 30. Effect of MRI power on the temperature variation of the wire.

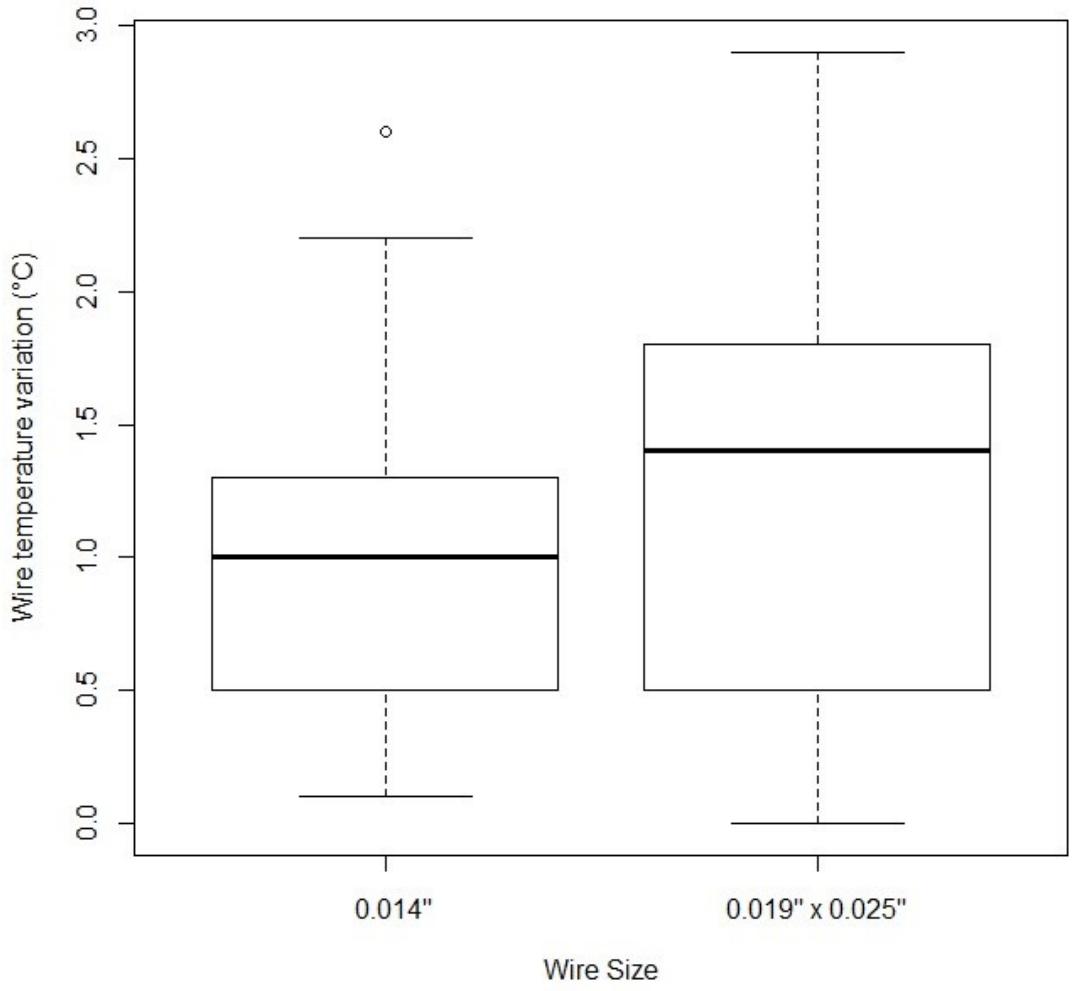

Figure 31. Effect of wire size on the temperature variation of the wire.

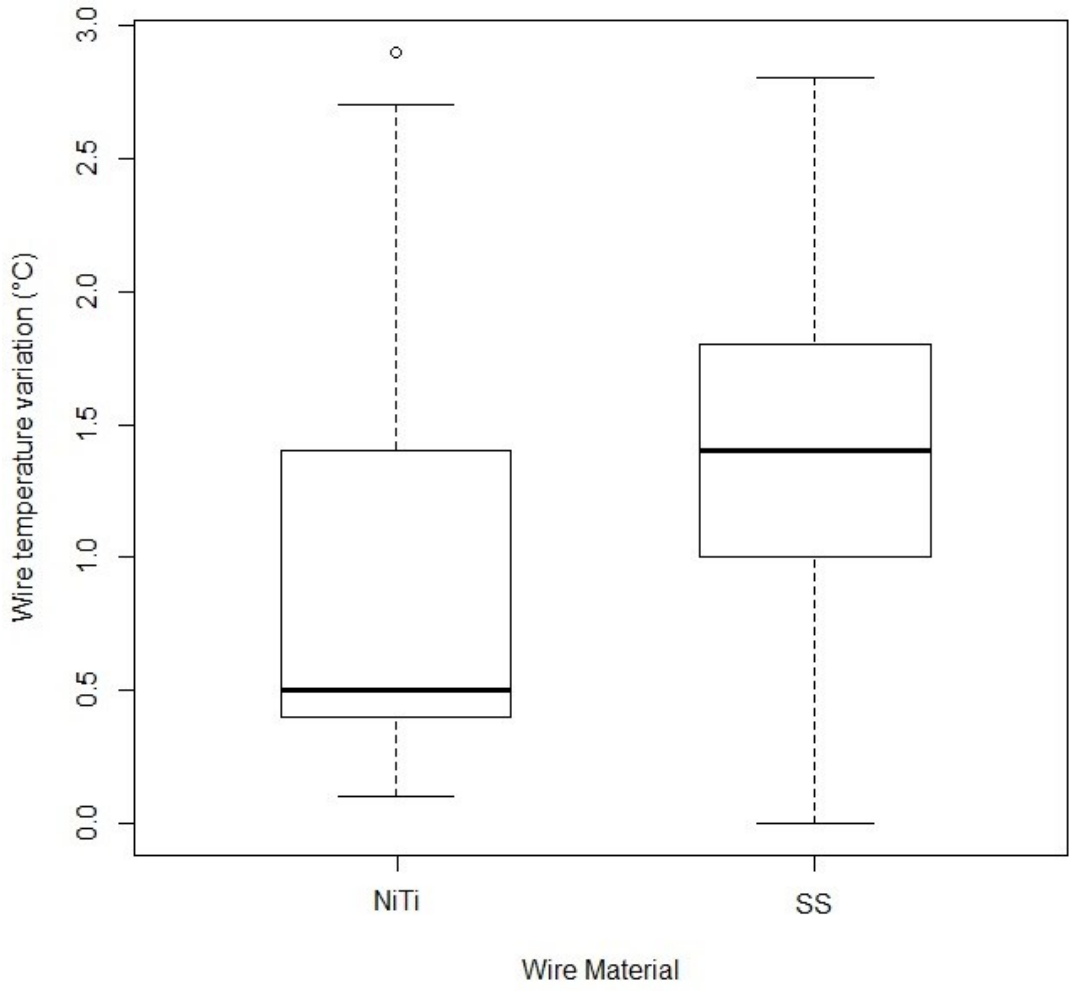

Figure 32. Effect of wire material on the temperature variation of the wire.

As Showed in Figures 33, 34 and 35, Concerning shear bond strengths, they were not significantly affected by wire material, wire dimension and MRI power (P>0.05).

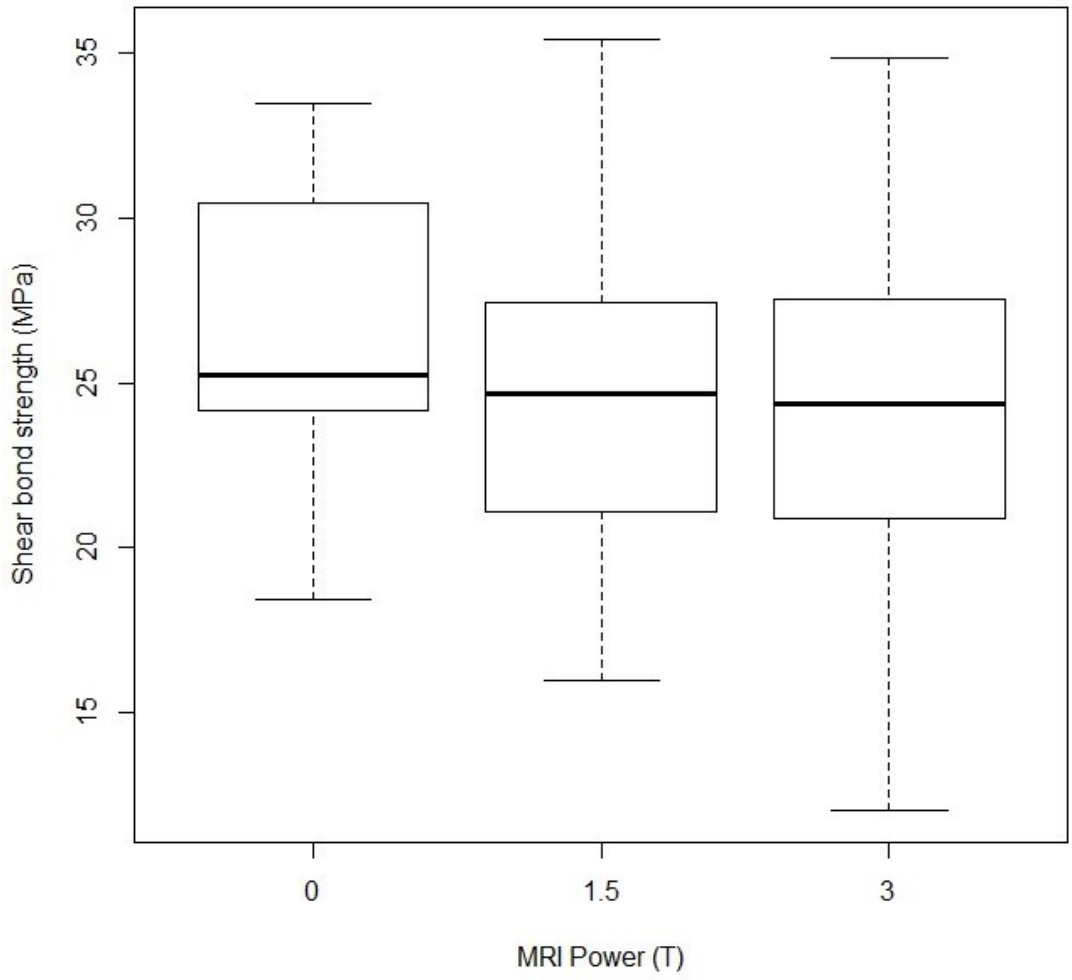

Figure 33. Effect of MRI power on the shear bond strength.

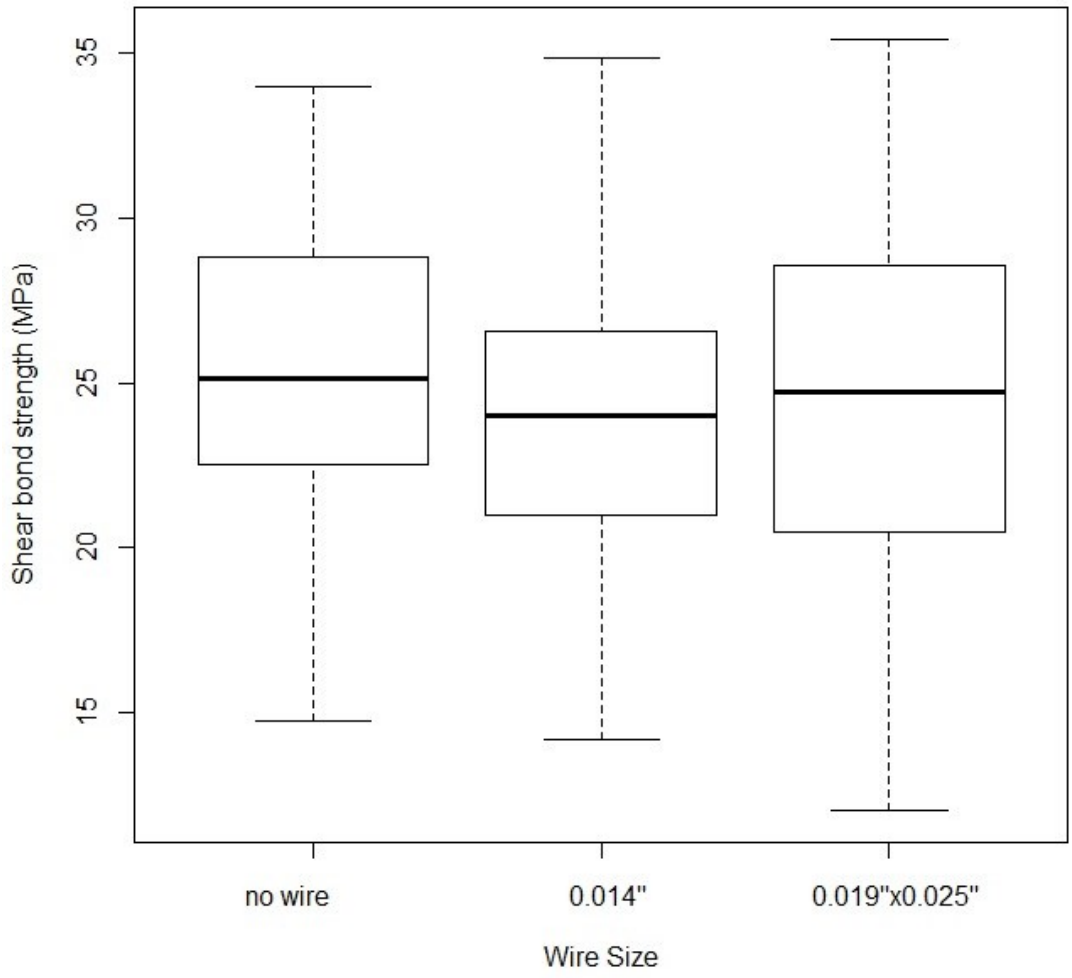

Figure 34. Effect of wire size on the shear bond strength.

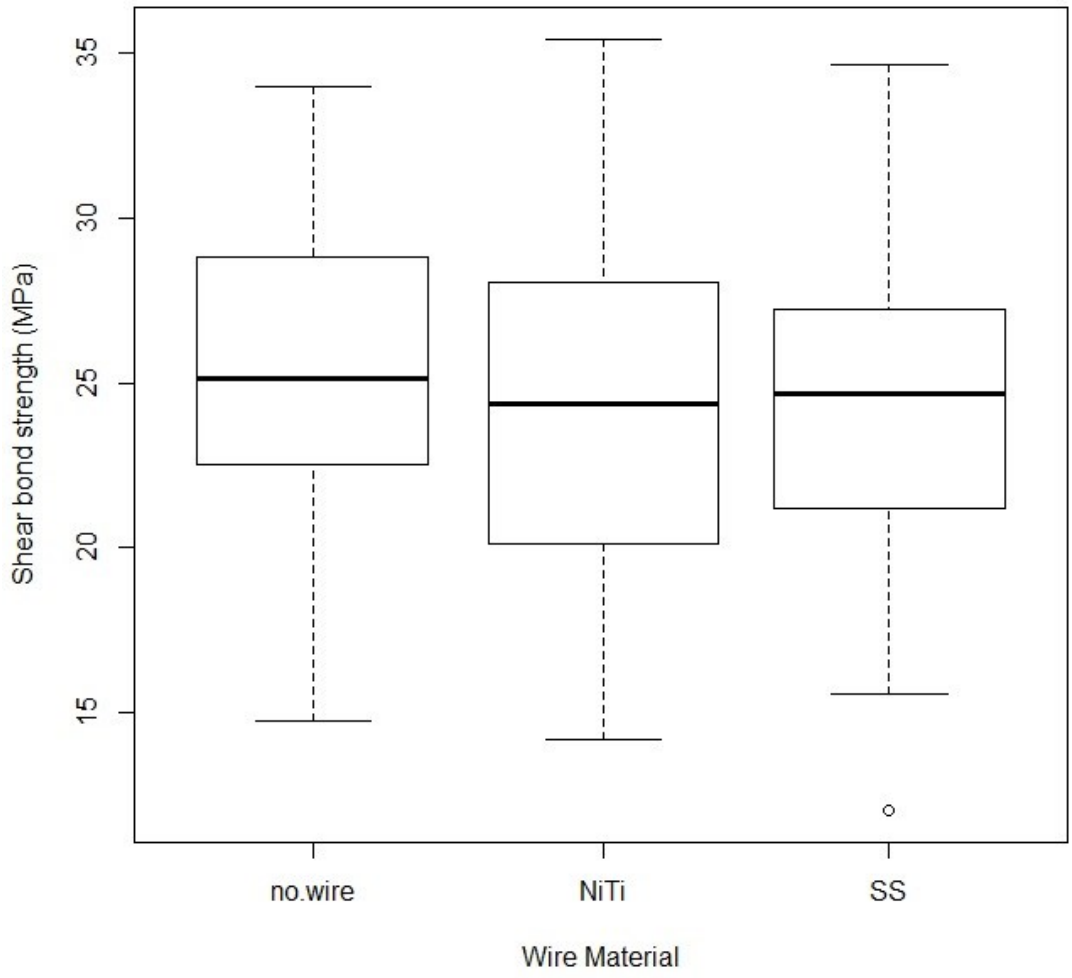

Figure 35. Effect of wire material on the shear bond strength.

5.2. Temperature test.

Descriptive statistics of the temperatures measured on brackets are reported in Table 5 and Figure 27.

Additionally, ANOVA showed the presence of significant differences among various groups ($P<0.05$). Tukey test showed that when evaluating brackets temperatures after 1.5T MRI no significant increase of temperature was recorded when brackets were tested with no wire engaged (group 2) and when nickel titanium wire was engaged (groups 5 and 6) ($P>0.05$). On the contrary a significant temperature increase ($P<0.05$) was measured after MRI when testing 0.014'' and 0.019''x0.025'' stainless steel wires with a mean temperature increase of 1.2°C and 2.2°C respectively.

On the other hand, after 3T MRI exposure a significant (P<0.05.) temperature increase of brackets was reported in all the conditions tested. Highest brackets temperatures were reported when 0.019"x0.025" stainless steel (group 9) and 0.019"x0.025" nickel titanium (group 11) wires were engaged, with a mean temperature rise of 1.94°C and 2.39°C respectively. No significant differences were reported between them (P>0.05). Significantly lower (P<0.05) bracket temperatures were recorded when no wire was used (group 7) and when 0.014" stainless steel (group 8) and 0.014" nickel titanium (group 10) wires were engaged, with a mean temperature rise of 0.97°C, 0.69°C and 0.77°C respectively. No significant differences were reported among them (P>0.05).

After MRI exams no significant differences were reported between 1.5T and 3T powers in terms of bracket temperatures (P>0.05) except when 0.014" nickel titanium and 0.019''x0.025'' nickel titanium wires were engaged, when significantly lower temperatures at 1.5T were reported if compared with 3T (P<0.05).

Group	Wire Size	Wire Material	MRI	Time	Mean	SD	Min	Mdn	Max	ΔT (T1-T0)	Significance*
1	No Wire	No Wire	No MRI	T0	23.84	0.13	23.50	23.90	24.10		A
	No Wire	No Wire	No MRI	T1	23.73	0.25	23.00	23.80	23.90	-0.11	A
2	No Wire	No Wire	1.5T	T0	23.69	0.27	23.10	23.80	24.00		A
	No Wire	No Wire	1.5T	T1	23.79	0.28	23.00	23.85	24.20	0.10	A
3	0.014"	Stainless Steel	1.5T	T0	23.83	0.27	23.40	23.80	24.50		A
	0.014"	Stainless Steel	1.5T	T1	25.02	0.20	24.80	25.00	25.30	1.20	B
4	0.019"x0.025"	Stainless Steel	1.5T	T0	23.79	0.14	23.50	23.80	24.10		A
	0.019"x0.025"	Stainless Steel	1.5T	T1	25.95	0.52	25.10	26.00	27.60	2.16	C
5	0.014"	Nickel Titanium	1.5T	T0	23.71	0.30	23.20	23.80	24.10		A
	0.014"	Nickel Titanium	1.5T	T1	23.76	0.25	23.30	23.75	24.20	0.05	A
6	0.019"x0.025"	Nickel Titanium	1.5T	T0	23.67	0.32	23.00	23.80	24.10		A
	0.019"x0.025"	Nickel Titanium	1.5T	T1	23.76	0.29	23.40	23.80	24.40	0.09	A
7	No Wire	No Wire	3T	T0	23.84	0.20	23.40	23.85	24.20		A
	No Wire	No Wire	3T	T1	24.81	0.56	24.00	24.80	25.90	0.97	B
8	0.014"	Stainless Steel	3T	T0	23.81	0.26	23.10	23.85	24.10		A
	0.014"	Stainless Steel	3T	T1	24.50	0.42	23.90	24.50	25.60	0.69	B
9	0.019"x0.025"	Stainless Steel	3T	T0	23.66	0.43	23.00	23.65	24.40		A
	0.019"x0.025"	Stainless Steel	3T	T1	25.60	0.24	25.10	25.55	26.00	1.94	C
10	0.014"	Nickel Titanium	3T	T0	23.73	0.31	23.00	23.70	24.20		A
	0.014"	Nickel Titanium	3T	T1	24.50	0.30	24.10	24.50	25.40	0.78	B
11	0.019"x0.025"	Nickel Titanium	3T	T0	23.66	0.39	22.70	23.70	24.20		A
	0.019"x0.025"	Nickel Titanium	3T	T1	26.05	0.61	24.60	26.20	26.70	2.40	C

Table 5. Descriptive statistics of the temperatures (°C) measured on orthodontic brackets in the various groups tested (T0: before MRI – T1: after MRI). *: Tukey grouping. Means with the same letters are not significantly different.

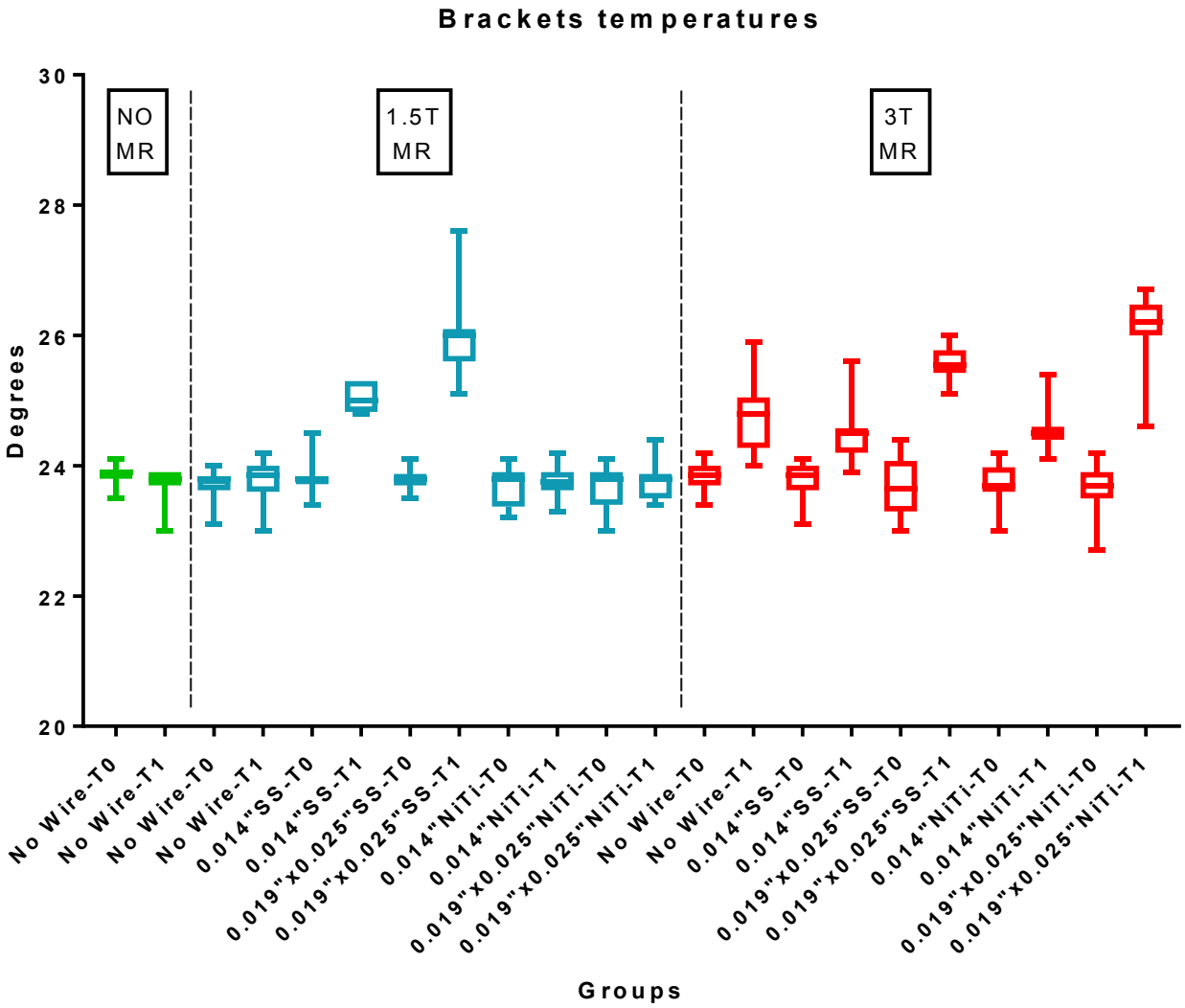

Figure 27. – Bracket temperatures (°C) of the various groups before (T0) and after (T1) 1.5T and 3T MRIs. SS: stainless steel wire – NiTi: nickel titanium wire.

Concerning temperatures of the wires, descriptive statistics are reported in Table 6 and Figure 28. ANOVA showed the presence of significant differences among various groups ($P<0.05$).

Tukey test showed that when evaluating wires temperatures after 1.5T MRI a significant temperature increase was reported in all the conditions tested ($P<0.05$). Highest temperatures ($P<0.05$) were recorded for 0.019"x0.025" stainless steel wires (group 4), that showed a mean temperature increase of 1.69°C. Significantly lower ($P<0.05$) values

were reported for 0.014” stainless steel wires (group 3) that exhibited a mean temperature increase of 1.01°C. The lowest values (P>0.05) were reported for 0.014” nickel titanium (group 5) and 0.019"x0.025” nickel titanium (group 6) wires that showed a mean temperature increase of 0.42°C and 0.39°C respectively, with no significant difference between them (P>0.05).

Conversely, after 3T MRI exposure, a significant wire temperature increase between T0 and T1 was reported in all the conditions tested (P<0.05). No significant differences were reported among various groups at T1 (P>0.05). The mean temperature increase for the wires was 1.26°C for 0.014” stainless steel (group 8), 1.74°C for 0.019"x0.025” stainless steel (group 9), 1.06°C for 0.014” nickel titanium (group 10), and 1.64°C for 0.019"x0.025” nickel titanium (group 11) wires.

After MRI exams no significant differences were reported between 1.5T and 3T powers in terms of wires temperatures (P>0.05) except for 0.014” nickel titanium wires, that showed significantly lower temperatures at 1.5T if compared with 3T (P<0.05).

Group	Wire Size	Wire Material	MRI	Time	Mean	SD	Min	Mdn	Max	ΔT (T1-T0)	Significance*
1	No Wire	No Wire	No MRI	T0	-	-	-	-	-		-
	No Wire	No Wire	No MRI	T1	-	-	-	-	-	-	-
2	No Wire	No Wire	1.5T	T0	-	-	-	-	-		-
	No Wire	No Wire	1.5T	T1	-	-	-	-	-	-	-
3	0.014"	Stainless Steel	1.5T	T0	23.91	0.33	23.20	23.90	24.60		A
	0.014"	Stainless Steel	1.5T	T1	24.92	0.13	24.70	24.90	25.10	1.02	B
4	0.019"x0.025"	Stainless Steel	1.5T	T0	23.94	0.35	23.30	23.90	24.70		A
	0.019"x0.025"	Stainless Steel	1.5T	T1	25.63	0.34	25.20	25.70	26.50	1.69	C
5	0.014"	Nickel Titanium	1.5T	T0	23.89	0.25	23.20	23.90	24.30		A
	0.014"	Nickel Titanium	1.5T	T1	24.31	0.25	23.70	24.30	24.80	0.42	D
6	0.019"x0.025"	Nickel Titanium	1.5T	T0	23.78	0.14	23.40	23.75	24.00		A
	0.019"x0.025"	Nickel Titanium	1.5T	T1	24.17	0.24	23.80	24.20	24.50	0.39	D
7	No Wire	No Wire	3T	T0	-	-	-	-	-		-
	No Wire	No Wire	3T	T1	-	-	-	-	-	-	-
8	0.014"	Stainless Steel	3T	T0	23.80	0.16	23.50	23.80	24.10		A
	0.014"	Stainless Steel	3T	T1	25.06	0.47	24.40	25.10	25.90	1.26	B,C
9	0.019"x0.025"	Stainless Steel	3T	T0	23.63	0.21	23.10	23.65	23.90		A
	0.019"x0.025"	Stainless Steel	3T	T1	25.37	0.68	23.60	25.25	26.30	1.74	B,C
10	0.014"	Nickel Titanium	3T	T0	23.98	0.39	23.30	24.00	24.50		A
	0.014"	Nickel Titanium	3T	T1	25.04	0.46	24.60	25.00	26.60	1.07	B,C
11	0.019"x0.025"	Nickel Titanium	3T	T0	23.48	0.28	23.00	23.50	24.00		A
	0.019"x0.025"	Nickel Titanium	3T	T1	25.12	0.51	24.30	25.00	26.00	1.65	B,C

Table 6. Descriptive statistics of the temperatures (°C) measured on orthodontic wires in the various groups tested (T0: before MRI – T1: after MRI). *: Tukey grouping. Means

with the same letters are not significantly different. Significance cut off was set at P<0.05.

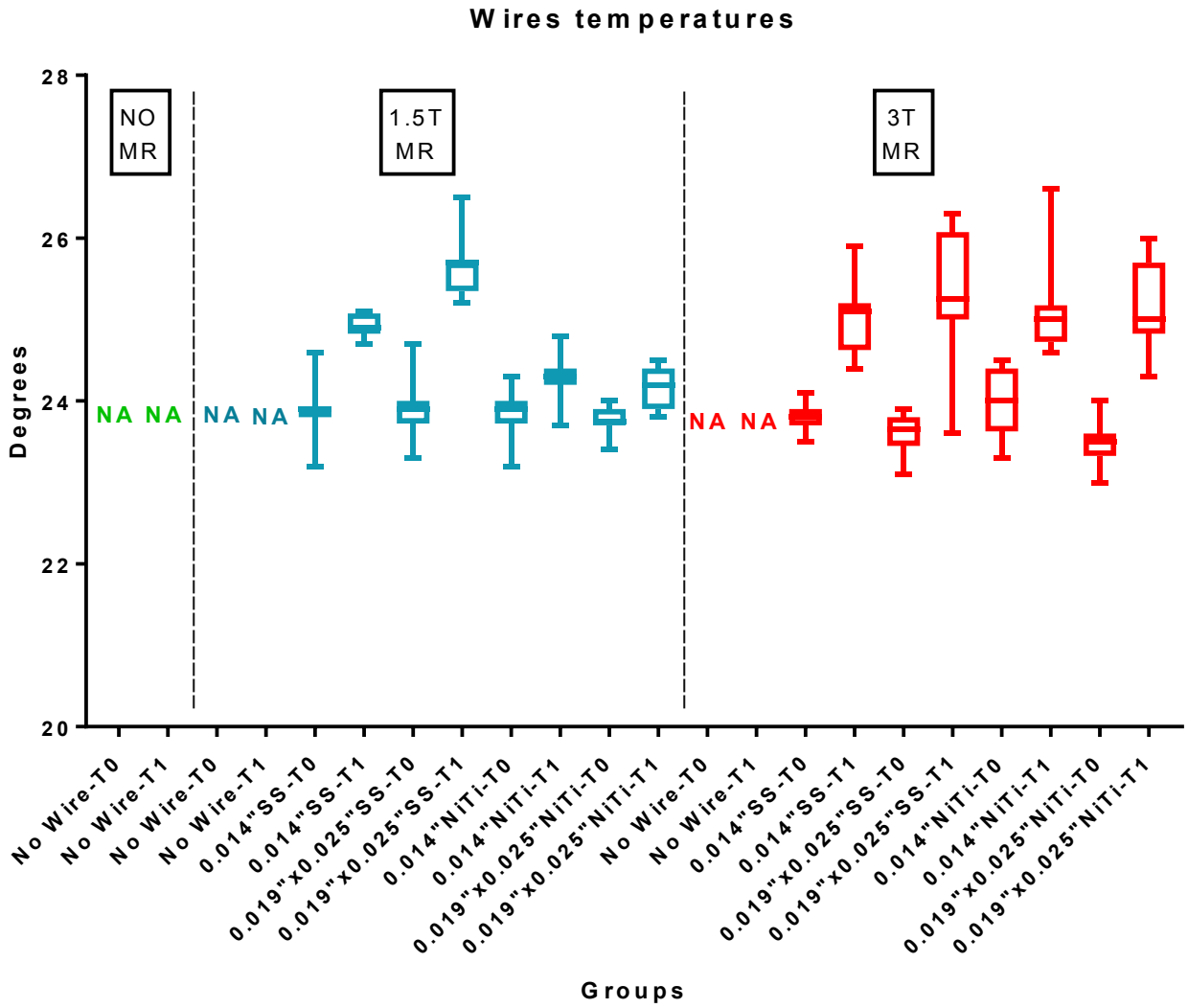

Figure 28. – Wire temperatures (°C) of the various groups before (T0) and after (T1) 1.5T and 3T MRIs. SS: stainless steel wire – NiTi: nickel titanium wire. NA: not applicable, since no wire was present.

When comparing brackets versus wires temperatures no significant differences were reported both at 1.5T and at 3T exposures (P<0.05). After 1.5T MRI exposure, the mean temperature rise was 0.87°C for brackets and 0.88°C for wires. After 3T MRI exposure, the mean temperature rise was 1.45°C for brackets and 1.43°C for wires. When comparing MRI powers, after 3T exposure, temperatures recorded were significantly

higher than after 1.5T exposure (P<0.05) with a mean temperature difference of 0.58°C for brackets and 0.55°C for wires.

5.3. Shear bond strength test.

Descriptive statistics of the shear bond strength values are reported in Table 7 and Figure 29. ANOVA showed no significant difference in shear bond strength values among various groups tested (P>0.05).

Group	RMN	Wire	Wire Material	Mean	SD	Min	Mdn	Max	Significance*
1	No RMN	No wire	No wire	26.45	4.64	18.44	25.26	33.44	A
2	1.5T	No wire	No wire	25.07	4.36	16.35	25.13	33.29	A
3	1.5T	0.014''	Stainless Steel	24.91	3.56	18.02	24.64	33.81	A
4	1.5T	0.019''x0.025''	Stainless Steel	24.49	4.30	18.23	24.85	31.99	A
5	1.5T	0.014''	Nickel Titanium	23.33	4.78	15.98	23.02	31.07	A
6	1.5T	0.019''x0.025''	Nickel Titanium	25.29	5.14	18.20	24.69	35.43	A
7	3T	No wire	No wire	24.39	5.56	14.76	24.68	33.95	A
8	3T	0.014''	Stainless Steel	24.21	4.71	16.20	24.01	34.62	A
9	3T	0.019''x0.025''	Stainless Steel	24.51	5.52	12.04	24.52	33.13	A
10	3T	0.014''	Nickel Titanium	24.38	5.44	14.18	23.82	34.83	A
11	3T	0.019''x0.025''	Nickel Titanium	24.34	5.24	14.94	24.77	31.85	A

Table 7. Descriptive statistics of shear bond strength values (MPa). *: ANOVA grouping. Means with the same letters are not significantly different. Significance cut off was set at P<0.05.

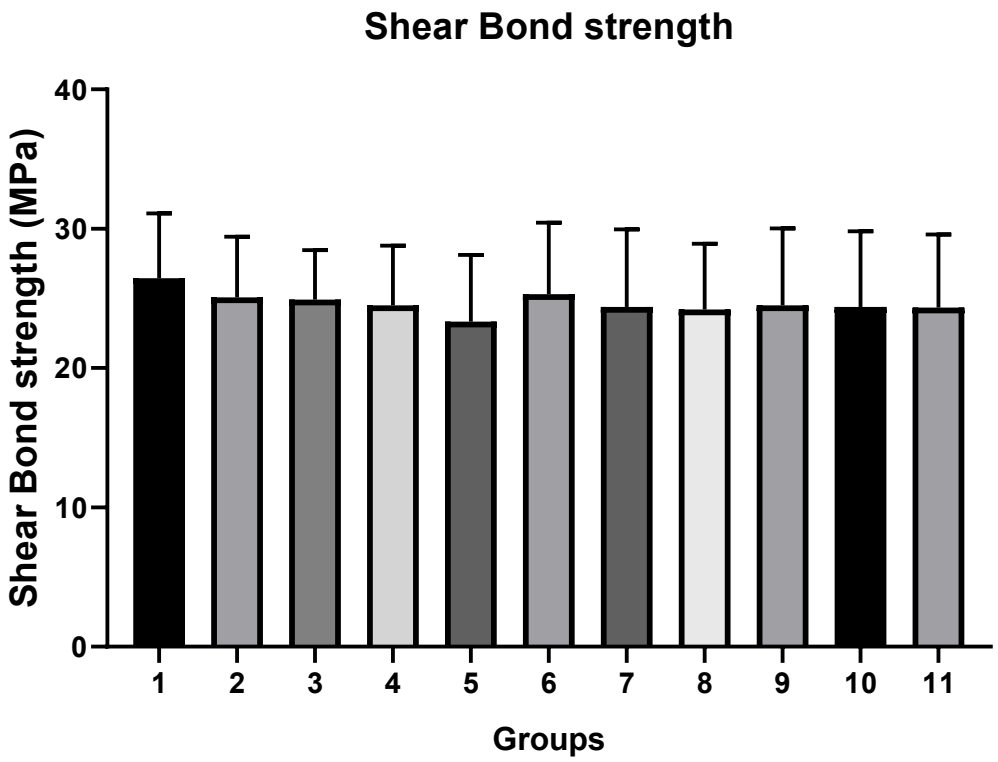

Figure 29. Shear bond strength values (MPa) of the various groups.

5.4. ARI scores analysis.

Frequency distributions of ARI Scores are reported in Table 8 and Figure 30. When no MRI was performed specimen showed a significantly higher frequency of ARI=1 ($P<0.05$), whereas after MRI all the groups (2 to 11) showed a significant prevalence of ARI=0 showing no significant difference among them regardless of wire size, wire shape or MRI power ($P>0.05$).

Group	MRI	Wire	Wire Material	ARI=0	ARI=1	ARI=2	ARI=3
1	No MRI	No wire	No wire	15	75	5	5
2	1.5T	No wire	No wire	50	45	5	0
3	1.5T	0.014"	Stainless Steel	55	30	10	5
4	1.5T	0.019"x0.025"	Stainless Steel	55	40	5	0
5	1.5T	0.014"	Nickel Titanium	45	30	25	0
6	1.5T	0.019"x0.025"	Nickel Titanium	45	40	15	0
7	3T	No wire	No wire	55	45	0	0
8	3T	0.014"	Stainless Steel	55	35	10	0
9	3T	0.019"x0.025"	Stainless Steel	55	45	0	0
10	3T	0.014"	Nickel Titanium	50	45	5	0
11	3T	0.019"x0.025"	Nickel Titanium	60	35	5	0

Table 8. Frequency distribution (%) of ARI scores (0: no adhesive left on enamel surface; 1: less than half of the adhesive left on enamel; 2: more than half of the adhesive left on enamel; 3: all the adhesive left on enamel).

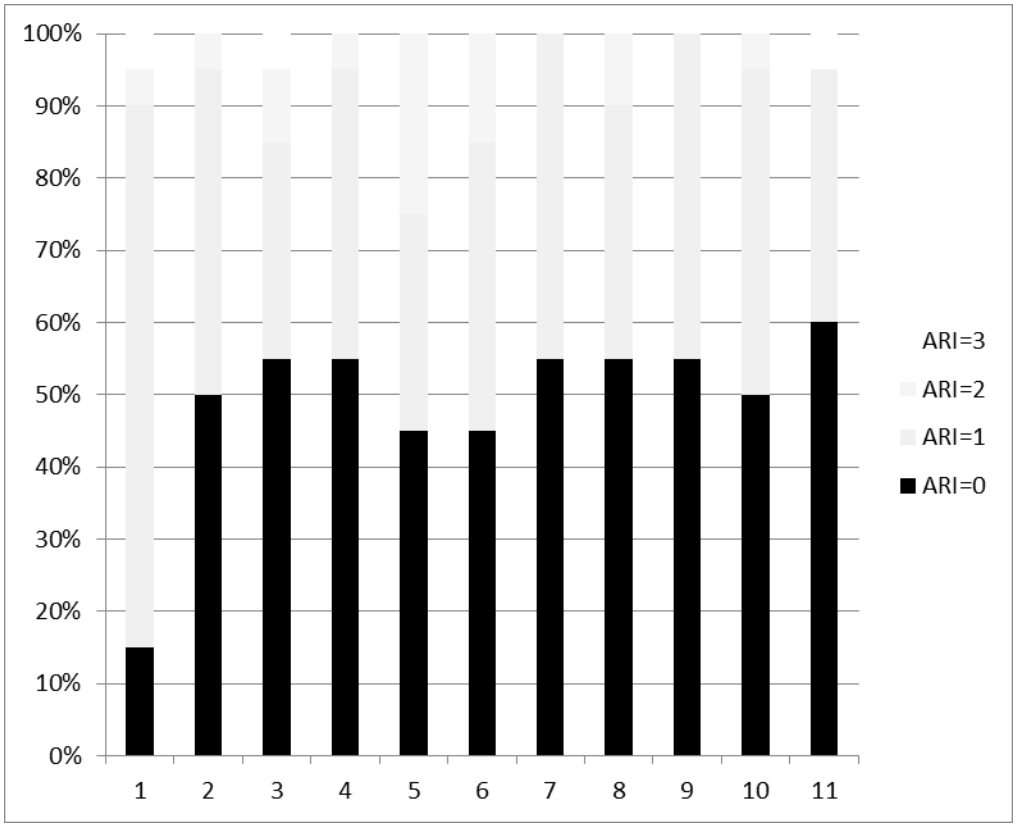

Figure 30. ARI score frequency distributions among various groups.

6. Discussion.

6. Discussion.

6.1. Overall.

Nowadays, there is a large literature about the interactions between MRI and metal orthodontic devices [Shalish et al., 2015]. Most research focuses on the evaluation of image artifacts, instead neglecting the issue of patient safety in terms of movement and overheating of metal objects [Görgülü et al., 2014]. In particular, no author has so far investigated any changes in the adhesion strength of the brackets due to interaction with the magnetic field. For these reasons, the objective of this experimental work was the analysis of multiple phenomena: the thermal variations (of brackets and wires), the adhesion strength of orthodontic brackets and the adhesive remnant index score.

6.2. The first null hypothesis. Temperature variations.

The first null hypothesis of the study was rejected. Significant differences in brackets and wires temperatures were reported. Linear regressions showed significant effects of MRI power, wire material and wire size on temperatures of orthodontic devices (brackets and wires). In fact, after MRI a significant increase in the temperature of the brackets was revealed in all the groups tested, except for group without wire and groups with 0.014'' nickel titanium and 0.019x0.025'' nickel titanium wires at 1.5T, where no significant difference was reported before and after MRI exam. The mean bracket temperature increase ranged between 0.05°C and 2.4°C. Concerning orthodontic wires tested, all the groups showed a significant increase in the temperature after MRI, both at 1.5T and 3T. The mean wire temperature increase ranged between 0.42°C and 1.74°C.

Previous studies evaluated the effect of 1.5T MRI on dental materials showing a mean temperature increase of 1°C-2°C for prosthodontic materials [Hasegawa et al., 2013]. Concerning orthodontic appliances, previous reports evaluated temperature changes of brackets and stainless steel wires, whereas no studies evaluated temperature changes of nickel titanium wires with different sizes. Significant changes in temperatures were less than 1°C [Yassi et al., 2007] at 1.5T, and the temperature rise is resulted higher in particular in the metal wire linking the brackets. At 3T the temperature increase ranged between 0.1°C [Regier et al., 2009] and 2.6°C [Hasegawa et al., 2013]. All authors concluded that increase of temperature of stainless steel devices after MRI was

numerically significant but not clinically relevant, as limited to few degrees. These findings are in agreement with the present report. Additionally our research showed similar results also for nickel titanium wires. Regarding this last material, nowadays, no studies evaluated temperature changes of nickel titanium wires with different sizes.

Orthodontic wires are used to provide the required force to move teeth to their correct positions. They can be made of many materials even if the most used are nickel titanium and stainless steel. The first is capable of exhibiting super-elasticity, which provides light, continuous force for physiological and efficient tooth movement. The second is used for torsional root moment [Maekawa et al., 2015]. Concerning wire size, the 0.014" round section is the most used size in the aligning phase and 0.019"x0.025" rectangular shape is the most used dimension for sliding mechanics [Yassir et al., 2019]. Based on these considerations these two materials and sizes were tested in the present report.

In the present research, the arches were organized according to a rectilinear arrangement to avoid changing the magnetic properties of the orthodontic wires and, at the same time, to facilitate the application of a cutting force parallel to the bracket-enamel interface. Previous Authors attested reduced interactions between titanium and magnetic resonance imaging [Klocke et al., 2005], but the magnetic behavior also depends on the crystalline structure of the alloy (austenitic, martensitic or ferritic) and on the specific composition [Blankenstein et al., 2015]. Therefore, it was decided to include both materials in the experimentation, testing both in the same rectangular and round formats to be able to evaluate any influences of shape and size [Kemper et al., 2007].

For the same reason, although the available literature affirms the absence of an important effect by the magnetic field on metal ligatures [Klocke et al., 2005], due to the lack of information and the variability of the studies, it was decided to choose elastic ligatures. These devices do not contain metallic material, so they are inert in an RM environment.

The placement of the samples in the machine region in which is usually positioned the patient's head and the presence of a radiofrequency coil for cranial imaging allowed reproducing the effects of the field acting on a real patient. Additionally this position maximized the radiofrequency action in view of the worst-case scenario, even if, due to

the generation of artifacts, the presence of orthodontic equipment could be incompatible with the tests for which the coil is dedicated [Elison et al., 2008].

Finally, as regards the analysis of overheating, it was decided to use a contact thermometer with thermocouple probes, as in previous reports [Regier et al., 2009; Görgülü et al., 2014].

The results obtained regarding the overheating of the devices appear to be consistent with results reported in various studies [Yassi et al., 2007; Hasegawa et al., 2013]: the increase in temperature is very low, therefore it is not dangerous for the patient. The maximum superheat values calculated, in fact, were 2 ° C in the brackets in combination with SS .019 "x.025" orthodontic wire, and 1.96 ° C for the single wire. In both cases, therefore, the thermal increase remains below the overheating limit threshold compatible with pulp viability, set at 5.6 °C or higher, depending upon the various Authors [Kagetsu et al., 1991; Swartz, 2007; Daronch et al., 2007].

Furthermore, the result of a previous report [Görgülü et al., 2014] regarding the finding of a more marked effect for stainless steel than NiTi is confirmed in the present report. Additionally, in our results the difference between the two materials is more important. However, within the various studies, there are considerable methodological differences (field power, type of thermometer, etc.) which do not allow a direct comparison among the results [Hasegawa et al., 2013].

Nowadays, there is a large literature about the interactions between MRI and metal orthodontic devices [Shalish et al., 2015]. Most recent research focuses on the evaluation of image artifacts. An artifact can be defined as a signal intensity distortion or a void, devoid of anatomical correspondence in the investigated plane, which determine an untrue representation of the tissue components of the area in question [Dalili Kajan et al., 2015].

One of the main drawbacks induced by orthodontic equipment during MRI is the creation of artifacts. The extent of the distortion is related to the composition of the material of which the device is made, the shape and size of the object, its position with respect to the axis of the magnetic field, the intensity of the field itself, the protocol used and the selected technical parameters. The distance of the equipment from the anatomical area under investigation is also an important discriminant. The signal loss will be maximum if the object is within 10 cm of the area of interest [Taniyama et al.,

2010]. In general, the greater the distance between the orthodontic appliance and the site to be investigated, the less there will be gaps and distortions of the image of interest [Poorsattar-Bejeh et al., 2016].

Some Authors have conducted a study aimed at defining a repeatable method of predicting the extent of the artifact produced by orthodontic attacks of different manufacturers, subjected to RM 1.5 T, with Turbo-Spin-Echo (TSE) and Gradient-Echo sequences (GRE). The authors found distortions with a radius of 11 mm for ceramic attachments, about 20 mm for Cr-Co attachments and between 10 and 74 mm for steel attachments, depending on the specific alloy and size [Blankestein, 2017].

For this reason, it is important to consider which area is being investigated and then decide whether it is necessary to remove the orthodontic appliance. In this regard, Cassetta el al. evaluated the diagnostic quality of 80 MRI images of patients with steel orthodontic brackets and concluded that the presence of the appliances compromises the diagnostic efficacy of MRI images of the cervical and paranasal regions, while it does not affect the effectiveness of the brain images and the temporal region. [Cassetta et al., 2017].

Another study has shown that, unlike steel brackets, ceramic, composite or titanium attachments cause insignificant artifacts on images obtained with a 1.5 T device [Elison et al., 2008]. However, in current clinical practice, 3T machines are spreading as they offer higher resolution images. Since the extent of the artifact also depends on the strength of the magnetic field, a device compatible with a 1.5 T MRI scanner may not be compatible with a 3 T scanner.

A recent study examined the production of cephalic imaging artifacts in ten patients undergoing 3 T MRI and wearing different orthodontic appliances (metal brackets, ceramic brackets in combination or not with direct tubes and metal wires braided by splinting). Authors concluded that ceramic brackets cause minimal distortion; steel braided splinting wires do not cause significant artifacts in the survey district. Additionally, none of the devices tested caused significant distortions for angiographic axial sequences without contrast medium, FLAIR (Fluid Attenuated Inversion Recovery) axial images, and axial T2 images. Steel connections and direct tubes make the brain image non-diagnostic for sagittal T1 images, for axial gradient-echo images (GRE) and Diffusion Weighted Imaging (DWI). The presence of ceramic brackets and

direct metal pipes make the image non-diagnostic in the case of axial sequences GRE and DWI. In axial T1-weighted images, the vestibular tubes distort the images of the oral cavity, pharynx and eyeballs. Sagittal T1 images instead maintain diagnostic value with this combination of devices [Zhylich et al., 2017].

The extent of the distortion is related also to the imaging sequence used and some sequences generate more extensive artifacts than others, in the presence of the same disturbing element. In particular, long TE sequences and GRE sequences produce extensive artifacts; on the contrary, spin echo sequences with short TE would, according to some authors, lead to less distortions [Harris et al., 2006]. However, other Authors deny this latest finding [Costa et al., 2009] and the question is still controversial.

In the present report, the artifact generation has not been taken into consideration, considering the wide existing literature on the topic. The present study focused firstly on temperature changes. In fact, in Literature little research has been conducted on the topic. Concerning the overheating of orthodontic devices, the intensity of the effect depends on the type of metal, the shape and orientation of the object, the magnetic field and the sequence of impulses [Hasegawa et al., 2013]. However, no overheating was reported for all the materials tested in the present report.

6.3. The second null hypothesis. The shear bond strength.

Taking into account the shear bond strength, the second null hypothesis of the present report was accepted. MRI Power, wire material and wire size had no significant effect on shear bond strength values. No significant differences in adhesion values were reported among various conditions tested. Nowadays, no studies evaluated bond strength of orthodontic appliances after MRI. Other dental materials have been investigated [Hubálková et al., 2002]. Some Authors evaluated the effect of MRI on metal-ceramic restorations showing that surface roughness increased and hardness decreased after 20 minutes of 1.5T exposure [El-Bediwi et al., 2014]. Additionally, Authors recommended Ni-Cr alloy over titanium in the fabrication of metal ceramic frameworks for patients with a recurring need for MRI. Regarding orthodontic devices, previous Authors [Oshagh et al., 2010] evaluated tensile strength of 0.016'' stainless steel orthodontic wires after 1.5T MRI, showing no significant difference in their mechanical properties. Additionally, some studies evaluated the risk of displacement in

magnetic resonance imaging measuring deflection angles and translational forces. The maximal forces observed were about 0.3 N and the deflection angles arrived at 45° in some cases, so they considered the risk of detachment and displacement to be non-existent at 1.5T [Yassi et al., 2007] and at 3T [Kemper et al., 2005] when the usual recommendations are respected. This is in agreement with the present report that evaluated shear bond strength. The values obtained in all the conditions tested in the present report are considerable clinically acceptable, as they are higher than 8 MPa [Patel et al., 2018].

Experimentally, bond strength can be assessed in terms of resistance to shear, to tension, compression or rotation [Oshagh et al., 2010; Linjawi et al., 2016; Khargekar et al., 2019; Milagres et al., 2019; Tanbakuchi et al., 2019]. The technique chosen for the present study was the evaluation of the shear bond strength (SBS). In fact, although it may not accurately represent intraoral stresses and may apply a load that is not homogeneously distributed at the tooth-bracket interface, this methodology presents lower coefficients of variation compared to the Tensile Tests and less tendency to produce detachment forces that would underestimate the adhesion force [Swartz, 2007].

In order to improve the validity of the in vitro study an attempt was made to represent the clinical conditions as closely as possible and to reduce confounding variables [Finnema et al., 2010]. The enamel was chosen as the substrate for adhesion, and appliances were bonded with an orthodontic adhesive. This is in contrast with other Authors, which bonded the brackets to resin teeth of a Typodont using a universal glue [Oshagh et al., 2010]. However, due to the increasing difficulty of finding extracted dental elements of human origin for research purposes, in the present report, bovine teeth were used [Schilke et al., 1999]. Specifically, the permanent mandibular incisors, in addition to the greater ease of finding, have wider vestibular surfaces that facilitate the preparation and placement of the brackets and have enamel tissue similar to the human one at both histochemical and anatomical level [Schilke et al., 2000]. Therefore, although human and bovine teeth differ considering their geometry and size, similar compositions and physical properties have been described between the two, allowing bovine teeth to be used as valid substitutes in bonding tests [Poggio et al., 2014]. Furthermore, results of in vitro studies might not be directly transferred to a clinical setting because of the different conditions to which materials are exposed in vivo

[Soares et al., 2016]. In the present investigation, brackets were bonded onto buccal surface. In fact, lingual surface of bovine teeth has been reported to be rougher and curve than vestibular side, thus reducing repeatability of bond strength measurements. Therefore, in order to minimize errors and bias during tests execution, buccal side has been selected [Godard et al., 2017]. Finally, in the interpretation of the results, the use of bovine teeth has to be taken into consideration, as recorded shear bond strength values could be slightly different from those reported with human enamel [De Carvalho et al., 2018].

The concern of bond strength is very important for appliances exposed to MRI. The strength of the magnetic field generated by MRI attracts objects containing iron (or other ferromagnetic materials) causing their uncontrolled and fast movement, thus making them dangerous “loose projectiles” in the magnetic field. This force is also able to attract metal objects placed inside the body [Hillebrand et al., 2013].

This phenomenon represents a potential risk for the patient and for anyone who is in the trajectory of the moving object within the field. According to a recent study by the US Food and Drug Administration (FDA), MRI-related incidents quintupled between 2001 and 2009, of which most are related to “bullet” burns and injuries [Mathew et al., 2013].

In recent years, several studies have been carried out to evaluate the effects of the attractive forces that act on orthodontic devices subjected to the magnetic field during MRI.

Some Authors tested a sample of 40 extracted human teeth on which orthodontic brackets were placed and 0.014 "Ni-Ti or 0.014" steel arches were applied and tied with continuous elastic or metal ligatures, thus obtaining four different experimental groups [Görgülü et al.,. 2014]. The translational attraction force and the torque, therefore the rotational force, induced by the static magnetic field generated by a 3T machine were evaluated. Translational force was measured using the standardized method proposed by the American Society for Testing and Materials (ASTM) in 2002 (F2052-02). For the measurement of the torque, Authors applied the method proposed by Shellock et al. [Shellock, 2002; Shellock et al., 2006], as the standardized method proposed by ASTM, regarding rotational force was practically not applicable. The results obtained from this experiment led the authors to conclude that none of the commonly used orthodontic

brackets was a risk to the patient during a 3T MRI. Conversely, the arches in NiTi or SS has been demonstrated to be removed for greater safety [Görgülü et al., 2014].

Given the latest updates proposed by ASTM regarding the displacement test (ASTM F2052-15, Standard Test Method for Measurement of Magnetically Induced Displacement Force on Medical Devices in the Magnetic Resonance Environment, ASTM International, West Conshohocken, PA, 2015) and the test of the torque (ASTM F2213-17, Standard Test Method for Measurement of Magnetically Induced Torque on Medical Devices in the Magnetic Resonance Environment, ASTM International, West Conshohocken, PA, 2017), it may be interesting to repeat the experimentation following the updated methods.

The forces of attraction suffered by orthodontic brackets when subjected to MRI are far below the force necessary for the debonding of such devices (about 60 N). The reason for this phenomenon is due to the reduced size of the brackets, whose compatibility with the environment of the MRI is therefore considered "conditioned": the condition to be satisfied for the brackets to be RM-compatible is the sufficient adhesion to the tooth [Blankenstein et al., 2017].

Kemper et al. analyzed the interactions of the main auxiliaries used during a fixed orthodontic treatment with both 1.5 T and 3 T magnetic fields [Kemper et al., 2007]. In addition, in this case, the translational and rotational forces were detected using methods comparable to those used in the previous study. Among the auxiliaries being tested there are different types of springs, devices such as Herbst, Jasper Jumper, Forsus, transpalatal bar, quadhelix, Hyrax screw, lip bumper and lingual arch. Most of the devices tested were "MR unsafe" according to the criteria drawn up by ASTM. However, all the forces exerted by the magnetic field on the auxiliaries were low (less than 1 N) and as such were not able to compromise the stability of the auxiliaries. The intensity of the force exerted by the magnetic field on some accessories was comparable to the forces normally produced by orthodontic equipment to induce dental movements. A feeling of discomfort for the patient is therefore foreseeable, similar to that experienced during orthodontic treatment. Therefore, the Authors conclude that removable devices, such as the lip bumper, do not create any problem as the patients can easily remove them before the examination. Bands and orthodontic brackets can be left in situ, but the adhesion and stability of each element must be carefully checked.

The same applies to orthodontic auxiliaries that cannot be removed, for which it is necessary to check that they are welds linked to the equipment and correctly held in place. On the other hand, these accessories are stabilized in such a way as to withstand considerable forces, such as chewing ones. It is therefore unlikely that these are displaced by minor forces, such as those exerted by the magnetic field [Kemper et al., 2007].

Another study analyzed the effects of translational and rotational forces induced by a 3T magnetic field on 21 orthodontic arches of different section, material and manufacturer. Additionally, 8 different metal ligatures and 3 different splinting wires were tested. Steel bows and splinting wires were not found to be safe according to the ASTM evaluation criteria. The detected forces, although exceeding the limits set by the aforementioned association, are comparable or lower than the normal orthodontic forces and should therefore not cause the detachment of correctly placed devices. Conversely, Ni-Ti or TMA bows and brass wires were safe [Klocke et al., 2006].

However, the retentive forces offered by the adhesion systems and by the various types of ties play an important role in opposing the attractive forces and reducing the potentials risks of dislocation of orthodontic devices. The Authors state that these "counter-forces" must therefore be verified before the examination and possibly replaced or reinforced. In order to define the overall risk represented by the interaction of non-removable orthodontic appliances with the static magnetic field produced during a magnetic resonance examination, it is also necessary to take into consideration other important aspects, such as overheating of the auxiliaries and the induction of electric currents through of them [Regier et al., 2009].

In literature a minimum bond strength of 6 to 8 MPa is reported to be adequate for most clinical orthodontic needs [Reynolds, 1975], but adhesion forces should not be too strong (over 40–50 MPa) in order to avoid enamel loss after debonding [Giannini et al., 2004]. Therefore, the ideal orthodontic biomaterial should have bonding forces included in the interval of 5–50 MPa, even if these limits are mostly theoretical [Scribante et al., 2016]. In the present report, SBS values ranged between these limits. Therefore, after MRI, all brackets exhibited clinically acceptable bond strength values, therefore appliances are expected to sustain masticatory forces without risk of enamel loss.

6.4. Third null hypothesis. The ARI Scores.

As far as ARI scores are concerned, the third null hypothesis of this study was rejected. ARI values were significantly lower after MRI, showing a shift from a significant prevalence of ARI=1 recorded in control group to ARI=0 measured in all other groups that underwent MRI. This is probably due to the heating of metal devices that seems to modify the quantitative of adhesive left on the tooth after bracket removal.

Generally, an ARI = 0 means a higher adhesion of bonding system, more to the bracket base than to the tooth, during the debonding process [Hadrous et al., 2019]. In this case, it is claimed that less time is involved for adhesive removal from tooth surface [Cardoso et al., 2014]. In contrast, an ARI = 3 indicates failure between the bracket and adhesive, thus lowering risk of enamel fracture upon removal [Holberg et al., 2014].

The results of the present study showed a significant change in the detachment interface for the groups subjected to MRI. Therefore possible to hypothesize a correlation between the variation in temperature and the different behavior of the composite, even if there are no sufficient evidence to support this theory.

Since ARI is based on subjective observations, several methods have been proposed to transform this index in order to gain more precision and repeatability [Hung et al., 2019; Pourhajibagher et al., 2019; Zarif Najafi et al., 2019]. An index expressed as a percentage of residual composite based on the bracket with respect to the area of the base itself has been proposed [O'Brien et al., 1988]. To carry out this measurement, the authors proposed acquiring a digital image of the enamel and enlarging it to facilitate operator observation. The use of digital image acquisition and the ability to provide an enlargement of the images to indicate the percentage of residual adhesive finds consensus among different authors [Mirzakouchaki et al., 2016]. The calculation can be even more accurate if performed using a program image processing, compared to a single naked eye analysis. A 20x magnification allows better discrimination of the indices [Montasser and Drummond, 2009].

In the literature previous reports that evaluated ARI scores showed contradicting results. Both insignificant [Knox et al., 2000] and significant [Merone et al., 2010] effects of base design or other bonding-related variables on ARI scores have been previously

reported. This is probably due to the different materials and study design presented in the various investigations [Dallel et al., 2019].

However, ARI Scores are not directly related to bond strength efficacy [Montasser and Drummond, 2009], but represent a more complex method to assess the failure between the bracket base and enamel. Low ARI Score can be linked to easier polishing procedures as no adhesive remains on tooth surface [Ahmadi et al., 2020] so both 1.5T and 3T MRIs seem to have no negative effects also on this variable.

6.5. Limitations and general considerations.

The present report demonstrated that the tested orthodontic materials are considerable as safe considering the variables of brackets and wires temperatures, appliance adhesion and residual adhesive. However, these devices can have a detrimental effect on final image quality depending on the anatomical district studied with the radiologic exam. A classification of dental materials according to their magnetic susceptibility has been proposed [Tymofiyeva et al., 2013] and studies evaluated the effect of orthodontic fixed metal appliances [Zhylich et al., 2017] and retainers [Shalish et al., 2015] on image quality. There is fair evidence to suggest orthodontic devices cause MRI image artefacts both at 1.5T [Blankenstein et al., 2017] and 3T [Ozawa et al., 2018]. The removal of metal orthodontic devices prior to MRI is recommended, especially if the area of interest is near the appliance [Beau et al., 2015], such as cervical vertebrae, cervical region, paranasal sinuses, and head and neck MRI scans. The brain and temporomandibular joint region MRI should not require the removal of such appliances [Ozawa et al., 2018].

A limitation of the present report could be that during a MRI exam the amount of magnetic field could change significantly depending on the distance from radiologic device or on the patient orientation [Sawyer-Glover and Shellock, 2000; Kainz, 2007; Blankenstein et al., 2017]. However, in our study orthodontic appliances were positioned in the centre of the MRI device, in the area where the magnetic field was the greatest [Oshagh et al., 2010].

Additionally, the results of the present report are reliable only for materials tested and they are not generalizable, as there could be variability in induced magnetic moment among appliances from different manufacturers. Moreover, clear information on the

exact alloy composition of orthodontic appliances is not readily available in most cases [Wang et al., 2015]. So, further in vitro and clinical studies on the topic would be welcomed in order to give clearer guidelines to clinicians and patients [Alshammery et al., 2020].

It is not always possible to predict whether a patient will need to undergo MRI during orthodontic treatment, but it is important to question the patient on the first visit about his medical history and the possible need to undergo periodic checks that require this type of examination. In this case, it may be advisable to use ceramic or titanium brackets and bands instead of tubes [Sawyer-Glover and Shellock, 2000]. The desired biomechanics, the type of anchor required and the specific treatment plan in each case guide the clinician's final decision regarding the choice of MRI compatible devices. For example, ceramic brackets can produce less image distortions but the brittleness of the attachment, the risk of damage to the enamel during debonding, the potential abrasion of the antagonist teeth and the greater sliding resistance can make this option disadvantageous. In these cases, titanium attachments are therefore more advisable [Fernández-Miñano et al., 2011].

Different brackets on the market have parts in various materials and the distortion of the image depends on the content of ferromagnetic components [Sawyer-Glover and Shellock, 2000; Blankenstein et al., 2017; Alshammery et al., 2020]. Even the composites usually used for bonding contain ferromagnetic materials (ferric oxide), albeit in minimal quantities, and can therefore cause distortions but limited to the tooth surface involved [Hasegawa et al., 2013].

Therefore, it is not always necessary to remove the device before an MRI and the decision must be made considering the area under investigation and the appliances present in each specific case. In general, steel arches must be removed beforehand due to the risk of artifacts, due to the important interactions with the magnetic field and to some possible thermal damage, albeit negligible [Sawyer-Glover and Shellock, 2000; Oshagh et al., 2010; Wang et al., 2015; Blankenstein et al., 2017; Alshammery et al., 2020]. The stability of other remaining devices inside the oral cavity (metal ligatures, brackets, bands and tubes) has to be meticulously checked. All removable metal devices must be removed and, if the oral cavity would be the main object of investigation, also

the fixed retainers and splints made with metal wires should be removed [Poorsattar-Bejeh et al., 2016].

Brackets can be made of SS, NiTi, SS without nickel or ceramic [Elsaka et al., 2014] so the decision should take into account the composition of the brackets and the distance from the survey sites. Removal is questionable if they are located near the maxillary sinus, the ATM or palatal zones [Sawyer-Glover and Shellock, 2000; Alshammery et al., 2020].

On these bases, the clinician should evaluate rational and careful considerations for each different patient.

7. Conclusions.

7. Conclusions.

The present report demonstrated that:

-a significant increase of temperatures was found both for brackets and wires in some groups, even if the mean temperature increase was clinically not significant (from 0.4°C to 2.2°C).

-MRI did not conditioned bracket adhesion in any group.

-ARI Scores were significantly lower after MRI.

Therefore, the removal of orthodontic appliance before MRI would not recommended routinely, but it is suggested only in case of void risk or interference in image quality.

8. Statements.

8. Statements.

Funding.
None.

Conflict of interests.
None.

Data availability statement.
All data are available upon request to Author.

Publication statement.
A research article has been extracted from the present Doctoral Thesis.
Title: Magnetic Resonance Imaging and Its Effects on Metallic Brackets and Wires: Does It Alter the Temperature and Bonding Efficacy of Orthodontic Devices?
Authors: Sfondrini MF, Preda L, Calliada F, Carbone L, Lungarotti L, Bernardinelli L, Gandini P, Scribante A.
Journal: Materials (Basel). 2019 Nov 30;12(23). pii: E3971.

Technical acknowledgements.
The Author would like to thank 3M and Leone for providing the materials tested in this study and Dr. Ivano Marrone and Dr. Luca Anemoni for excellent technical assistance.

9. References.

9. References.

1. Ahmadi H, Haddadi-Asl V, Ghafari HA, Ghorbanzadeh R, Mazlum Y, Bahador A. Shear bond strength, adhesive remnant index, and anti-biofilm effects of photoexcited a modified orthodontic adhesive containing curcumin doped poly lactic-co-glycolic acid nanoparticles; An ex-vivo biofilm model of S. mutans on the enamel slab bonded brackets. Photodiagnosis Photodyn Ther. 2020 Jan 26:101674.
2. Almosa N, Zafar H. Incidence of orthodontic brackets detachment during orthodontic treatment: A systematic review. Pak J Med Sci. 2018 May-Jun;34(3):744-750.
3. Alshammery FA. Three dimensional (3D) imaging techniques in orthodontics-An update. J Family Med Prim Care. 2020 Jun 30;9(6):2626-2630.
4. Altmann AS, Collares FM, Leitune VC, Samuel SM. The effect of antimicrobial agents on bond strength of orthodontic adhesives: a meta-analysis of in vitro studies. Orthod Craniofac Res. 2016 Feb;19(1):1-9.
5. Artun J, Bergland S. Clinical trials with crystal growth conditioning as an alternative to acid-etch enamel pretreatment. Am J Orthod. 1984 Apr;85(4):333-40.
6. Arun A, Thomas TJ, Rani JS, Gorthi RKSS. Efficient directionality-driven dictionary learning for compressive sensing magnetic resonance imaging reconstruction. J Med Imaging (Bellingham). 2020 Jan;7(1):014002.
7. Assaf C, Fahd JC, Sabbagh J. Assessing Dental Light-curing Units' Output Using Radiometers: A Narrative Review. J Int Soc Prev Community Dent. 2020 Jan 24;10(1):1-8.
8. Attishia R, Van Sickels JE, Cunningham LL. Incidence of bracket failure during orthognathic surgery: a comparison of two techniques to establish interim maxillomandibular fixation. Oral Maxillofac Surg. 2015;19(2):143–147.
9. Aydın B, Pamir T, Baltaci A, Orman MN, Turk T. Effect of storage solutions on microhardness of crown enamel and dentin. Eur J Dent. 2015 Apr-Jun;9(2):262-266.

10. Bakhadher W, Halawany H, Talic N, Abraham N, Jacob V. Factors Affecting the Shear Bond Strength of Orthodontic Brackets - a Review of In Vitro Studies. Acta Medica (Hradec Kralove). 2015;58(2):43-8.
11. Banks P, Elton V, Jones Y, Rice P, Derwent S, Odondi L. The use of fixed appliances in the UK:a survey of specialist orthodontists. J Orthod. 2010;37(1):43–55.
12. Beau A, Bossard D, Gebeile-Chauty S. Magnetic resonance imaging artefacts and Fixed Orthodontic Attachments. Orthod Fr 2017;88:131-138.
13. Behr A. Production and efficiency analysis with R (Book). Springer 2015
14. Beltrami R, Chiesa M, Scribante A, Allegretti J, Poggio C. Comparison of shear bond strength of universal adhesives on etched and nonetched enamel. J Appl Biomater Funct Mater. 2016 Apr 6;14(1):e78-83.
15. Bishara SE, Laffoon JF, VonWald L, Warren JJ. The effect of repeated bonding on the shear bond strength of different orthodontic adhesives. Am J Orthod Dentofacial Orthop. 2002;121(5):521–525.
16. Blankenstein FH, Asbach P, Beuer F, Glienke J, Mayer S, Zachriat C. Magnetic permeability as a predictor of the artifact size caused by orthodontic appliances at 1.5 T magnetic resonance imaging. Clin Oral Investig. 2017 Jan;21(1):281-289.
17. Blankenstein FH, Truong BT, Thomas A, Thieme N, Zachriat C. Predictability of magnetic susceptibility artifacts from metallic orthodontic appliances in magnetic resonance imaging. J Orofac Orthop 2015;76:14-29.
18. Blokdyk B. Ad Hoc Testing (Book). 5STARCooks 2018.
19. Bovali E, Kiliaridis S, Cornelis MA. Indirect vs direct bonding of mandibular fixed retainers in orthodontic patients: a single-center randomized controlled trial comparing placement time and failure over a 6-month period. Am J Orthod Dentofacial Orthop. 2014;146(6):701–708.
20. Brown JD. Advanced Statistics for the Behavioral Sciences: A Computational Approach with R (Book). Springer 2019.
21. Caplin J, Han MD, Miloro M, Allareddy V, Markiewicz MR. Interceptive Dentofacial Orthopedics (Growth Modification). Oral Maxillofac Surg Clin North Am. 2020 Feb;32(1):39-51.

22. Cardoso LA, Valdrighi HC, Vedovello Filho M, Correr AB. Effect of adhesive remnant removal on enamel topography after bracket debonding. Dental Press J Orthod. 2014;19:105–12.
23. Carlyle TD, Chamma A, Moir RW, Williams PT. An evaluation of the shear bond strength developed between a glass ionomer cement and enamel. J Dent Res. 1978 Feb;57(2):232.
24. Cassetta M, Pranno N, Stasolla A, Orsogna N, Fierro D, Cavallini C, Cantisani V. The effects of a common stainless steel orthodontic bracket on the diagnostic quality of cranial and cervical 3T- MR images: a prospective, case-control study. Dentomaxillofac Radiol. 2017 Aug;46(6):20170051.
25. Cerroni S, Pasquantonio G, Condò R, Cerroni L. Orthodontic Fixed Appliance and Periodontal Status: An Updated Systematic Review. Open Dent J. 2018 Sep 28;12:614-622.
26. Cetik S, Ha TH, Sitri L, Duterme H, Pham V, Atash R. Comparison of Shear Strength of Metal and Ceramic Orthodontic Brackets Cemented to Zirconia Depending on Surface Treatment: An In Vitro Study. Eur J Dent. 2019 May;13(2):150-155.
27. Chockattu SJ, Suryakant DB, Thakur S. Unwanted effects due to interactions between dental materials and magnetic resonance imaging: a review of the literature. Restor Dent Endod. 2018 Aug 30;43(4):e39.
28. Cohen Y, Cohen JY. Statistics and Data with R: An applied approach through examples (Book). Wiley 2008.
29. Contreras-Bulnes R, Scougall-Vilchis RJ, Rodríguez-Vilchis LE, Centeno-Pedraza C, Olea-Mejía OF, Alcántara-Galena Mdel C. Evaluation of self-etching adhesive and Er:YAG laser conditioning on the shear bond strength of orthodontic brackets. ScientificWorldJournal. 2013 Oct 8;2013:719182.
30. Cope F, Damadian R. Cell potassium by 39K spin echo nuclear magnetic resonance. Nature 1970;228(5266):76–77.
31. Corradi-Dias L, Paiva SM, Pretti H, Pordeus IA, Abreu LG. Impact of the onset of fixed appliance therapy on adolescents' quality of life using a specific condition questionnaire: A cross-sectional comparison between male and female individuals. J Orthod. 2019 Sep;46(3):195-204.

32. Costa AL, Appenzeller S, Yasuda CL, Pereira FR, Zanardi VA, Cendes F. Artifacts in brain magnetic resonance imaging due to metallic dental objects. Med Oral Patol Oral Cir Bucal. 2009 Jun 1;14(6):E278-82.
33. Cox RJ, Kau CH, Rasche V. Three-dimensional ultrashort echo magnetic resonance imaging of orthodontic appliances in the natural dentition. Am J Orthod Dentofacial Orthop. 2012;142:552-561.
34. Crawley MJ. The R Book: Second Edition (Book). Wiley 2012.
35. Currie S, Hoggard N, Craven IJ, Hadjivassiliou M, Wilkinson ID. Understanding MRI: basic MR physics for physicians. Postgrad Med J. 2013;89:209-¬223.
36. Da Rocha JM, Gravina MA, da Silva Campos MJ, Quintão CC, Elias CN, Vitral RW. Shear bond resistance and enamel surface comparison after the bonding and debonding of ceramic and metallic brackets. Dental Press J Orthod. 2014 Jan-Feb;19(1):77-85.
37. Dalili Kajan Z, Khademi J, Alizadeh A, Babaei Hemmaty Y, Atrkar Roushan Z. A comparative study of metal artifacts from common metal orthodontic brackets in magnetic resonance imaging. Imaging Sci Dent 2015; 45: 159-68.
38. Dallel I, Lahwar S, Jerbi MA, Tobji S, Ben Amor A, Kassab A. Impact of adhesive system generation and light curing units on orthodontic bonding: In vitro study. Int Orthod. 2019 Dec;17(4):799-805.
39. Daronch M, Rueggeberg FA, Hall G, De Goes MF. Effect of composite temperature on in vitro intrapulpal temperature rise. Dent Mater. 2007;23:1283-1288.
40. De Carvalho MFF, Leijôto-Lannes ACN, Rodrigues MCN, Nogueira LC, Ferraz NKL, Moreira AN, Yamauti M, Zina LG, Magalhães CS. Viability of Bovine Teeth as a Substrate in Bond Strength Tests: A Systematic Review and Meta-analysis. J Adhes Dent. 2018;20(6):471-479.
41. Degrazia FW, Genari B, Ferrazzo VA, Santos-Pinto AD, Grehs RA. Enamel Roughness Changes after Removal of Orthodontic Adhesive. Dent J (Basel). 2018 Aug 6;6(3).
42. Ekizer A, Zorba YO, Uysal T, Ayrikcila S. Effects of demineralizaton-inhibition procedures on the bond strength of brackets bonded to demineralized enamel surface. Korean J Orthod. 2012 Feb;42(1):17-22.

43. Ekstrøm CT, Sørensen H. Introduction to statistical data analysis for the life sciences (Book). Taylor and Francis 2010.
44. El-Bediwi AB, El-Fallal A, Saker S, Ozcan M. Effect of non-ionizing radio frequency signals of magnetic resonance imaging on physical properties of dental alloys and metal-ceramic adhesion. J Adhes Dent. 2014 Oct;16(5):407-13.
45. Elison JM, Leggitt VL, Thomson M, Oyoyo U, Wycliffe ND. Influence of common orthodontic appliances on the diagnostic quality of cranial magnetic resonance images. Am J Orthod Dentofacial Orthop. 2008;134:563-572.
46. Elsaka SE, Hammad SM, Ibrahim NF. Evaluation of stresses developed in different bracket-cement-enamel systems using finite element analysis with in vitro bond strength tests. Prog Orthod. 2014 Apr 16;15(1):33.
47. Elster AD. An index system for comparative parameter weighting in MR imaging. J Comput Assist Tomogr 1988; 12:130-134.
48. Fernández-Miñano E, Ortiz C, Vicente A, Calvo Guirado JL, Ortiz AJ. Metallic ion content and damage to the DNA in oral mucosa cells of children with fixed orthodontic appliances. Biometals. 2011 Oct;24(5):935.
49. Finnema KJ, Özcan M, Post WJ, Ren Y, Dijkstra PU. In-vitro orthodontic bond strength testing: A systematic review and meta-analysis. Am J Orthod Dentofacial Orthop 2010;137:615-622.
50. Fjeld M, Øgaard B. Am J Orthod Dentofacial Orthop. Scanning electron microscopic evaluation of enamel surfaces exposed to 3 orthodontic bonding systems. 2006 Nov;130(5):575-81.
51. Fleming PS, Springate SD, Chate RA. Myths and realities in orthodontics. Br Dent J. 2015 Feb 16;218(3):105-10.
52. Foersch M, Schuster C, Rahimi RK, Wehrbein H, Jacobs C. A new flash-free orthodontic adhesive system: A first clinical and stereomicroscopic study. Angle Orthod. 2016 Mar;86(2):260-4.
53. Fox NA, McCabe JF, Buckley JG. A critique of bond strength testing in orthodontics. Br J Orthod. 1994 Feb;21(1):33-43.
54. Garcia-Contreras R, Scougall-Vilchis RJ, Contreras-Bulnes R, Sakagami H, Morales-Luckie RA, Nakajima H. Mechanical, antibacterial and bond strength

properties of nano-titanium-enriched glass ionomer cement. J Appl Oral Sci. 2015 May-Jun;23(3):321-8.

55. Gaur A, Maheshwari S, Verma SK, Tariq M. Effects of adhesion promoter on orthodontic bonding in fluorosed teeth: A scanning electron microscopy study. J Orthod Sci. 2016;5:87-91.
56. Giannini M, Soares CJ, de Carvalho RM. Ultimate tensile strength of tooth structures. Dent Mater. 2004 May;20(4):322-9.
57. Gittner R, Müller-Hartwich R, Engel S, Jost-Brinkmann PG. Shear bond strength and enamel fracture behavior of ceramic brackets Fascination® and Fascination®2. J Orofac Orthop. 2012;73:49-57.
58. Godard M, Deuve B, Lopez I, Hippolyte MP, Barthélemi S. Shear bond strength of two 2-step etch-and-rinse adhesives when bonding ceramic brackets to bovine enamel. Int Orthod. 2017 Sep;15(3):388-404.
59. Görgülü S, Ayyildiz S, Kamburoglu K, Gökçe S, Ozen T. Effect of orthodontic bracket and different wires on radiofrequency heating and magnetic field interactions during 3-T MRI. Dentomaxillofacial Radiology 2014;43:20130356
60. Haacke E.M.,Brown R.W., Thompson M.R., Venkatesan R. Magnetic Resonance Imaging: Physical Principles and Sequence Design. Wiley Blackwell 2014
61. Hadrous R, Bouserhal J, Osman E. Evaluation of shear bond strength of orthodontic molar tubes bonded using hydrophilic primers: An in vitro study. Int Orthod. 2019 Sep;17(3):461-468.
62. Harris TMJ, Faridrad MR, Dickson JAS. The benefits of aesthetic orthodontic bracket in patients requiring multiple MRI scanning. J Orthod. 2006;33:90-94.
63. Hasanin M, Kaplan SEF, Hohlen B, Lai C, Nagshabandi R, Zhu X, Al-Jewair T. Effects of orthodontic appliances on the diagnostic capability of magnetic resonance imaging in the head and neck region: A systematic review. Int Orthod. 2019 Jul 6. pii: S1761-7227(19)30076-2.
64. Hasegawa M, Miyata K, Abe Y, Ishigami T. Radiofrequency heating of metallic dental devices during 3.0 T MRI. Dentomaxillofac Radiol. 2013;42:20120234.

65. Hatch JP, Deahl TS 2nd, Matteson SR. CAT of the month: Remove metallic orthodontic appliances prior to MRI imaging UT CAT #2166. Tex Dent J. 2014;131:26.
66. Hillebrand A, Fazio P, de Munck JC, van Dijk BW. Feasibility of clinical magnetoencephalography (MEG) functional mapping in the presence of dental artefacts. Clin Neurophysiol. 2013 Jan;124(1):107-13.
67. Hioki M, Shin-Ya A, Nakahara R, Vallittu PK, Nakasone Y, Shin-Ya A. Shear bond strength and FEM of a resin-modified glass ionomer cement--effects of tooth enamel shape and orthodontic bracket base configuration. Dent Mater J. 2007 Sep;26(5):700-7.
68. Holberg C, Winterhalder P, Holberg N, Wichelhaus A, Rudzki-Janson I. Orthodontic bracket debonding: risk of enamel fracture. Clin Oral Investig. 2014 Jan;18(1):327-34.
69. Hubálková H, Hora K, Seidl Z, Krásenský J. Dental materials and magnetic resonance imaging. Eur J Prosthodont Restor Dent. 2002 Sep;10(3):125-30.
70. Hung CY, Yu JH, Su LW, Uan JY, Chen YC, Lin DJ. Materials (Basel). Shear Bonding Strength and Thermal Cycling Effect of Fluoride Releasable/Rechargeable Orthodontic Adhesive Resins Containing LiAl-F Layered Double Hydroxide (LDH) Filler. 2019 Sep 30;12(19):3204.
71. Inam O, Basit A, Qureshi M, Omer H. FPGA-based hardware accelerator for SENSE (a parallel MR image reconstruction method). Comput Biol Med. 2020 Feb;117:103598.
72. Kagetsu NJ, Litt AW. Important considerations in measurement of attractive force on metallic implants in MR imagers. Radiology. 1991;179:505-508.
73. Kainz W. MR heating tests of MR critical implants. J Magn Reson Imaging. 2007 Sep;26(3):450-1.
74. Karunakaran C. Spin resonance spectroscopy: Principles and applications (Book). Elsevier 2018.
75. Ke Y, Zhu Y, Zhu M. A comparison of treatment effectiveness between clear aligner and fixed appliance therapies. BMC Oral Health. 2019 Jan 23;19(1):24.

76. Kemper J, Klocke A, Kahl-Nieke B, Adam G. Orthodontic brackets in high field MR imaging: experimental evaluation of magnetic field interactions at 3.0 Tesla. Rofo. 2005 Dec;177(12):1691-8.
77. Kemper J, Priest AN, Schulze D, Kahl-Nieke B, Adam G, Klocke A. Orthodontic springs and auxiliary appliances: assessment of magnetic field interactions associated with 1.5 T and 3 T magnetic resonance systems. European Radiology. 2007;17:533-540.
78. Khargekar NR, Kalathingal JH, Sam G, Elpatal MA, Hota S, Bhushan P. Evaluation of Different Pretreatment Efficacy with Fluoride-releasing Material on Shear Bond Strength of Orthodontic Bracket: An In Vitro Study. J Contemp Dent Pract. 2019 Dec 1;20(12):1442-1446.
79. Kim Y, Park HI, Lee HK, Nam HS, Lee YW, Lee SG, Park Y, Lee W, Nam MH, Song SH, Chung JW, Lee J. Development of Statistical Software for the Korean Laboratory Accreditation Program Using R Language: LaboStats. Ann Lab Med. 2019 Nov;39(6):552-560.
80. Klocke A, Kahl-Nieke B, Adam G, Kemper J. Magnetic forces on orthodontic wires in high field magnetic resonance imaging (MRI) at 3 Tesla. J Orofac Orthop. 2006;67:424-429.
81. Klocke A, Kahl-Nieke B. Effect of debonding force direction on orthodontic shear bond strength. Am J Orthod Dentofacial Orthop. 2006 Feb;129(2):261-5.
82. Klocke A, Kemper J, Schulze D, Adam G, Kahl-Nieke B. Magnetic field interactions of orthodontic wires during magnetic resonance imaging (MRI) at 1.5 Tesla. J Orofac Orthop. 2005;66:279-287.
83. Knox J, Hubsch P, Jones ML, Middleton J. The influence of bracket base design on the strength of the bracket-cement interface. J Orthod. 2000 Sep;27(3):249-54.
84. Koide K, Tanaka S, Endo T. Use of the Er,Cr:YSGG laser for removing remnant adhesive from the enamel surface in rebonding of orthodontic brackets. Odontology. 2020 Apr;108(2):271-279.
85. Linjawi AI, Abbassy MA. Comparison of shear bond strength to clinically simulated debonding of orthodontic bracket: an in vitro study. J Orthod Sci. 2016;5:25-29.

86. Maekawa M, Kanno Z, Wada T, Hongo T, Doi H, Hanawa T, Ono T, Uo M. Mechanical properties of orthodontic wires made of super engineering plastic. Dent Mater J. 2015;34(1):114-9.
87. Mandall NA, Hickman J, Macfarlane TV, Mattick RC, Millett DT, Worthington HV. Adhesives for fixed orthodontic brackets. Cochrane Database Syst Rev. 2018 Apr 9;4(4):CD002282.
88. Mathew CA, Maller S, Maheshwaran. Interactions between magnetic resonance imaging and dental material. J Pharm Bioallied Sci. 2013 Jun;5(Suppl 1):S113-6.
89. Matias M, Freitas MR, Freitas KMS, Janson G, Higa RH, Francisconi MF. Comparison of deflection forces of esthetic archwires combined with ceramic brackets. J Appl Oral Sci. 2018;26:e20170220. Sanchez DJ, Walker MP, Kula K, Williams KB, Eick JD. Fluoride prophylactic agents effect on ceramic bracket tie-wing fracture strength. Angle Orthod. 2008 May;78(3):524-30.
90. Matthews DE, Farewell VT. Using and understanding medical statistics: 5th, revised and extended edition (Book). Karger 2015
91. Merone G, Valletta R, De Santis R, Ambrosio L, Martina R. A novel bracket base design: biomechanical stability. Eur J Orthod. 2010 Apr;32(2):219-23.
92. Miao X, Wu Y, Liu D, Jiang H, Woods D, Stern MT, Blair NIS, Airan RD, Bettegowda C, Rosch KS, Qin Q, van Zijl PCM, Pillai JJ, Hua J. Whole-Brain Functional and Diffusion Tensor MRI in Human Participants with Metallic Orthodontic Braces. Radiology. 2020 Jan;294(1):149-157.
93. Milagres FDSA, Oliveira DD, Silveira GS, Oliveira EFF, Antunes ANDG. Bond Strength and Failure Pattern of Orthodontic Tubes Adhered to a Zirconia Surface Submitted to Different Modes of Application of a Ceramic Primer. Materials (Basel). 2019 Nov 27;12(23):3922.
94. Miller RG. Beyond ANOVA: Basics of Applied Statistics. Chapman & Hall 1997.
95. Mirzakouchaki B, Shirazi S, Sharghi R, Shirazi S, Moghimi M, Shahrbaf S. Shear bond strength and debonding characteristics of metal and ceramic brackets bonded with conventional acid-etch and self-etch primer systems: An in-vivo study. J Clin Exp Dent. 2016 Feb 1;8(1):e38-43.

96. Mitchell D. G. MRI Principles Saunders, 1999.
97. Mollabashi V, Rezaei-Soufi L, Farhadian M, Noorani AR. Effect of Erbium, Chromium-Doped: Yttrium, Scandium, Gallium, and Garnet and Erbium: Yttrium-Aluminum-Garnet Laser Etching on Enamel Demineralization and Shear Bond Strength of Orthodontic Brackets. Contemp Clin Dent. 2019 Apr-Jun;10(2):263-268.
98. Monahan JF. Numerical methods of statistics. (Book). Cambridge University Press 2011.
99. Montasser MA, Drummond JL. Reliability of the adhesive remnant index score system with different magnifications. Angle Orthod. 2009 Jul;79(4):773-6.
100. Montasser MA, Taha M. Effect of enamel protective agents on shear bond strength of orthodontic brackets. Prog Orthod. 2014 Jul 18;15:34.
101. Montasser MA. Effect of applying a sustained force during bonding orthodontic brackets on the adhesive layer and on shear bond strength. Eur J Orthod. 2011 Aug;33(4):402-6.
102. Morris P. Biomedical Imaging: Applications and Advances (Book). Woodhead Publishing Limited 2014.
103. Mortazavi SMJ, Paknahad M. Effect of orthodontic bracket and different wires on radiofrequency heating and magnetic field interactions during 3.0-T MRI. Dentomaxillofac Radiol. 2016; 45: 20150266.
104. Mostafiz W. Fundamentals of Interceptive Orthodontics: Optimizing Dentofacial Growth and Development. Compend Contin Educ Dent. 2019 Mar;40(3):149-154.
105. O'Brien KD, Watts DC, Read MJ. Residual debris and bond strength--is there a relationship? Am J Orthod Dentofacial Orthop. 1988 Sep;94(3):222-30.
106. Oduncuoğlu BF, Yamanel K, Koçak ZŞ. In Vitro Evaluation of Direct and Indirect Effects of Sonic and Ultrasonic Instrumentations on the Shear Bond Strength of Orthodontic Brackets. Turk J Orthod. 2020 Mar 1;33(1):37-42.
107. Okano Y, Yamashiro M, Kaneda T, Kasai K. Magnetic resonance imaging diagnosis of the temporomandibular joint in patients with orthodontic appliances. Oral Surg Oral Med Oral Pathol Oral Radiol Endod. 2003;95:255-263.

108. Oshagh M, Hematian MR, Shahidi S, Feizi N, Bayani F, Pishbin L. Effect of MRI on the mechanical properties of stainless steel orthodontic wires. World J Orthod. 2010 Winter;11(4):e72-7.

109. Ozawa E, Honda EI, Parakonthun KN, Ohmori H, Shimazaki K, Kurabayashi T, Ono T. Influence of orthodontic appliance-derived artifacts on 3-T MRI movies. Prog Orthod. 2018 Feb 19;19(1):7.

110. Ozcan M, Vallittu PK, Peltomäki T, Huysmans MC, Kalk W. Bonding polycarbonate brackets to ceramic: effects of substrate treatment on bond strength. Am J Orthod Dentofacial Orthop. 2004 Aug;126(2):220-7.

111. Oztürk B, Malkoç S, Koyutürk AE, Catalbas B, Ozer F. Influence of different tooth types on the bond strength of two orthodontic adhesive systems. Eur J Orthod. 2008 Aug;30(4):407-12.

112. Panagiotakos DB. The Value of p-Value in Biomedical Research. Open Cardiovasc Med J. 2008; 2: 97–99.

113. Papageorgiou SN, Keilig L, Hasan I, Jäger A, Bourauel C. Effect of material variation on the biomechanical behaviour of orthodontic fixed appliances: a finite element analysis. Eur J Orthod. 2016 Jun;38(3):300-7. doi: 10.1093/ejo/cjv050. Epub 2015 Jul 14.

114. Pardoe I. Applied Regression Modeling: Second Edition (Book). Wiley 2013

115. Parker JA. Image reconstruction in radiology (Book). CRC Press 2018.

116. Pasha A, Vishwakarma S, Narayan A, Vinay K, Shetty SV, Roy PP. Comparison of Frictional Forces Generated by a New Ceramic Bracket with the Conventional Brackets using Unconventional and Conventional Ligation System and the Self-ligating Brackets: An In Vitro Study. J Int Oral Health. 2015 Sep;7(9):108-13.

117. Patel A, Bhavra GS, O'Neill JRS. MRI scanning and orthodontics. Journal of Orthodontics 2006;33:246-249

118. Patel N, Bollu P, Chaudhry K, Subramani K. The effect of orthodontic bracket pad shape on shear bond strength, an in vitro study on human enamel. J Clin Exp Dent. 2018 Aug 1;10(8):e789-e793.

119. Phukaoluan A, Khantachawana A, Kaewtatip P, Dechkunakorn S, Kajornchaiyakul J. Improvement of mechanical and biological properties of TiNi alloys by addition of Cu and Co to orthodontic archwires. Int Orthod. 2016 Sep;14(3):295-310.

120. Poggio C, Scribante A, Della Zoppa F, Colombo M, Beltrami R, Chiesa M. Shear bond strength of one-step self-etch adhesives to enamel: effect of acid pretreatment. Dent Traumatol. 2014 Feb;30(1):43-8.

121. Poorsattar-Bejeh Mir A., Rahmati-Kamel M. Should the orthodontic bracket always be removed prior to magnetic resonance imaging (MRI)? J Oral Biol Craniofac Res. 2016; 6:142–152

122. Pourhajibagher M, Salehi Vaziri A, Takzaree N, Ghorbanzadeh R. Physico-mechanical and antimicrobial properties of an orthodontic adhesive containing cationic curcumin doped zinc oxide nanoparticles subjected to photodynamic therapy. Photodiagnosis Photodyn Ther. 2019 Mar;25:239-246.

123. Rabi II, Zacharias JR, Millman S, Kusch P. A New Method of Measuring Nuclear Magnetic Moment. Physical Review. 1938;53 (4): 318–327.

124. Regier M, Kemper J, Kaul MG, Feddersen M, Adam G, Kahl-Nieke B, Klocke A. Radiofrequency-induced heating near fixed orthodontic appliances in high field MRI systems at 3.0 Tesla. J Orofac Orthop. 2009;70:485-494.

125. Reichardt E, Geraci J, Sachse S, Rödel J, Pfister W, Löffler B, Wagner Y, Eigenthaler M, Wolf M. Qualitative and quantitative changes in the oral bacterial flora occur shortly after implementation of fixed orthodontic appliances. Am J Orthod Dentofacial Orthop. 2019 Dec;156(6):735-744.

126. Reynolds IR. A review of direct orthodontic bonding. Br J Orthod 1975;2:171-78.

127. Richter AE, Arruda AO, Peters MC, Sohn W. Incidence of caries lesions among patients treated with comprehensive orthodontics. Am J Orthod Dentofacial Orthop. 2011 May;139(5):657-64.

128. Roelofs T, Merkens N, Roelofs J, Bronkhorst E, Breuning H. A retrospective survey of the causes of bracket- and tube-bonding failures. Angle Orthod. 2017;87(1):111–117.

129. Romano FL, Valerio RA, Gomes-Silva JM, Ferreira JT, Faria G, Borsatto MC. Clinical evaluation of the failure rate of metallic brackets bonded with orthodontic composites. Braz Dent J. 2012;23(4):399–402.

130. Rüttermann S, Braun A, Janda R. Shear bond strength and fracture analysis of human vs. bovine teeth. PLoS One. 2013;8(3):e59181.

131. Sadowsky PL, Bernreuter W, Lakshminarayanan AV, Kenney P. Orthodontic appliances and magnetic resonance imaging of the brain and temporomandibular joint. Angle Orthod. 1988;58:9-20.

132. Santana FR, Pereira JC, Pereira CA, Fernandes Neto AJ, Soares CJ. Influence of method and period of storage on the microtensile bond strength of indirect composite resin restorations to dentine. Braz Oral Res. 2008 Oct-Dec;22(4):352-7.

133. Sawitzki G. Computational Statistics: An Introduction to R (Book). Taylor and Francis 2009.

134. Sawyer-Glover AM, Shellock FG. Pre-MRI procedure screening: recommendations and safety considerations for medical implants and devices. J Magn Reson Imaging. 2000;12:92-106.

135. Schenck JF. The role of magnetic susceptibility in magnetic resonance imaging: MRI magnetic compatibility of the first and second kinds. Med Phys 1996;23:815¬-850.

136. Schilke R, Bauss O, Lisson JA, Schuckar M, Geurtsen W. Bovine dentin as a substitute for human dentin in shear bond strength measurements. Am J Dent. 1999 Apr;12(2):92-6.

137. Schilke R, Lisson JA, Bauss O, Geurtsen W. Comparison of the number and diameter of dentinal tubules in human and bovine dentine by scanning electron microscopic investigation. Arch Oral Biol. 2000 May;45(5):355-61.

138. Schweber B. Magnetic resonance imaging (MRI), Part 1: How it works. March 11, 2019. https://www.analogictips.com/magnetic-resonance-imaging-part-1-how-it-works-faq/

139. Scougall-Vilchis RJ, Gonzalez-Lopez BS, Contreras-Bulnes R, Rodriguez-Vilchis LE, Garcia-Niño de Rivera MW, Kubodera-Ito T. Influence

of four systems for dental bleaching on the bond strength of orthodontic brackets. Angle Orthod. 2011 Jul;81(4):700-6

140. Scribante A, Cacciafesta V, Sfondrini MF. Effect of various adhesive systems on the shear bond strength of fiber-reinforced composite. Am J Orthod Dentofacial Orthop. 2006 Aug;130(2):224-7.

141. Scribante A, Contreras-Bulnes R, Montasser MA, Vallittu PK. Orthodontics: Bracket Materials, Adhesives Systems, and Their Bond Strength. Biomed Res Int. 2016;2016:1329814.

142. Scribante A, Sfondrini MF, Fraticelli D, Daina P, Tamagnone A, Gandini P. The influence of no-primer adhesives and anchor pylons bracket bases on shear bond strength of orthodontic brackets. Biomed Res Int. 2013;2013:315023. A

143. Scribante A, Sfondrini MF, Gatti S, Gandini P. Disinclusion of unerupted teeth by mean of self-ligating brackets: effect of blood contamination on shear bond strength. Med Oral Patol Oral Cir Bucal. 2013 Jan 1;18(1):e162-7. B

144. Scribante A, Vallittu PK, Özcan M. Fiber-Reinforced Composites for Dental Applications. Biomed Res Int. 2018 Nov 1;2018:4734986.

145. Sfondrini MF, Cacciafesta V, Scribante A, Boehme A, Jost-Brinkmann PG. Effect of light-tip distance on the shear bond strengths of resin-modified glass ionomer cured with high-intensity halogen, light-emitting diode, and plasma arc lights. Am J Orthod Dentofacial Orthop. 2006 Apr;129(4):541-6.

146. Sfondrini MF, Fraticelli D, Gandini P, Scribante A. Shear bond strength of orthodontic brackets and disinclusion buttons: effect of water and saliva contamination. Biomed Res Int. 2013;2013:180137

147. Sfondrini MF, Gandini P, Castroflorio T, Garino F, Mergati L, D'Anca K, Trovati F, Scribante A. Buccolingual Inclination Control of Upper Central Incisors of Aligners: A Comparison with Conventional and Self-Ligating Brackets. Biomed Res Int. 2018 Nov 29;2018:9341821.

148. Sfondrini MF, Gatti S, Scribante A. Shear bond strength of self-ligating brackets. Eur J Orthod. 2011 Feb;33(1):71-4. A

149. Sfondrini MF, Xheka E, Scribante A, Gandini P, Sfondrini G. Reconditioning of self-ligating brackets. Angle Orthod. 2012 Jan;82(1):158-64.

150. Sfondrini MF, Scribante A, Cacciafesta V, Gandini P. Shear bond strength of deciduous and permanent bovine enamel. J Adhes Dent. 2011 Jun;13(3):227-30. B

151. Sha HN, Choi SH, Yu HS, Hwang CJ, Cha JY, Kim KM. Debonding Force and Shear Bond Strength of an Array of CAD/CAM-based Customized Orthodontic Brackets, Placed by Indirect Bonding- An In Vitro Study. PLoS One. 2018 Sep 11;13(9):e0202952.

152. Shafiei F, Honda E, Takahashi H, Sasaki T. Artifacts from dental casting alloys in magnetic resonance imaging. J Dent Res 2003;82: 602–606.

153. Shalish M, Dykstein N, Friedlander-Barenboim S, Ben-David E, Gomori JM, Chaushu S. Influence of common fixed retainers on the diagnostic quality of cranial magnetic resonance images. Am J Orthod Dentofacial Orthop. 2015;147:604-609.

154. Shellock FG, Crues JV. High-field-strength MR imaging and metallic biomedical implants: an ex vivo evaluation of deflection forces. AJR Am J Roentgenol. 1988;151:289-392

155. Shellock FG, Habibi R, Knebel J. Programmable CSF shunt valve: in vitro assessment of MR imaging safety at 3T. AJNR Am J Neuroradiol. 2006; 27:661–5;

156. Shellock FG. Biomedical implants and devices: assessment of magnetic field interactions with a 3.0-Tesla MR system. J Magn Reson Imaging. 2002; 16: 721–32;

157. Shinchi MJ, Soma K, Nakabayashi N. The effect of phosphoric acid concentration on resin tag length and bond strength of a photo-cured resin to acid-etched enamel. Dent Mater. 2000 Sep;16(5):324-9.

158. Shinya M, Shinya A, Lassila LV, Gomi H, Varrela J, Vallittu PK, Shinya A. Treated enamel surface patterns associated with five orthodontic adhesive systems--surface morphology and shear bond strength. Dent Mater J. 2008 Jan;27(1):1-6.

159. Soares FZ, Follak A, da Rosa LS, Montagner AF, Lenzi TL, Rocha RO. Bovine tooth is a substitute for human tooth on bond strength studies: A

systematic review and meta-analysis of in vitro studies. Dent Mater. 2016 Nov;32(11):1385-1393.

160. Staley, R.N., Reske, N.T. Essentials of orthodontics: Diagnosis and treatment (Book). Wiley Blackwell 2013.

161. Strikman M, Spartalian K, Cole MW. Applications of modern physics in medicine (Book). Princeton University Press 2014.

162. Swartz ML. Limitations of in vitro orthodontic bond strength testing. J Clin Orthod 2007;51:207-210.

163. Tanbakuchi B, Hooshmand T, Javad Kharazifard M, Shekofteh K, Hesam Arefi A. Shear Bond Strength of Molar Tubes to Enamel Using an Orthodontic Resin-Modified Glass Ionomer Cement Modified with Amorphous Calcium Phosphate. Front Dent. 2019 Sep-Oct;16(5):369-378.

164. Taniyama T, Sohmura T, Etoh T, Aoki M, Sugiyama E, Takahashi J. Metal artifacts in MRI from non-magnetic dental alloy and its FEM analysis. Dent Mater J. 2010;29:297-302.

165. Templ M. Statistical disclosure control for microdata: Methods and applications in R (Book). Springer 2017.

166. Thompson RM, Fowler E, Culo B, Shellock FG. MRI safety and imaging artifacts evaluated for a cannulated screw used for guided growth surgery. Magn Reson Imaging. 2020 Feb;66:219-225.

167. Tian KV, Festa G, Basoli F, Laganà G, Scherillo A, Andreani C, Bollero P, Licoccia S, Senesi R, Cozza P. Orthodontic archwire composition and phase analyses by neutron spectroscopy. Dent Mater J. 2017 May 31;36(3):282-288.

168. Tymofiyeva O, Vaegler S, Rottner K, Boldt J, Hopfgartner AJ, Proff PC, Richter E-J, Jakob PM. Influence of dental materials on dental MRI. Dentomaxillofac Radiol. 2013;42:20120271.

169. Van Meerbeek B, Peumans M, Poitevin A, Mine A, Van Ende A, Neves A, De Munck J. Relationship between bond-strength tests and clinical outcomes. Dent Mater. 2010 Feb;26(2):e100-21.

170. Vicente A, Bravo LA, Romero M, Ortíz AJ, Canteras M. Effects of 3 adhesion promoters on the shear bond strength of orthodontic brackets: an in-vitro study. Am J Orthod Dentofacial Orthop. 2006 Mar;129(3):390-5.

171. Wang ZJ, Park YJ, Morriss MC, Seo Y, Nguyen T, Hallac RR, Nava A, Chopra R, Chatzinoff Y, Price K, Rollins NK. Correcting B0 Field Distortions in MRI Caused by Stainless Steel Orthodontic Appliances at 1.5 T Using Permanent Magnets - A Head Phantom Study. Sci Rep. 2018 Apr 9;8(1):5706.

172. Wang ZJ, Rollins NK, Liang H, Park YJ. Induced magnetic moment in stainless steel components of orthodontic appliances in 1.5 T MRI scanners. Med Phys. 2015 Oct;42(10):5871-8.

173. Wenger NA, Atack NE, Mitchell CN, Ireland AJ. Perioperative second molar tube failure during orthognathic surgery: two case reports. J Orthod. 2007;34(2):75–79.

174. White SC, Pharoah MJ. Oral radiology, Principles and interpretations (Book). Elsevier 2009.

175. Wiley JF, Pace LA. Beginning r: An introduction to statistical programming (Book). Apress 2015.

176. Wylezinska M, Pinkstone M, Hay N, Scott AD, Birch MJ, Miquel ME. Impact of orthodontic appliances on the quality of craniofacial anatomica) magnetic resonance imaging and real-time speech imaging. Eur J Orthod. 2015;37:610-617.

177. Yassaei S, Aghili H, KhanPayeh E, Goldani Moghadam M. Comparison of shear bond strength of rebonded brackets with four methods of adhesive removal. Lasers Med Sci. 2014 Sep;29(5):1563-8.

178. Yassaei S, Aghili HA, Davari A, Mostafavi SM. Effect of Four Methods of Surface Treatment on Shear Bond Strength of Orthodontic Brackets to Zirconium. J Dent (Tehran). 2015 Apr;12(4):281-9.

179. Yassi K, Ziane F, Bardinet E, Moinard M, Veyret B, Chateil JF. Évaluation des risqué d'échauffement et de déplacement des appareils orthodontiques en imagerie par resonance magnétique. Journal de Radiologie 2007;88:263-268

180. Yassir YA, McIntyre GT, Bearn DR. Variation in bracket slot sizes, ligation methods and prescriptions: UK national survey. Int Orthod. 2019 Jul 1.

181. Zachriat C, Asbach P, Blankenstein KI, Peroz I, Blankenstein FH. MRI with intraoral orthodontic appliance-a comparative in vitro and in vivo study of image artefacts at 1.5 T. Dentomaxillofac Radiol. 2015;44(6):20140416.

182. Zarif Najafi H, Bagheri R, Pakshir HR, Tavakkoli MA, Torkan S. Effect of different surface treatment on the shear bond strength of metal brackets to bleached and desensitized enamel. Int Orthod. 2019 Mar;17(1):73-79.

183. Zhylich D, Krishnan P, Muthusami P, Rayner T, Shroff M, Doria A, Tompson B, Lou W, Suri S. Effects of orthodontic appliances on the diagnostic quality of magnetic resonance images of the head. Am J Orthod Dentofacial Orthop. 2017 Mar;151(3):484-499.